Modeling Driving Behavior at Single-Lane Roundabouts

Min Zhao

Berichte aus dem DLR-Institut
für Verkehrssystemtechnik

Band 34

DLR Deutsches Zentrum
für Luft- und Raumfahrt

ISSN 1866-721X

Modeling Driving Behavior at Single-Lane Roundabouts

Von der Fakultät für Maschinenbau

der Technischen Universität Carolo-Wilhelmina zu Braunschweig

zur Erlangung der Würde

einer Doktor-Ingenieurin (Dr.-Ing.)

genehmigte Dissertation

von:	Min Zhao
aus:	Nei Mongol, China

eingereicht am:	04.01.2018
mündliche Prüfung am:	09.03.2018

Gutachter:	Prof. Dr.-Ing. Karsten Lemmer
	Prof. Dr.-Ing. Dirk Söffker
	PD Dr. rer. soc. Meike Jipp

2019

Berichte aus dem DLR-Institut für Verkehrssystemtechnik

Band 34

Modeling Driving Behavior at Single-Lane Roundabouts

Min Zhao

Herausgeber:
Deutsches Zentrum für Luft- und Raumfahrt e. V.
Institut für Verkehrssystemtechnik
Lilienthalplatz 7, 38108 Braunschweig

ISSN: 1866-721X

DLR-TS 1.34

Braunschweig, im Januar 2019

Institutsdirektorin:
Prof. Dr.-Ing. Katharina Seifert

Verfasserin:
Min Zhao

Vorwort der Herausgeberin

Liebe Leserinnen und Leser,

in Ihren Händen halten Sie einen Band unserer Buchreihe "Berichte aus dem DLR-Institut für Verkehrssystemtechnik". In dieser Reihe veröffentlichen wir spannende, wissenschaftliche Themen aus dem Institut für Verkehrssystemtechnik des Deutschen Zentrums für Luft- und Raumfahrt e.V. (DLR) und aus seinem Umfeld. Einen Teil der Auflage stellen wir Bibliotheken und Fachbibliotheken für ihren Buchbestand zur Verfügung. Herausragende wissenschaftliche Arbeiten und Dissertationen finden hier ebenso Platz wie Projektberichte und Beiträge zu Tagungen in unserem Hause von verschiedenen Referenten aus Wirtschaft, Wissenschaft und Politik.

Mit dieser Veröffentlichungsreihe verfolgen wir das Ziel, einen weiteren Zugang zu wissenschaftlichen Arbeiten und Ergebnissen zu ermöglichen. Wir nutzen die Reihe auch als praktische Nachwuchsförderung durch die Publikation der wissenschaftlichen Ergebnisse von Dissertationen unserer Mitarbeiter und auch externer Doktoranden. Veröffentlichungen sind wichtige Meilensteine auf dem akademischen Berufsweg. Mit der Reihe "Berichte aus dem DLR-Institut für Verkehrssystemtechnik" erweitern wir das Spektrum der möglichen Publikationen um einen Baustein. Darüber hinaus verstehen wir die Kommunikation unserer Forschungsthemen als Beitrag zur nationalen und internationalen Forschungslandschaft auf den Gebieten Automotive, Bahnsysteme und Verkehrsmanagement.

Der vorliegende Band stellt einen datengetriebenen Ansatz zur Erhöhung der Verkehrssicherheit an Kreisverkehren vor. Der Ansatz basiert auf einem empirischen Forschungsparadigma, im Rahmen dessen Fahrdaten sowie Daten von Blick- und Kopfbewegungen im Realverkehr und in der Simulation erhoben wurden. Diese Daten wurden mit Hilfe von Methoden der künstlichen Intelligenz mit Informationen über das Verhalten anderer Verkehrsteilnehmer und über das geographische Layout des Kreisverkehrs miteinander in Beziehung gesetzt. Darauf aufbauend wurde ein Algorithmus entwickelt und validiert, der insbesondere Daten über den zeitlichen Verlauf der Lenkradbewegung und Daten zum geographischen Layout des aktuellen Kreisverkehrs nutzt, um vorherzusagen, ob die jeweiligen Fahrer den Kreisverkehr bei der nächsten Ausfahrt verlassen oder nicht. Dies gelingt in einer Distanz von bis zu 10 m vor der Ausfahrt in über 95% der Fälle. Diese Quote kann bei einer Individualisierung des Modells noch deutlich früher erreicht werden. Somit erscheint es auch realistisch, mit Hilfe dieses Ansatzes die Verkehrssicherheit an Kreisverkehren zu erhöhen: Fahrer können damit nämlich rechtzeitig vor der Durchführung eines intendierten Abbiegemanövers gewarnt werden, sollte eine Kollision mit einem anderen (schwächeren) Verkehrsteilnehmer drohen.

Prof. Dr.-Ing. Katharina Seifert

Acknowledgments of the author

The research presented in this thesis was carried out when I worked at German Aerospace Center (Deutsches Zentrum für Luft- und Raumfahrt, DLR) as a PhD student. In this thesis, the problem of driving behavior prediction at roundabouts was investigated with data driven algorithms, which is an essential component of the advanced driver-assistance systems (ADAS) and could contribute to the future autonomous driving. I am proud to be involved in the big trend of intelligent transportation system (ITS) and make my own contribution. It is my honor here to thank all the people who have supported me in completing this research.

I would like to thank my supervisor Prof. Dr.-Ing. Karsten Lemmer who gave me the chance to undertake my thesis at the Institute of Transportation Systems at DLR. I am grateful for our regular meetings, his encouragement, suggestions as well as the friendly and positive working environment he maintained at our institute.

Further, I express my gratitude to PD Dr. rer. soc. Meike Jipp for her constant support, detailed discussions and practical suggestions for my research and how I should do research in Germany. Many aspects of this work, from measurement conduction to thesis revision, are supported by her. I have learned a lot from her in the last few years. Her professional attitude in scientific work, friendliness, calmness and passion are always exemplary to me.

Also, I would like to thank Prof. Dr.-Ing. Dirk Söffker for being the second referee of this thesis. I have learned a lot with the experience of exchanging at his institute and the discussions with him. With his advice, not only my doctoral work but my writing and presentation skills were improved. Furthermore, I would like to thank Dr.-Ing. Uwe Becker for being the chair of my examination board.

I would also like to thank my colleagues at DLR. In particular, I am grateful to David Käthner for his significant help, from his assistance in measurement even during weekend to his inspiring suggestion during our discussions. His comprehensive knowledge helped me not only with my research, but also various aspects of the German culture. Also, I thank my colleagues Uwe Drewitz, Klas Arne Ihme, Meng Zhang, Björn Hendriks, Paulin Pekezou Fouopi, Eric Nicolay, Dirk Assmann, Fabian Utesch, and Robert Kaul for providing me assistance in my studies and enjoyable working environment throughout the whole time of my PhD.

Finally, I would like to give my special thanks to my family. I thank my parents Yonghong Pei and Pingyuan Zhao for their constant love and their understanding when I seek my way to live the life. Most importantly, I wish to thank my husband Bile Peng for his company at each important moment during my PhD as well as his understanding and encouragement when we seek our way to live the life together.

Min Zhao

Contents

List of Figures

List of Tables

Abstract

Roundabouts are considered important because converting an intersection into a roundabout has been proven to improve safety. However, the absolute number of crashes at roundabouts is still high. Many crashes occur because car drivers fail to yield. Intelligent systems can increase safety if they can prevent crashes by precisely predicting driver maneuvers. Therefore, a reliable and trustworthy predictive model of driver maneuvers is needed.

A few studies analyze human behavior at roundabouts. However, they focus on an operational timescale rather than on maneuvers on a tactical timescale. Tactical maneuvers have mostly been investigated in scenarios about typical intersections and overtaking. Thus, there is still a lack of research on driver maneuver prediction at roundabouts. To fill this gap, the objective of this thesis is to develop a model that can predict driver maneuvers at single-lane roundabouts.

Two types of driver maneuvers are possible in front of each exit of a roundabout: exiting the roundabout and staying in the roundabout. To predict which maneuver a driver will execute in front of an exit, a driver maneuver predictive model was developed on the basis of an analysis of driver behavior data acquired from a field study and a simulator study. Soft-classification algorithms were proposed to train the predictive model. The model consisted of four sub-models for four different scenarios, which were defined by the correlation between roundabout layouts and drivers' steering behavior. The sub-models make it possible to predict the exiting or staying maneuvers executed in the corresponding scenarios. Furthermore, a personalized predictive model was developed to adapt to individual drivers because different drivers have different driving styles.

The driver maneuver predictive model shows excellent predictability: In the scenarios without traffic, the model reported prediction results for more than 97.60% of test drives at the position 10 m from the exits of the roundabouts. Of these drives, more than 97.10% were predicted correctly. The personalized predictive model provided even better prediction results for individual drivers with significantly different driving styles. Moreover, the driver maneuver predictive model also successfully predicts drivers' maneuvers in most scenarios with cyclists. The prediction results show that steering angle, steering angle speed, velocity, and acceleration of the ego car provide the most important information. With this information, the model can predict the maneuver of a driver with any type of driving style at a single-lane roundabout with any type of layout.

Kurzfassung

Kreisverkehre gelten als ein wichtiger Bestandteil der Verkehrsinfrastruktur, da ihre Verwendung anstelle von traditionellen Kreuzungen einen wesentlichen Beitrag zur Verkehrssicherheit leistet. Die absolute Anzahl von Unfällen bleibt jedoch auch an Kreisverkehren noch hoch. Viele Kollisionen werden dabei durch Missachtung der Vorfahrt verursacht. Intelligente Fahrzeugassistenzsysteme könnten hier eingreifen, vorausgesetzt sie verfügen über eine zuverlässige Vorhersage des Fahrerverhaltens. Hierfür wird ein robustes und präzises Modell für die Vorhersage von Fahrmanövern im Kreisverkehr benötigt.

Empirische Studien zu menschlichem Verhalten an Kreisverkehren fokussieren in der Regel auf die operationale Ebene der Fahraufgabe, also auf eine zeitlich hoch aufgelöste Zeitskala. Die taktische Ebene, auf der Manöver wie “Verlassen des Kreisverkehr” stattfinden, wurde dabei jedoch nicht ausreichend analysiert. Insbesondere fehlen Modelle, die Fahrmanöver im Kreisverkehr vorhersagen. Ziel dieser Arbeit ist es daher, ein solches Modell für einspurige Kreisverkehre zu entwickeln.

Zwei Arten von Manövern sind innerhalb eines einspurigen Kreisverkehrs möglich: Im Kreisel zu bleiben, oder ihn zu verlassen. Um möglichst früh eines der beiden Manöver vorherzusagen wurden im Rahmen dieser Arbeit verschiedene Modelle entwickelt, welche auf Fahrdaten aus dem Realverkehr sowie Simulationsstudien basieren. Für das Training der jeweiligen Modelle werden Soft-Klassifikationsalgorithmen vorgeschlagen, die auf einem Quasi-Hidden-Markov-Modell basieren.

Dieses Modell besteht aus vier Teilmodellen für jeweils vier verschiedene Szenarien, die durch die Korrelation zwischen Kreisverkehrlayouts und Lenkverhalten von Fahrern definiert wurden. Mit den Teilmodellen können die in den entsprechenden Szenarien ausgeführten Manöver "Verlassen" oder "Bleiben" vorhergesagt werden. Des Weiteren wurde ein personalisiertes Vorhersagemodell entwickelt, um sich an den individuellen Fahrer anzupassen, da verschiedene Fahrer unterschiedliche Fahrstile aufweisen.

Das Fahrmanöver-Vorhersagemodell zeigt eine ausgezeichnete Performanz: In den Szenarien ohne Verkehr lieferte das Modell in einem Abstand von 10 m vor der Kreisverkehrsausfahrt Vorhersagen für mindestens 97,60% aller Testfahrten. Von diesen Fahrten wurden wiederum über 97,10% korrekt vorhergesagt. Personalisierte Modelle erreichen noch bessere Vorhersageergebnisse. Sind weitere Verkehrsteilnehmer in den analysierten Szenarien anwesend liegt die Vorhersagegüte etwas darunter. Die Ergebnisse zeigen, dass Lenkwinkel, Lenkwinkelgeschwindigkeit sowie Eigengeschwindigkeit und -beschleunigung die wichtigsten Informationen liefern. Hiermit kann das Modell das Manöver eines Fahrers mit jeder Art von Fahrstil an einem Kreisverkehr mit jeder Art von Layout vorhersagen.

1 Introduction

1.1 Motivation

Roundabouts are considered important because converting an intersection into a roundabout results in fewer injury accidents for both car drivers and pedestrians [Bri11, EHVS09, RPGL01, HV00]. A study by Montella shows that roundabouts reduce the total number of injury crashes by 76% and the total number of fatal crashes by more than 90% compared to signalized intersections [Mon11]. However, many crashes with cyclists occur at roundabouts [HOB07]. Roundabouts increase cyclist injury accidents by 27% and fatal accidents by 46% [DNW08]. The most dangerous situations are those in which a) a car enters a roundabout when a cyclist is circulating or b) in which they both circulate in parallel and the car driver exits the roundabout [SLSH10]. In almost one-third of the crashes between cars and cyclists, the failure of car drivers to give way is the main contributing factor in terms of road users. For instance, turn signals were used incorrectly in about 20% of all turn maneuvers [Eur08][LKB+13]. Therefore, an important factor for accidents is when drivers indicate their planned behavior to leave or stay in the roundabout incorrectly, or make incorrect predictions about other road users' maneuvers.

Advanced Driver Assistance Systems (ADASs) can decrease the probability of crashes or mitigate the damage caused by accidents [HKBL11]. In risky situations, ADASs can assist drivers by warning them of dangers, activating blinkers automatically to warn other road users, or activating the braking system to avoid potential crashes [DMT11]. These systems work efficiently only when they can predict drivers' upcoming maneuvers correctly and offer appropriate help based on these predictions, otherwise, drivers might feel annoyed by the interference and disable the ADAS [DMT11][HZW12]. Therefore, an ADAS that can effectively mitigate accidents at roundabouts must include a reliable and trustworthy driver maneuver predictive model. This model must be able to predict future driver maneuver of exiting or staying in roundabouts. The prediction result will allow the ADAS to decide whether and how to assist the driver in considering her/his future maneuver.

Predicting driver maneuvers correctly at roundabouts is still an open research question, and is thus the focus of this thesis. Specifically, a model for predicting driver maneuver at generic roundabouts was developed and evaluated in this thesis.

1.2 Objective

The objective underlying this thesis is to develop a driver maneuver predictive model that can predict future driver maneuvers at roundabouts with different layout designs and in different traffic situations for all drivers with their different driving styles. It should be noted that the focus of this thesis is on compact roundabouts, which are defined as roundabouts with a single

circulating lane and a diameter of 26 - 40 m [Bri11][Hof14]. Two types of driver maneuvers in front of each exit of compact roundabouts are possible: exiting the roundabout or staying in the roundabout (see Figure 1-1). To predict these two maneuvers, the following challenges need to be addressed:

- Identify the driving behavior information that provides indications for the upcoming driver maneuver. Although driver maneuvers cannot be observed before they are executed, certain information (e.g., driving velocity, steering wheel angle) can be used to infer which maneuver a driver is going to execute.
- Identify the effect of different roundabout geometric layouts on driving behavior. Drivers behave differently when driving through roundabouts with different radii and entry-exit angles. Only when the effects of the geometric design on human driver behavior are considered can driving behavior effectively predict driver maneuvers.
- Identify a classification algorithm that can distinguish between pieces of driving behavior data that are related to the two maneuvers.
- Identify a modeling method that can make use of driving behavior and the classification algorithm to predict driver maneuvers in different scenarios in a valid manner.
- Identify an evaluation method to evaluate the performance of the driver maneuver predictive model.

Addressing these challenges will allow the objective of developing a driver maneuver predictive model to be achieved.

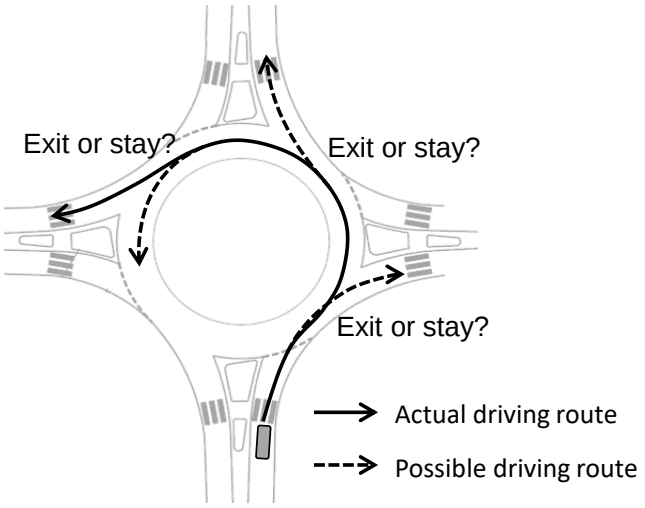

Figure 1-1: Two driver maneuvers in front of an exit of a roundabout.

1.3 Methodology

Here, the methodology for developing a driver maneuver predictive model is introduced in a general way. The specific details of the methodology are provided in Chapters 3, 4, and 5.

Driver maneuvers are both a cause and a consequence of driving behavior. Thus, driving behavior can be used to predict driver maneuvers. However, drivers may behave differently when they drive through roundabouts with different geometric layouts. This is why the effects of roundabout layouts need to be controlled for. Otherwise, driver maneuver can hardly be predicted effectively. Hence, driving behavior data relevant to roundabouts with different layouts were acquired and analyzed to develop an understanding of the effects of the roundabout layout on driving behavior. Then, machine-learning algorithms were used to train classifiers to distinguish between different patterns of driving behavior to understand what maneuvers drivers are going to execute in the immediate future. The workflow of the thesis is presented in Figure 1-2, the details of which are explained in this chapter.

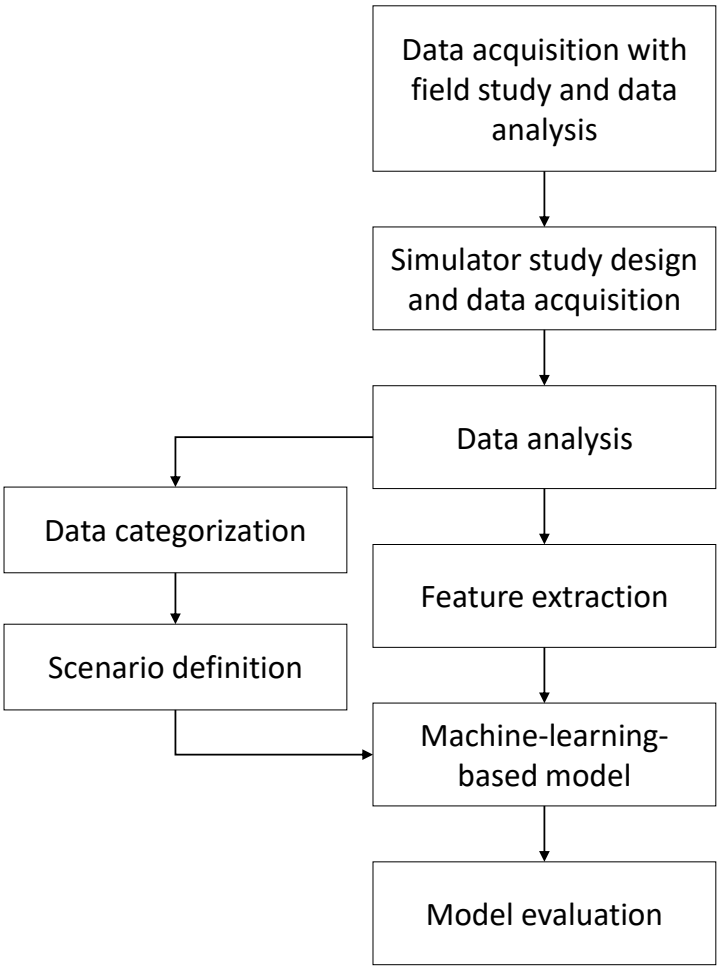

Figure 1-2: Modeling workflow.

Driving Data Acquisition

A field study was conducted to acquire data about how drivers drive through roundabouts. In this field study, participants drove on a standardized route through compact roundabouts in real traffic with a sensor-equipped experimental car. Each participant drove through every combination of entries and exits in accordance with an experimenter's instructions. Thus, data on participants' naturalistic driving behavior were acquired, including steering angle, steering

angle velocity, acceleration, velocity, yaw, and driver gaze and head direction. The data showed that information about steering wheel behavior is useful for predicting driver maneuvers at the investigated roundabouts [ZKJ+17]. The limitations of the field study were that the driving behavior was mediated by uncontrolled factors related to surrounding traffic and that driving behavior data were only captured at three roundabouts. To complement these limitations, a simulator study was designed to acquire driving behavior data at more generic roundabouts with varied geometric layouts (in Session 1) and varied traffic situations (in Session 2). In Session 1, two geometric features of roundabout layout design, *radius* and *entry-exit angle*, were manipulated experimentally. In Session 2, four types of surrounding cyclists were placed at or near the roundabouts to see how they would affect the participants' driving behavior. In the simulator study sessions, the participants drove through tracks that had been produced to match the roundabouts with the varied geometric features and the varied traffic discussed above. The following variables were recorded during the two sessions for each scenario:

- Steering angle
- Steering angle velocity
- Acceleration
- Velocity
- Position
- Gaze direction
- Head direction

Therefore, relevant driving behavior data were acquired and analyzed. The details of the studies and the analysis are provided in Chapter 3.

Scenario Definition

The driver behavior data acquired from the simulator study were analyzed to identify the impact of roundabout layout on driving behavior. The local extremum of steering angles (θ_e) and the integrated geometric feature (Geo) were defined to characterize the steering wheel information and the geometric features of roundabouts, respectively. The mathematical correlation of these two variables was calculated to define each scenario. Subsequently, a method of scenario categorization for roundabouts was proposed using this correlation, so that all scenarios at roundabouts could be categorized into four categories. This allows the effect of geometric features of roundabouts on driving behavior to be eliminated in each scenario category. The details of the scenario definition are also provided in Chapter 3.

Modeling

A driver maneuver predictive model was developed for the four scenarios. The model includes four sub-models that correspond to each of the four scenarios. Each sub-model consists of a series of classifiers corresponding to a series of prediction sites. Prediction sites are locations where a prediction is made along the route between the entry and the exit of a roundabout. The information on driving behavior at each prediction site were used to train the corresponding classifier. With the classifiers, two driver maneuvers of test drives at each prediction site were classified. The features and the algorithms used for classifier training are as follows:

- Features for classifier training. The relevant features are those that significantly differ between exiting a roundabout VS. staying in the roundabout. Steering angle and steering angle velocity proved to be important features [ZKJ+17]. The other features, including acceleration, velocity, and driver gaze and head direction, were also tested. The values for steering angle, steering angle velocity, speed, acceleration, heading direction, and gaze direction at each prediction site were extracted as features for training the classifiers. Different features and different combinations of features provide different predictabilities. Thus, all combinations of features were used as inputs to train the classifiers, and the most important ones were selected.

- Algorithms for classifier training. The algorithms were developed based on those that have proven to be successful in earlier studies (see Chapter 2). Soft-classification algorithms were used because hard-classification algorithms are inappropriate for driver maneuver prediction: hard classifiers output discrete values of "Exiting" or "Staying" when fed with feature data [LZW11], and thus always offer results even when predictability is still weak at the very beginning of drives. In contrast, soft classifiers output continuous values of the likelihood of "Exiting" or "Staying" [LZW11]. This output is known as soft-decision output. Soft classifiers decide whether or not to report the results of "Exiting" or "Staying" with a soft-decision output and an output threshold: The classifiers will not report results if the soft-decision outputs of "Exiting" and "Staying" are lower than the threshold. Thus, the prediction results had three possible stati: correct, incorrect, or not available. In this work, two types of soft-classification algorithms were investigated: simple algorithms and complex algorithms. The simple classification algorithms include support vector machines, random forest, AdaBoost, and logistic regression. The complex algorithms are the algorithms proposed by integrating the hidden Markov model and the above simple algorithms. So, the classifiers were trained with these soft-classification algorithms.

A personalized predictive model was then developed for individual drivers because drivers have different driving styles even in the same roundabout scenario. This model was obtained by updating the original predictive model, which was trained using data about generic drivers, to include the specific driver's driving data. Details on this process are provided in Chapter 4.

Evaluation

Evaluation is needed to select the feature and the algorithm with the best performance. Five-fold cross validation was used for the model evaluation, so one-fifth of the driving behavior data are test data for the predictive model. The test data set contained driving samples with the exiting maneuver and samples with the staying maneuver. When the models were tested with these samples, they labeled the samples as "Exiting", "Staying", or "NA (no result available)" using the soft-decision outputs and an output threshold. Traditional evaluation scores for hard classification such as accuracy, F1 score, detection rate, and false alarm rate are not appropriate in this case because these scores would treat "no result available" as an incorrect result. Therefore, a unique grading system was proposed to evaluate the soft-decision based models. The basic principle of the grading system is that a correct prediction is the best situation, an incorrect prediction is the worst situation, and no result available is neutral. Following this principle, the models receive one positive point when they offered a correct prediction result, one negative point when they offered an incorrect prediction result, and zero points when they did not offer a result for a given test drive. However, the scores the models acquired in this way depended not only on the prediction results but also on the number of test drives. Therefore, the points were converted into percentages, so that the scores for all scenarios varied in the same range, from -100 (incorrectly predicting all test drives) to 100 (correctly predicting all test drives). Performance scores were calculated for all combinations of the algorithms and the features at each prediction site in each of the four scenarios.

The performance scores of better models reached 100 at earlier prediction sites, therefore, the prediction sites for which scores were close to 100 were selected as key sites. Performance of the algorithm-feature combinations at each key site in each scenario could be ranked using the comparison method. The rank allowed for the selection of the best feature and the best algorithm. Afterwards, the model that was trained using the selected feature and the selected algorithm was evaluated in the traffic scenarios.

The evaluation showed that the model performs well when it comes to predicting driver maneuvers at roundabouts. Therefore, the objective of this thesis was achieved. The details of the evaluation are provided in Chapter 5.

1.4 Contributions

The work presented in this thesis makes the following contributions:

1. Empirical proof that human driving behavior in roundabouts is affected by the geometric features of roundabouts. The mathematical relationship between driving behavior and roundabout geometric features is introduced in Chapter 3.
2. A method for categorizing roundabout scenarios according to relevant geometric features and human driving behavior–a prerequisite for modeling human behavior at generic roundabouts. This method is also introduced in Chapter 3.

3. A generic structure for the driver maneuver predictive model. The model consists of sub-models for each scenario category. Each sub-model consists of a series of classifiers trained with data captured at roundabouts to predict drivers' future maneuvers. The model's structure and training are introduced in Chapter 4.
4. A grading system for evaluating the model. This grading system rewards correct predictions, punishes incorrect predictions, and ignores unavailable results. The grading system is introduced and defined in Chapter 5.
5. Identification of information that can be captured automatically and be used to best predict future behavior. This information includes steering wheel information and car motion parameters. The advantage of this information is that it can be acquired at a low cost and without violating drivers' privacy. The evaluation of the driving information can be found in Chapter 5.
6. A complex algorithm that integrates hidden Markov model and logistic regression is well suited for predicting driver behavior. The evaluation of the algorithms can also be found in Chapter 5.
7. A driver maneuver predictive model that is successful in scenarios with and without surrounding traffic. The performance of the model can be found in Chapter 5.
8. Empirical proof that human behavior depends not only on the geometric features of roundabouts but also on person-specific parameters such as driving style. A personalized predictive model was developed on the basis of this knowledge. The performance of the personalized model can also be found in Chapter 5.

1.5 Outline

Chapter 2 presents the state-of-the-art regarding driver maneuver prediction [TIS+07, NMI+08, BED08, BD09, SH14, GJW+16, TMF16]. Many researchers have focused on turning behavior at (urban) intersections [TIS+07][BLSIG17]. Fewer researchers have investigated driving behavior at roundabouts and how cyclists impact driving behavior [Rom05][Raa17]. Predicting driver maneuvers at roundabouts has not yet been investigated at all.

Chapter 3 introduces a method for categorizing scenarios. In each scenario category, the effect of the geometric features of roundabouts on driving behavior is eliminated, increasing the predictability of driving behavior.

Chapter 4 presents the development of the driver maneuver predictive model. Multiple forms of driving behavior information were used as classification features and multiple machine-learning algorithms were used as classification algorithms. Additionally, a method for personalizing the model was proposed for individual drivers. The final driver maneuver predictive model achieves universality for both: roundabouts and drivers, i.e., the model can predict the maneuvers of all drivers with all driving styles at compact roundabouts with any types of layouts.

Chapter 5 presents the evaluation of the driver maneuver predictive model. First, the features and the algorithm with the best predictive performance were selected and the positions where

reliable prediction can be obtained were investigated. Second, the impact of cyclists at or near a roundabout on the driver maneuver prediction was analyzed. Finally, a personalized model that was trained to predict the behavior of a specific driver was evaluated.

Chapter 6 summarizes the modeling process and provides conclusions about driver maneuver prediction. Limitations and further work are also presented.

2 Current State of Driver Maneuver Prediction

Research on driver maneuver prediction incorporates many aspects, from cognition to the behavior of human drivers [Ran94, Mac03, PE07, DT11, MM15]. Driving behavior can be planned on operational, tactical, and strategic timescales [Ran94][PE07]. The operational timescale, the shortest timescale of human interaction, is on the order of hundreds of milliseconds. The tactical timescale, which includes successive operations, is on the order of seconds. The strategic timescale, meanwhile, is associated with minutes or hours of prior planning [DT11]. Therefore, driver maneuvers related to turning at roundabouts are on the tactical timescales, on the order of seconds.

Some studies analyze human behavior at roundabouts, however, on the operational timescale rather than the tactical timescale [Rom05][SASMMI13][MHCG14]. Tactical maneuvers have been investigated in intersection and overtaking scenarios. In this chapter, turning maneuver prediction at intersections is focused because roundabouts are a special type of intersection. Previous work is summarized as the state of the art in following parts: driving behavior data, algorithms, and evaluation methods.

2.1 Driving Behavior Data

Driver maneuver studies are usually based on driving data collected either from real driving, in a simulator, or via a mixture of both [BLSIG17]. Data that are captured in a realistic traffic scenario can be generalized to reality, whereas simulator studies can control for more variables, such as surrounding traffic [DT11]. Studies on driver maneuvers at intersections show that the data used for prediction generally include driver information, ego car information, surrounding traffic information, and geometric information on the intersections [TIS+07, NMI+08, LIGL11, LLIG11, SSH12, LKB+13, GKO14, SH14, TKG15, GJW+16, TMF16, BLSIG17, PWK17].

Driver information and ego car information

Driver information includes head, eye, foot, or hand positions that are usually collected using camera-based systems inside the car [TMF16]. Ego car information is generally collected from a CAN bus or off-the-shelf portable devices [SSH12]. The car information includes steering wheel angle, pedal position, turn signal state, lateral and longitudinal position, velocity, and acceleration [TIS+07, NMI+08, SH14, GJW+16, TMF16]. To acquire driving information at specific sites of intersections, driving data are usually assigned to potential routes and transformed from time-based to distance-based representation [GJW+16].

Surrounding traffic information

Surrounding traffic information includes the position, yaw angle, and velocity of the other vehicles, which are usually collected using sensors and cameras equipped on the outside of the car [TMF16]. In some studies [LKB+13][LRKS13], traffic information is not directly used to predict driver maneuver but to investigate how traffic affects predictions. Liebner et al. (2013) predicted driver maneuvers at urban intersections in the presence of preceding vehicles. With no preceding vehicles, they achieved a false positive rate of 5% and a true positive rate of 95%; the true positive rate decreased to 55% in the presence of preceding vehicles. Hence, this approach allows for the expression of uncertainty in the presence of a preceding vehicles [LKB+13][GJW+16][LRKS13].

Geometric information of intersections

Geometric information of intersections includes information about the geometrical and topological characteristics of the road intersection, which are usually collected from a geographic information system (GIS) and digital map [LIGL11, LLIG11, TKG15]. This information can be combined with car information and traffic information to predict driver maneuvers [LIGL11][LLIG11].

2.2 Algorithms

Machine-learning approaches have been demonstrated to perform well in driver maneuver prediction due to their ability to learn from large amounts of available data [TB13]. The machine-learning algorithms SVM, RF, Adaboost, and logistic regression are explained here because previous research has found them to be suitable classification algorithms for the binary classification problem [TIS+07, SH14, GJW+16, TMF16, BLSIG17, GKO14, TKG15].

2.2.1 Support Vector Machines

Support vector machines (SVM) is a classification and regression method for categorizing data [CV95][BSB+96]. It has been used for driver maneuver prediction at intersections and exhibited good prediction ability: A turn prediction accuracy of 90% was achieved 1.6 seconds before the intersection [TKG15].

The main idea of SVM for a binary classification is to map data to a higher dimensional space with a kernel function, so that the two categories are more easily separated (see Figure 2-1). Typical kernel functions include linear functions, Gaussian functions, and polynomial functions. Then, the mapped data are separated with the hyper-plane, which can be identified by solving an optimization problem. The hyper-plane is based on support vectors, which are a set of boundary training data. New data are classified according to which side of the hyper-plane they fall into.

There can be more than one hyper-plane for a given set of data. The goal is to find a hyper-plane that maximizes the margin between these two classes. The margin is defined as the sum of distances from the closest data points of both classes to the hyper-plane. A larger margin is good because it reduces the overfitting problem. Overfitting occurs when the solution is too customized for the training data and cannot be generalized to new data [Ben12]. The correct choice of kernel and data representation leads to good solutions [MS05]. In machine learning, Platt scaling or Platt calibration is a way of transforming the outputs of a classification model into a probability distribution over classes [HMK06].

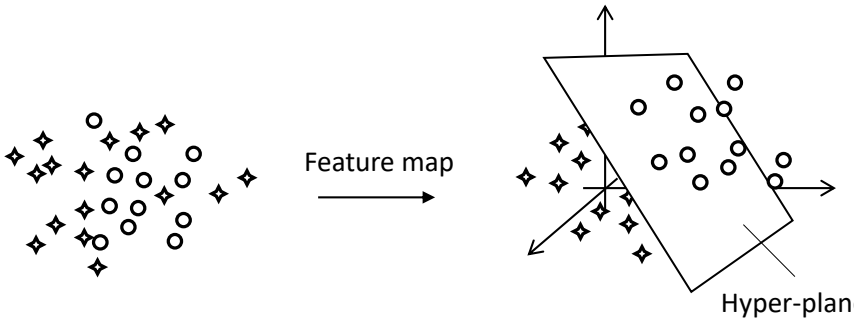

Figure 2-1: Feature map from a lower dimension to a higher dimension.

2.2.2 Logistic Regression

Logistic regression has also shown success when used for decision prediction at intersections [TIS+07]. Logistic regression is generally well-suited for describing relationships between a categorical outcome variable and one or multiple continuous predictor variables [PLI02]. For the case of multiple predictors x, a logistic regression can be constructed for one dichotomous outcome variable Y as follows [PLI02]

$$\text{logit}(Y) = \ln\left(\frac{\pi}{1-\pi}\right) = \alpha + \beta_1 X_1 + \beta_2 X_2 \tag{2.2.1}$$

Therefore,

$$\begin{aligned}\pi &= Probability(Y = outcome\ of\ interest \mid X_1 = x_1, X_2 = x_2, a\ specific\ value\ of\ X) \\ &= \frac{e^{\alpha+\beta_1 X_1+\beta_2 X_2}}{1+e^{\alpha+\beta_1 X_1+\beta_2 X_2}}\end{aligned} \tag{2.2.2}$$

where π is the probability of the event, α is the Y intercept, βs are regression coefficients, and Xs are a set of predictors. α and βs are typically estimated using the maximum likelihood (ML) method [PLI02].

2.2.3 AdaBoost

The AdaBoost algorithm [FHT+00] is the first practical realization of the boosting algorithm and remains a widely used approach in numerous applications. However, it has never been used in

driver maneuver prediction. The basic idea of boosting is to make accurate predictions based on heterogeneous data by combining several relatively simple and less accurate predictions [Sch13]. Consider m training data (x_1, y_1), ..., (x_m, y_m) where x_i is the observed data (e.g., steering wheel angle, vehicle velocity), $x_i \in X$ and y_1 is the classification label, $y_i \in \{-1, +1\}$, where -1 and 1 stand for two different maneuvers.

T simple predictors (a predictor with simple rules to map the data set and classification label with a high error rate) are applied to construct an AdaBoost predictor, and the tth simple predictor is denoted as $h_t : X \to \{-1, +1\}$. The combined predictor is the weighted combination of the simple predictors

$$H(x) = \sum_{t=1}^{T} \alpha_t h_t(x). \tag{2.2.3}$$

In plain text, $H(x)$ is the weighted vote of the simple predictors where the tth predictor is assigned weight α_t.

The error rate of each simple predictor is only expected to be slightly lower than 50%, i.e., no individual predictor has to be good, which is called the *weak learning condition*. Under this condition, it can be proven that the error rate in the training data set decreases to zero quickly [FS95] with a few simple predictors (i.e., T) of boosting and with a reasonable complexity measured according to the Vapnik and Chervonenkis (VC) dimension.

According to [FS95, BH89], the VC dimension of the final predictor increases roughly proportionally to the number of simple predictors T. Furthermore, the error rate in the training data set decreases monotonously with T and achieves, and then stays at 0 as further simple predictors are added. However, the error rate in the test set, which is different from but has identical statistical characteristics to the training set, decreases first and then increases again as the number of simple predictors grows. This problem is referred to as *overfitting*. Therefore, with a view to both complexity and the error rate, the number of simple predictors should be chosen as the smallest number that reduces the error rate in the training set to 0.

2.2.4 Random Forest

Random forest (RF) has also shown good predictability in driver maneuver prediction at intersections [GJW+16, TMF16, BLSIG17]. A study by Gross (2016) showed that maneuvers can be predicted with a recall of 76% 30 m before the relevant intersection center using RF.

Random forest comprises several predictors in the form of decision trees, with the final decision based on the votes of the individual decision trees [LWWL13]. Decision trees are a widely-used classification algorithm that splits the data space into two or more classes on the basis of significant features. Fig. 2-2 shows an example of a decision tree. Beginning with the root node (also a decision node), each decision node splits the data space according to the currently most significant feature. The currently most significant feature is excluded from the decision nodes beneath it, and the second most significant feature is applied to split the data space. The classification is complete when a terminal node is reached.

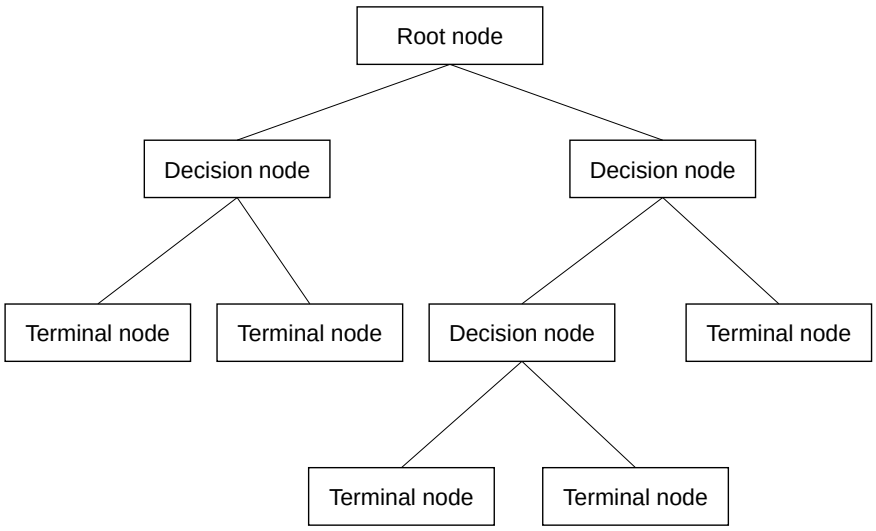

Figure 2-2: An example of the decision tree.

The decision tree outperforms linear models (e.g., SVM and logistic regressions) when the problem at hand involves non-linearities or the relationship between dependent and independent features is highly complex. However, one common issue of decision trees is the overfitting problem. To deal with this, one can use bagging to reduce the variance of the estimation [Bre96]. Bagging splits the complete training data into several sub-samples and uses each of them to train a decision tree. This algorithm is called *Random Forest*, because the training data is selected randomly and because there are quite a large number of decision trees. The final decision in RF is the class receiving the most votes from the decision trees. The RF algorithm is particularly suitable for complicated input data with a large number of dimensions with a wide range of relative importances.

2.2.5 Hidden Markov Models

Hidden Markov models (HMM) are also a suitable method for driver maneuver prediction at intersections [SH14, GKO14]. A study by Streubel (2014) [SH14] showed that HMM accomplished a robust prediction with high accuracy, above 90%, as early as 7 seconds before entering an intersection.

An HMM [RJ86] comprises *hidden states* and *observations*, as shown in Fig. 2-3. The observations are the measured data, which depend on unobserved states (hidden states) but are disturbed by random factors. The hidden states are assumed to have the Markov property, i.e., that each state in the sequence depends on the previous state and is independent of all other states, which can be formulated as

$$p(S_i|S_1, S_2, \ldots, S_{i-1}) = p(S_i|S_{i-1}) \tag{2.2.4}$$

where $p(a|b)$ is the conditional probability of a given b, S_i is the state at time i.

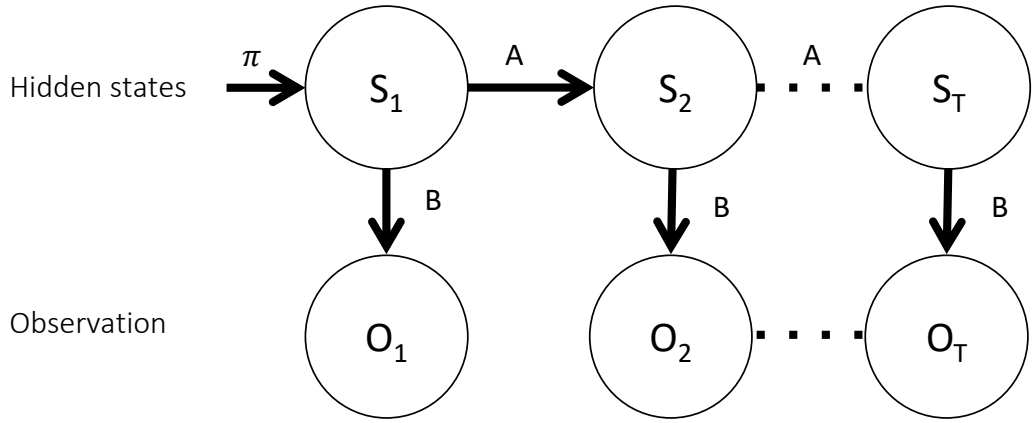

Figure 2-3: Typical hidden Markov structure.

Each observation is used to predict a sequence of states starting from an initial state. The prior probability of states given the previous posterior state probability is defined as the *state transition probabilities*. The probability of observations given the state is the *emission probability*. The notations used in the following text are defined as follows:

- N is the number of states, the individual states are denoted as $X = \{x_1, x_2, \ldots, x_N\}$, and the state at time t is denoted as S_t.
- A is the transition probability matrix, its element a_{ij} at row i and column j is the conditional probability $a_{ij} = p(S_{t+1} = x_i | S_t = x_j)$, where $1 \leq i, j \leq N$,
- O is the set of observations. Its elements v are possible continuous or discrete observations,
- B is the emission probability, i.e. the conditional probability of an observation v given a certain state x_i,
- π is the initial state probability vector. Its ith element is $\pi_i = p(S_1 = x_i)$, where $1 \leq i \leq N$.

A complete specification of an HMM requires specification of possible states S, possible observations O and three probabilities A, B, and π. Therefore, the complete parameter set of an HMM is $\lambda = (A, B, \pi)$.

In an HMM, the *prior probability* is defined as the probability of a state and the previous observations, i.e.,

$$\alpha(S_i = x) = p(O_1, \ldots, O_{i-1}, S_i = x). \tag{2.2.5}$$

The *posterior probability* is defined as the probability of a state and the previous and current observations, i.e.,

$$\beta(S_i = x) = p(O_1, \ldots, O_i, S_i = x) \tag{2.2.6}$$

which can be iteratively derived as

$$\begin{aligned}
\beta(S_i = x) &= p(O_1, \ldots, O_i, S_i = x) \\
&= \sum_{\kappa \in X} p(O_1, \ldots, O_i, S_i = x, S_{i-1} = \kappa) \\
&= \sum_{\kappa \in X} p(O_i, S_i = x | O_1, \ldots, O_{i-1}, S_{i-1} = \kappa) p(O_1, \ldots, O_{i-1}, S_{i-1} = \kappa) \\
&= \sum_{\kappa \in X} p(O_i, S_i = x | S_{i-1} = \kappa) p(O_1, \ldots, O_{i-1}, S_{i-1} = \kappa) \\
&= \sum_{\kappa \in X} p(O_i | S_i = x) p(S_i = x | S_{i-1} = \kappa) p(O_1, \ldots, O_{i-1}, S_{i-1} = \kappa) \\
&= \sum_{\kappa \in X} p(O_i | S_i = x) p(S_i = x | S_{i-1} = \kappa) \beta(S_{i-1} = \kappa)
\end{aligned} \tag{2.2.7}$$

where $p(O_i|S_i = x)$ is the emission probability, i.e., the probability that observation O_i happens given $S_i = x$, which can be obtained from the classification algorithms mentioned above; $p(S_i = x|S_{i-1} = \kappa)$ is the transition probability, i.e., the probability that the system state at time slice i is x given that the system state at time slice $i - 1$ is κ, which determines how "resistant" the algorithm is. A high transition probability of $p(S_i = x|S_{i-1} = x)$ suggests that a previous estimate is unlikely to change in the future and vice visa. The second line of (2.2.7) is the marginalization. The third line is the application of Bayes' rule. The fourth line is because O_i and S_i are independent of $O_1, \ldots, O_{i-1}$ given S_{i-1}. The fifth line is the application of Bayes' rule again and the last line is the iterative application of the definition of posterior probability.

Hidden Markov models can be used to predict future driving behavior for two reasons. First, driving maneuvers can be represented as the implementation of the driver's future plan on the tactical level [Mic85]. As this future behavior is a plan of the driver and cannot be observed directly, it has to be inferred from observable signals within the driver's current behavior and the environment in which the driver is operating. Many signals that describe how drivers influences vehicle dynamics, such as the steering wheel angle and velocity, are appropriate for making this observation [MS04]. Second, HMM supports recognition of temporal data patterns. This is important because humans perform different actions on different timescales. Even within a simple maneuver, internal states may vary over time. HMM provide an excellent framework for such temporal mappings. Thus, HMM is a good method to solve the driving behavior prediction problem.

Driver behavior can be successfully modeled with HMM by solving the following problems:

1. Given an observation sequence O and definition of states S, find the model $\lambda = (A, B, \pi)$ that maximizes the probability of O. This can be seen as training a model to best fit the observed data.
2. Given $\lambda = (A, B, \pi)$ and an observation sequence O, find an optimal state sequence for the underlying Markov process, i.e., to estimate the states of the HMM.

The conventional method for solving these two problems is as follows [Sta04]:

1. The solutions to Problem 1 can be used to obtain a specific HMM that represents driving

behavior at roundabouts. This is a model training process. The Baum-Welch algorithm can be used for parameter estimation based on the training set. In addition to the match between the HMM properties and the time series data, the expectation maximization (EM) algorithm provides an efficient class of training methods. Given plenty of data generated by some hidden power, a HMM architecture can be created and the EM algorithm can be used to find the best model parameters that maximize the likelihood of the observed training data.

2. The solution to Problem 2 can be used to estimate the driver's future behavior in new drives, which is an evaluation process. Two conventional methods to solve this problem are the Viterbi algorithm and the forward algorithm. The former finds the path in the state space with the maximum likelihood, whereas the latter chooses the state in every step to maximize the likelihood. For the considered problem, the two algorithms are equivalent. These methods allow a typical HMM to be determined, thus predicting future driver maneuver on the basis of the observations of driver behavior.

2.2.6 Summary

In summary, support vector machines, logistic regression, AdaBoost, and random forest algorithms have all proved to be effective for driver maneuver prediction. These four algorithms were tested in this work. In addition, complex algorithms that integrate these four algorithms and HMM were also developed in this work to improve the model's predictability, see the process of the model development in Chapter 4 and their predictive performance in Chapter 5.

2.3 Evaluation

A prediction method can be considered effective if its predictions are precise enough. An evaluation method is necessary to evaluate the precision of predictions, such as a confusion matrix [Pow11] or receiver operating characteristic (ROC) curve [Han98]. In the field of machine learning for binary classification, a confusion matrix is used to visualize the performance of an algorithm: Each row of the matrix represents the instances in a predicted class, whereas each column represents the instances in an actual class [Pow11]. The visualization allows to check whether the system is confusing two classes. The confusion matrix generates some widely-used scores to represent the proportion of target examples that are correctly or incorrectly predicted, such as accuracy, detection rate, false alarm rate, and F-measure. The performances of different models can be compared using a ROC curve [DT11].

The time lag or the distance lag of the prediction is also important to consider when evaluating a predictive model. As the time gets closer to maneuver execution, prediction performance generally increases. Some studies have been able to predict the maneuver just before it occurs [OYT04, GSBD06, KYSL00, Kru08], whereas others have been able to predict the maneuver at earlier times (e.g., several seconds before the maneuver) or some distance before the relevant intersection (e.g., 30 m before the intersection) [NMI+08, SH14, GJW+16, TMF16, TKG15,

PWK17].

2.4 Conclusion

The driving behavior data, algorithms, and evaluation methods found in the previous literature are summarized in Table 2-1. However, no study focusing on driver maneuver prediction at roundabouts is available. This thesis will fill this research gap.

Table 2-1: State of the art.

Study	Measure	Algorithm	Evaluation	Result
Taguchi et al. (2007) [TIS+07]	Ego car velocity, leading-car velocity, and the distance between the ego car and leading cars	Logistic regression	Detection rate	Detection rate of 80.0%
Naito et al. (2008) [NMI+08]	Accelerator throttle, brake, and velocity of the ego car	K-means	Accuracy	95.6% as early as 5 seconds before the intersections
Lefevre et al. (2011) [LIGL11, LLIG11]	Turn signal of the ego car and the information about the entry lanes	Bayesian network	Accuracy	100% approximately 10 m away from the exit of the intersection.
Sathyanaray-ana et al. (2012) [SSH12]	Velocity, steering wheel angle, engine RPM, and gas/brake pedal pressure information	SVM	Accuracy	Accuracy of 89%
Liebner et al. (2013) [LRKS13, LKB+13]	Ego car velocity	Intelligent driver model (IDM)	Detection rate	Detection rate of 95% Without traffic whereas 55% in the presence of preceding vehicles
Gadepally et al. (2014) [GKO14]	Velocity, position, and orientation of the ego car	HMM	Number of correct predictions	Correct recognition for 38 of the 40 observation sequences.
Streubel et al. (2014) [SH14]	Velocity, acceleration, and yaw value of ego car	HMM	Accuracy	Above 90% as early as 7 seconds before entering the intersections
Tang et al. (2015) [TKG15]	Position, velocity, acceleration, yaw value of the ego car and lane-level maps	SVM	accuracy	90% as early as 1.6 seconds before the intersection

Continued on next page

Table 2-1 – continued from previous page

Study	Measure	Algorithm	Evaluation	Result
Gross et al. (2016) [GJW+16]	Position, heading, acceleration, and velocity of the ego car	RF	Recall	76% at 30 m before the relevant intersection center
Tawari et al. (2016) [TMF16]	The information extracted from driver camera, scene camera, and navigation camera	RF	Accuracy	Over 80% 2 seconds before the maneuver event
Barbier et al. (2017) [BLSIG17]	Velocity, position, and heading of the ego car (20% of real driving data and 80% of data from simulated environment)	RF	Accuracy	Accuracy of 80.3%
Phillips et al. (2017) [PWK17]	Ego car velocity and acceleration, the lane-relative heading, the number of lanes, and the headway distance to the preceding vehicle	Recurrent Neural Networks (RNNs)	Accuracy	85% as early as 150 m before the intersection

3 Scenario Categorization Method

In this chapter, a scenario categorization method was developed to categorize any drive through a roundabout. The driver maneuver is both, a cause and a consequence of driving behavior, which can be used to predict the driver maneuver. However, drivers behave differently when driving through roundabouts with different geometric features. For this reason, it is important to eliminate the effect of geometric features on driving behavior. Otherwise, the driver maneuver can hardly be predicted effectively with the driving behavior. In this chapter, the relationships between driving behavior and the geometric features of roundabouts are described, achieving Contribution 1 presented in Chapter 1.4. The effects will then be used to propose a scenario categorization method that can categorize any drive through a roundabout. This finding is Contribution 3 presented in Chapter 1.4. In each category, the effect of the geometric features of roundabouts on driving behavior is eliminated, increasing the predictability of the driving behavior.

Two studies were conducted to identify the appropriate scenario categorization method and develop a model to predict driver maneuver with driving behavior data. These studies are described in detail in this chapter. First, a field study was conducted to gain an empirically well-founded understanding of driving behavior at roundabouts. Driving behavior data from participants were acquired in real driving environment as they drove through a track including three roundabouts with different geometric features. The limitations of the field study were that the driving behavior was mediated by uncontrolled factors related to surrounding traffic and that driving behavior data were only captured at three roundabouts. Thus, a simulator study was designed, taking the results of the field study into consideration. The simulator study was conducted in a laboratory in which the experimental conditions could be controlled and undesired disturbances could be eliminated. In the simulator study, driving behavior data from participants were acquired as they drove through tracks including roundabouts with controlled geometric features and a controlled traffic situation. On the basis of these two studies, a method of scenario categorization was proposed to make progress towards achieving the goal of developing the driver maneuver predictive model. This method can be used to propose the structure of the driver maneuver predictive model.

The relevant definitions used in this chapter are listed below:

- A driver maneuver is either exiting a roundabout via an oncoming exit or staying in the roundabout by following the circulating lane. The goal of this thesis is to predict the driver maneuver of exiting /staying in a roundabout in front of an oncoming roundabout exit.

- Driving behavior is the car status and driver actions in a driving task, such as turning the steering wheel turning and controlling velocity.

- Driving behavior data are the values of the driving behavior, i.e., data on the steering angle, steering angle velocity, velocity, acceleration, car yaw, driver gaze direction, and driver head direction.

- Entry-exit angle is the angle between the entry a driver takes to enter the roundabout and the exit she/he takes to exit the roundabout.
- The local extremum of steering angle θ_e is the value of the steering wheel rotation angle when the steering wheel is turned to leftmost.
- The integrated geometric feature Geo is a feature that integrates the information about the roundabout radius and the entry-exit angle.
- Geometric features of roundabouts is a general term for the features that can characterize roundabout layout geometry, such as radius, entry-exit angle, and the integrated geometric feature Geo.

3.1 Field Study

3.1.1 Method

The field study took place on a route leading through three roundabouts in the city of Braunschweig (Germany), see Figure 3-1 for details. Of the seven study participants, three were female and four male. Their age ranged from 22 to 33 years (M = 25.28, SD = 4.11). Each participant had at least one year of driving experience and drove more than 1000 km per year. They were paid 10 Euro per hour to participate in this study. During the drive, an experimenter instructed the participants which exit to choose in the roundabout. This assured that each participant drove through every combination of entries and exits. The order of roundabouts and exits were changed randomly across participants to eliminate potential effects of order on driving behavior.

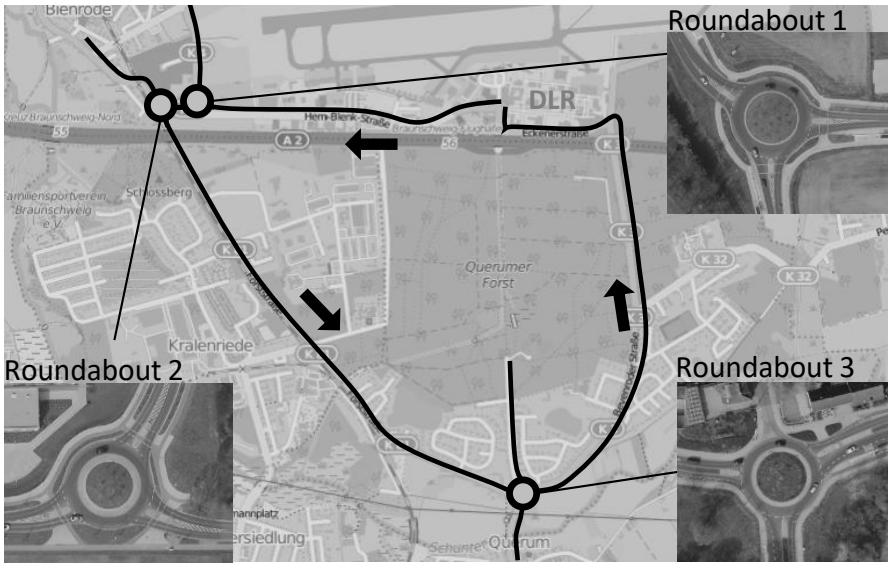

Figure 3-1: Driving route in the field study.

An experimental car was used for the study. It is an equipped research vehicle, dedicated to the

observation of driving behavior in real traffic. Using a logging frequency of 100 Hz, the following variables were recorded:

- Steering angle
- Steering angle velocity
- Acceleration
- Velocity
- Yaw
- GPS position

Further, information of the participants' gaze and head direction was obtained with an eye-tracking system using a logging frequency of 120 Hz. Therefore, the participants' naturalistic driving behavior data including car state and human gaze and head direction were acquired. The driving behavior data were contained in 1239 drives generated by all participants when they drove through each combination of entries and exits of the three roundabouts.

3.1.2 Data Selection

The driving behavior data regarding the driver maneuvers lie in the path covered by the vehicle. Trivially, a driver taking the first exit of a three-exit roundabout produced a different path than a driver exiting the roundabout at the third exit. As Figure 3-2 (a) shows, there are three different possible drives when a driver drove through a roundabout. The blue path leads the vehicle out of the first exit, the red one out of the second, and the yellow one out of the third exit. This consideration was used to filter the relevant observations from the recorded data. To filter for data in which the driver potentially took the first exit, the observations positioned between the entry and the first exit were selected. To filter for data in which the driver potentially took the second exit, the observations positioned between the first and the second exit were selected. GPS data were used as a filter criterion, see the yellow zones in Figure 3-2. Data falling into the yellow zone depicted in Figure 3-2 (b) were considered relevant for the driver maneuver regarding the first exit, whereas data located within the yellow zone in panel (c) were considered relevant for the driver maneuver regarding the second exit. The panels (d) and (e) show the result of the data filtering. These data were used for analyzing and modeling: The data falling in panel (d) were used to predict whether or not drivers will leave the roundabout at the first exit, whereas data from panel (e) were used to predict whether or not drivers will leave at the second exit.

The observations selected by the GPS data-based filter criterion contained errors because the GPS data contained measurement errors due to GPS signal multi-paths, signal reflections from buildings and trees, or a low number of GPS satellites in a line-of-sight to the antenna. Figure 3-3 depicts a typical erroneous observation at a roundabout: The solid red line denotes a drive

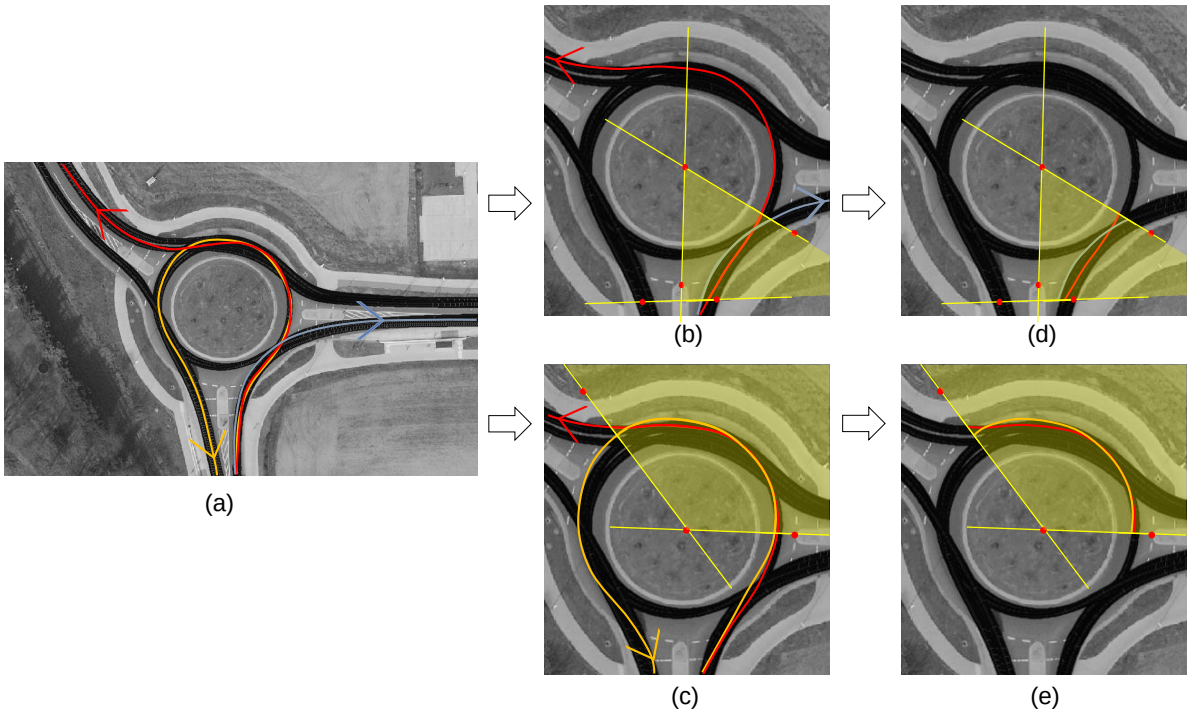

Figure 3-2: Selection of relevant data.

from the entry to the exit of the roundabout. From the shape of the line, it can be determined that the car's actual position was at the position of the dashed red line, i.e., the driving behavior data were actually related to the position of the dashed line. Hence, the information could not be used to predict the driver maneuver at the position where it appeared to be. Therefore, the observations with error needed to be excluded.

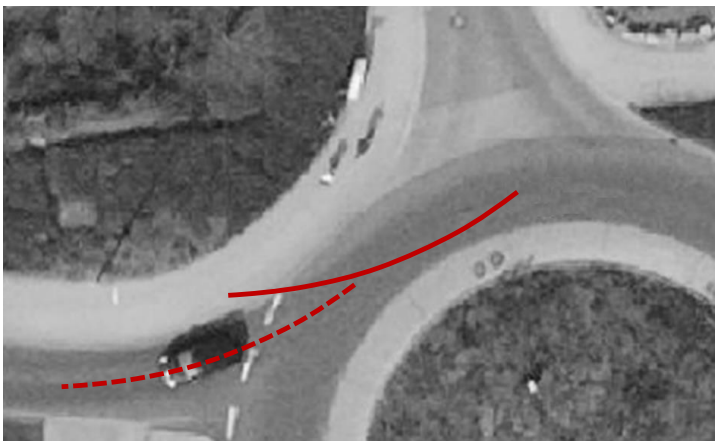

Figure 3-3: A typical erroneous observation at a roundabout.

Measurement errors also led to incorrect yaw values. Due to all paths being on the same roundabout with the same curvature, the yaw of correct measurements hardly varied, whereas the yaw of erroneous measurements varied markedly from the correct ones. Thus, the first yaw value and the last yaw value for each drive were checked to detect whether they contained an error. Figure 3-4 shows the direction of the first and the last yaw values of two drives with four arrows: Two black arrows denote the first yaw value and the last yaw value for a drive with correct measurement, that is denoted by a black line. Two red arrows denote the first

yaw value and the last yaw value for a drive with erroneous measurement, denoted by a red line. It can be observed that the first and the last yaw values of these two drives are different. Hence, drives with erroneous measurements can be detected by comparing the first and last yaw values with those of the correct observation. In this study, the median of the first/last yaw values over all drives was considered as the value for a standard correct drive. Therefore, only the observations whose first/last yaw values were within a 15° deviation from the median were considered acceptable for analysis, whereas observations outside this 30° range were considered errors and were excluded. To further illustrate this, the first and last yaw values for 22 drives are depicted in Figure 3-5 (a) and (b) respectively. These drives were all between the same entry and exit of a roundabout. The solid lines in the figure represent the median values, whereas the dashed lines mark the 30° borders. Most values fall into the range of 30° although five of the first yaw values and five of the last yaw values fall outside this range. These ten drives are shown in Figure 3-6: The drives denoted in blue were detected by checking the first yaw values, those denoted in yellow were detected by checking the last values, and the drive denoted in pink was detected by both. These drives were positioned either off the road or on an unrealistic driving track, validating the procedure of selecting erroneous GPS values via the first/last yaw angle outliers. Out of 1239 drives, 178 drives with measurement errors were excluded.

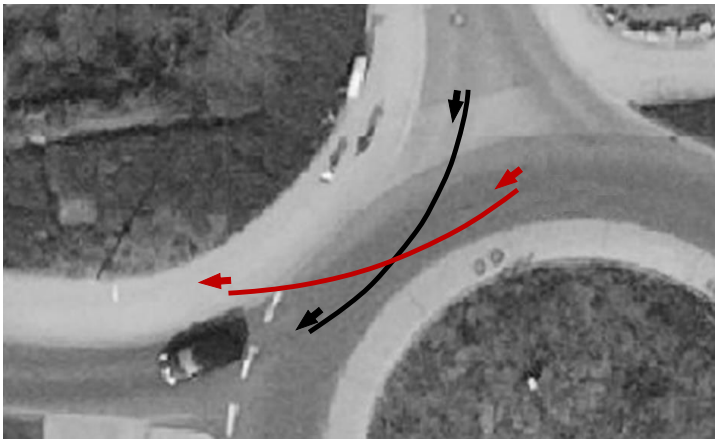

Figure 3-4: Direction of the first and the last yaw vectors of two drives.

3.1.3 Summary

A field study was conducted to acquire naturalistic driving behavior data on a route that included three roundabouts. GPS data were used as a filter criterion to select the driving behavior data relevant to the research objective of driver maneuver prediction. Furthermore, data with measurement errors were excluded by defining an acceptable range of yaw values. After all this, the driving behavior data were ready for the next step: identifying an approach to categorize the scenarios of these three roundabouts (see next section).

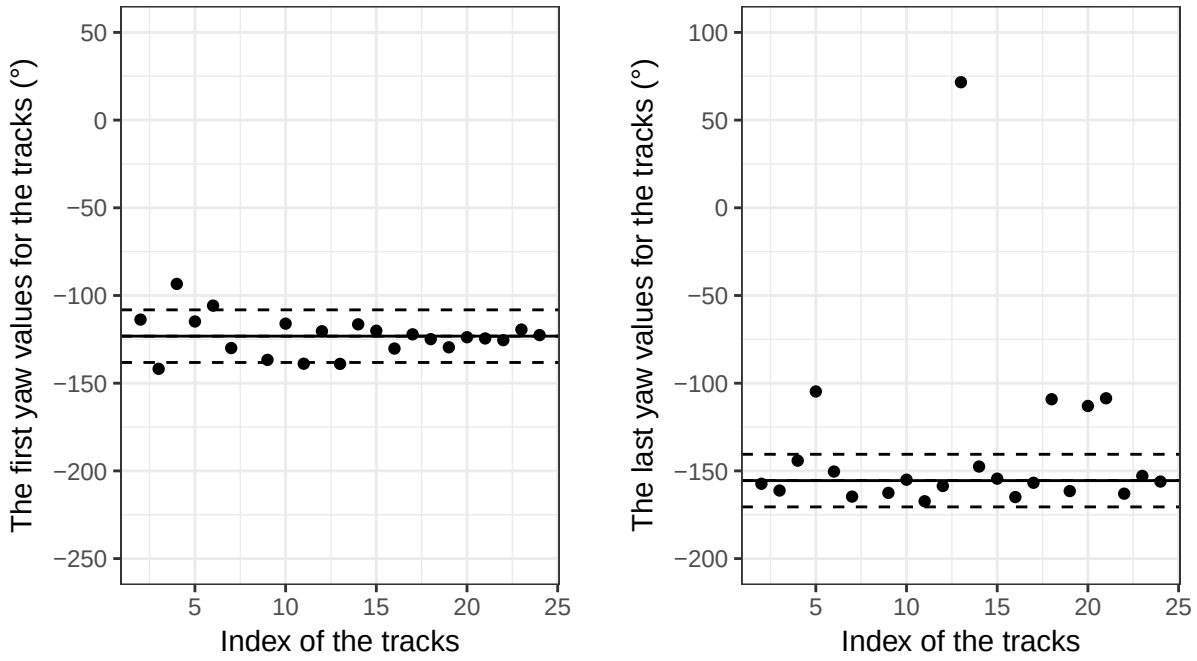

(a) Checking the first yaw values.

(b) Checking the last yaw values.

Figure 3-5: Checking the first/last yaw values to detect the drives with measurement errors.

Figure 3-6: Drives with measurement errors detected by checking the first/last yaw values.

3.2 Approach to Scenario Categorization

Scenario categorization is crucial to eliminating the effects of geometric features of roundabouts on driving behavior. Because the driving behavior data that are used to predict driver maneuvers certainly depend on these geometric features, scenario categorization enables driver maneuvers to be better predicted. In this subsection, an approach for scenario categorization was developed on the basis of an analysis of driving behavior.

3.2.1 An Approach to Scenario Categorization

Steering angle and steering angle velocity were assumed to be effective variables for predicting driver maneuvers for the following reasons:

- The steering angle and steering angle velocity vary only with driving direction, and driving direction is directly related to the driver maneuver of exiting/staying in a roundabout.
- The yaw value varies with roundabout entry positions.
- The speed and acceleration are strongly affected by surrounding traffic.

Thus, scenario categorization approach was proposed to eliminate the effect of the geometric features of roundabouts on steering wheel position when using it to predict the driver maneuver.

Participants' driving behavior data for the same time slice were hardly at the same position because each participant drove through the roundabout at a different speeds. Thus, to analyze steering wheel information from all participants at the same position, the data on steering angle and steering angle velocity were mapped from a time line with 0.02 s intervals to a distance line with 0.5 m intervals using interpolation. The origin of the distance line for each drive was the first point of the drive that was intercepted by the filter criterion. Analyzing the steering angles for all participants revealed that the steering wheel had different motion patterns when they drove through roundabouts with different entry-exit angles, even though the driver maneuvers at these roundabouts were the same. For example, Figure 3-7 shows the driver maneuver of taking the first exit: When the entry-exit angle was relatively small (see Figure 3-7 (a)), the steering angle was always smaller than 0°, i.e., the drivers kept the steering wheel at a right position when entering and exiting the roundabout. In contrast, when the entry-exit angle was large (see Figure 3-7 (b)), the steering angle was smaller than 0° at the beginning, then larger than 0°, and finally smaller than 0° again, i.e., the drivers kept the steering wheel at a right position to enter the roundabout, then at a left position to follow the roundabout, and finally at a right position to exit the roundabout. Yet another steering wheel pattern was observed when the drivers took the non-first exit, as shown in Figure 3-8: The steering angle was larger than 0° at the beginning and then smaller than 0° at the end, i.e., the drivers kept the steering wheel at a left position to follow the roundabout and then at a right position to exit the roundabout. The drivers did not steer to the right at the beginning of the analysis because they were already in the roundabout. Drawing upon these findings, three scenarios were categorized on the basis

of the relationship between the steering wheel motion pattern and the entry-exit angle:

- In Scenario 1, drivers tended to keep steering to the right when they drove through the roundabout. This was the case when the entry-exit angle was less than 110° and the entry and exist were adjacent to each other.
- In Scenario 2, drivers tended to first steer to the right to enter the roundabout, then steered to the left to follow it, and finally turned to the right to leave it. This was the case when the entry-exit angle was larger than 110° and the entry and exit were adjacent to each other.
- In Scenario 3, drivers tended to steer to the left to follow the roundabout, and steer to the right to exit. This was the case when the entry and exit were not adjacent to each other.

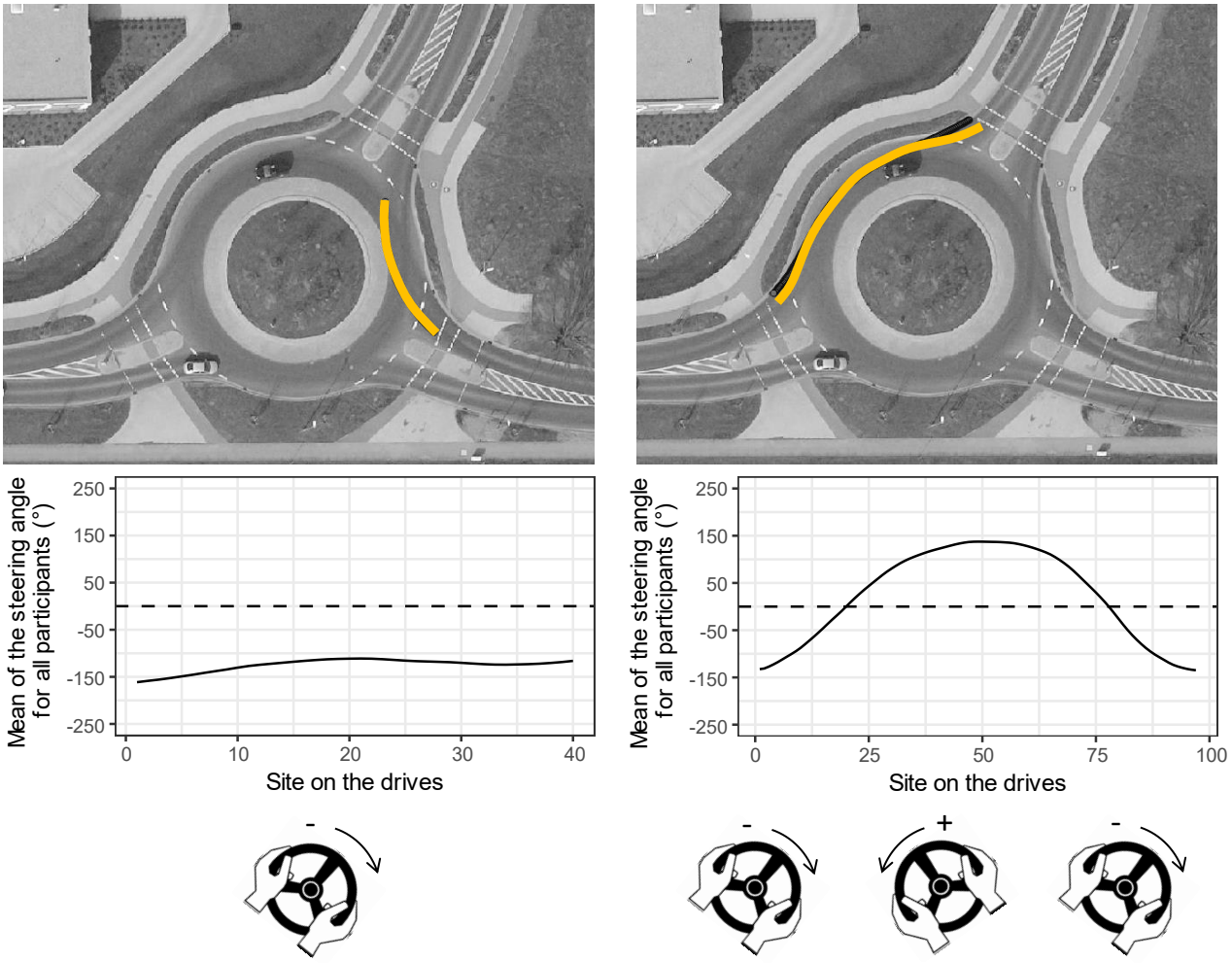

(a) Steering status when the entry-exit angle was small. **(b)** Steering status when the entry-exit angle was large.

Figure 3-7: Steering wheel information for the maneuver exiting through the first exit.

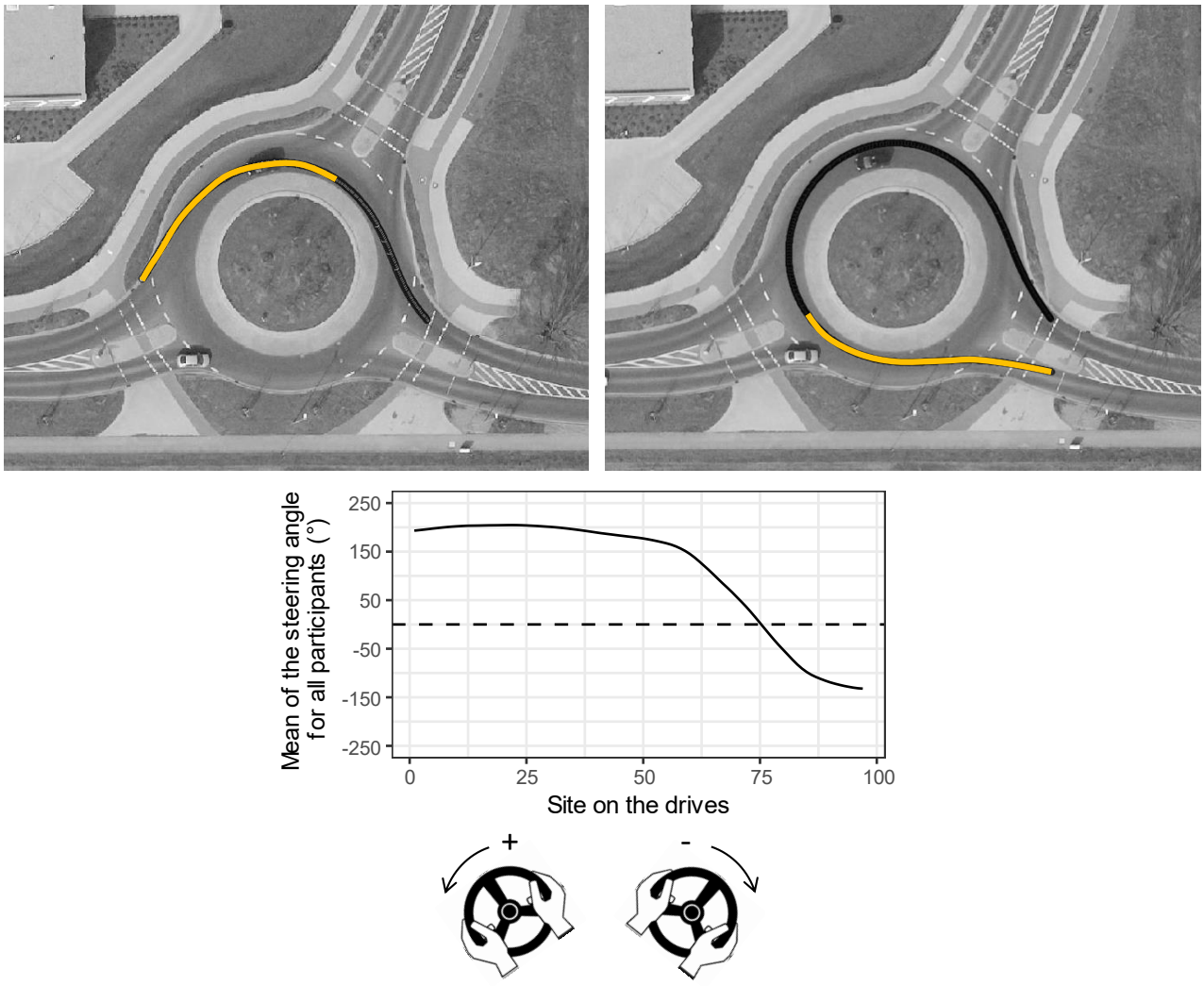

Figure 3-8: Steering wheel information for the maneuver exiting through the non-first exit.

3.2.2 Evaluation of the Approach to Scenario Categorization

A model consisting of three sub-models was developed to predict driver maneuvers in three scenarios (sub-model for Scenario 1, sub-model for Scenario 2, and sub-model for Scenario 3 respectively) and evaluate the approach to scenario categorization. For instance, when a driver enters a roundabout, either the sub-model for Scenario 1 or sub-model for Scenario 2 (the choice depends on the entry-exit angle) can be used to predict whether or not the driver will take the first exit to leave the roundabout. If the answer is no, then the sub-model for Scenario 3 is used to predict whether the driver will leave the roundabout at each of the next exits. Each sub-model consists of a series of "classifiers" corresponding to a series of "prediction sites". The "prediction sites" are the locations where predictions being made in the scenario. There were 11 prediction sites for each scenario, evenly dividing the drives into 10 parts. The driving behavior data for all drives from participants at each prediction site were clustered to train the classifiers. One classifier was trained for each prediction site. The classifiers classified the driving behavior data for two driver maneuvers at each prediction site. Support Vector Machine has been proven to be an effective and robust method for binary classification problems, see Chapter 2. Thus, SVM was used to develop the classifiers for each sub-model.

A four-step procedure was executed for classifier training [ZKJ+17]:

- Step 1: Feature extraction. Two features were extracted from the steering angle and steering angle velocity at each prediction site.
- Step 2: Scaling the features. Both features were scaled to the range [-1, 1] to avoid having variables with larger ranges dominate those with smaller ranges [HL02].
- Step 3: Splitting the scaled data. The scaled data were split into a training data set (80%) and a test data set (20%). These numbers were selected to assure that there were enough data to both train and test the model. There were 849 cases in the training data set for the three scenarios and 212 the cases in test data set.
- Step 4: Applying cross validation. Five-fold cross-validation was applied to train and test the SVM classifiers.

This four-step procedure was applied at each prediction site for each scenario, and one SVM classifier was trained to make the prediction at each prediction site.

Afterwards, the prediction accuracies of the classifiers were used to evaluate the effectiveness of the model that was developed using the scenario categorization approach, the steering angle and the steering angle velocity, and the SVM. The prediction accuracy was defined as the ratio between the number of instances correctly classified and the number of instances presented in the test data set to measure the performances of the sub-models. Its mathematical expression is

$$ACC = (TP + TN)/(P + N) \tag{3.2.1}$$

where P (Positive) was defined as the number of exiting maneuver samples in the test data set, N (Negative) was defined as the number of staying maneuver samples in the test data set, TP (True positive) was defined as the number of the samples that were correctly detected as exiting maneuvers (the exiting maneuver samples were labeled as "Exiting"), and TN (True negative) was defined as the number of the samples that were correctly detected as staying maneuvers (the staying maneuver samples were labeled as "Staying"). The prediction accuracy at each prediction site was calculated. The distance from each prediction site to the oncoming exit was also calculated, meaning that the relative position of the prediction site was known. Finally, the first prediction site where the prediction accuracy was above 95% and its distance to the exit was identified.

The results are visualized in Figures 3-9 for the three scenarios:

- Scenario 1: Prediction accuracy increased as the prediction site got closer to the exit. It reached 98.1% at Prediction Site 4 at a distance of 13.8 m before the exit (see Figure 3-9 (a)).
- Scenario 2: Prediction accuracy increased as the prediction site got closer to the exit. It reached 97.4% at Prediction Site 7 at a distance of 11.4 m before the exit (see Figure 3-9 (b)).

- Scenario 3: Prediction accuracy increased as the prediction site got closer to the exit. It reached 98.5% at Prediction Site 6 at a distance of 14.1 m before the exit (see Figure 3-9 (c)).

This level of prediction accuracy is promising: Future behavior could be predicted with a high level of accuracy (larger than 95%) at a distance of approximately 11 m (about 2 seconds) before the exit. These results proved that 1) the selected scenario categorization approach effectively predicts driver maneuvers for driver maneuver predictive at the investigated roundabouts, 2) the steering angle and steering angle velocity provide important information for driver maneuver prediction and the predictability increases as the prediction site gets closer to the exit, and 3) SVM successfully predicts driver maneuvers by classifying the data for the exiting maneuver and the staying maneuver. The linear kernel for SVM with C = 100 performed best. The classification process for each site required 0.01 s [ZKJ+17].

3.2.3 Summary

In this section, a scenario categorization approach for the three investigated roundabouts was proposed. This approach categorized the scenarios into three classes. Subsequently, three sub-models were developed using SVM for these three scenario categories to predict driver maneuvers. The results proved that the selected scenario categorization approach, the steering angle and the steering angle velocity as prediction features, and SVM as the classification algorithm, effectively predict driver maneuvers at the investigated roundabouts. One limitation of this approach is that it may only work for the investigated roundabouts. Another limitation is that surrounding traffic is not controlled for in the field study. Thus, a simulator study was conducted to generalize the approach to generic roundabouts and develop a model that can predict driver maneuvers in generic situations, which is introduced in the next section.

3.3 Simulator Study

3.3.1 Simulator Study Design

The objective of the simulator study was to generalize the scenario categorization method to generic roundabouts and then develop a model to predict driver maneuvers in generic roundabouts with different geometric features and in different traffic situations. Three research questions were pursued to reach these objective:

- Question 1: What is the quantitative relationship between driving behavior and the geometric features of generic roundabouts? In the field study, this relationship was investigated for three specific roundabouts. The quantitative relationship between driving behavior and the geometric features of generic roundabouts needs to be investigated in order to more precisely handle a more generic situation.

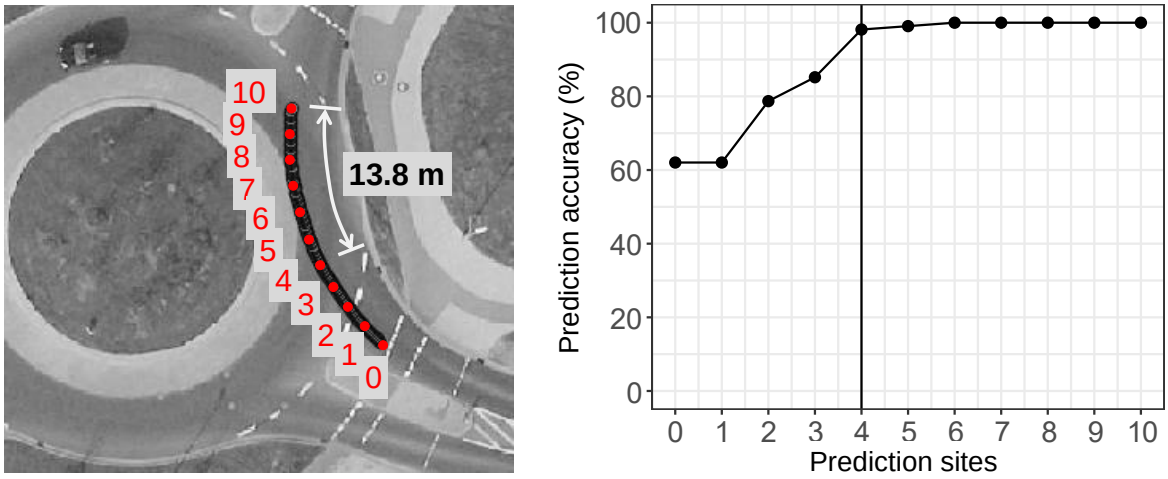

(a) Prediction sites and accuracies for Scenario 1.

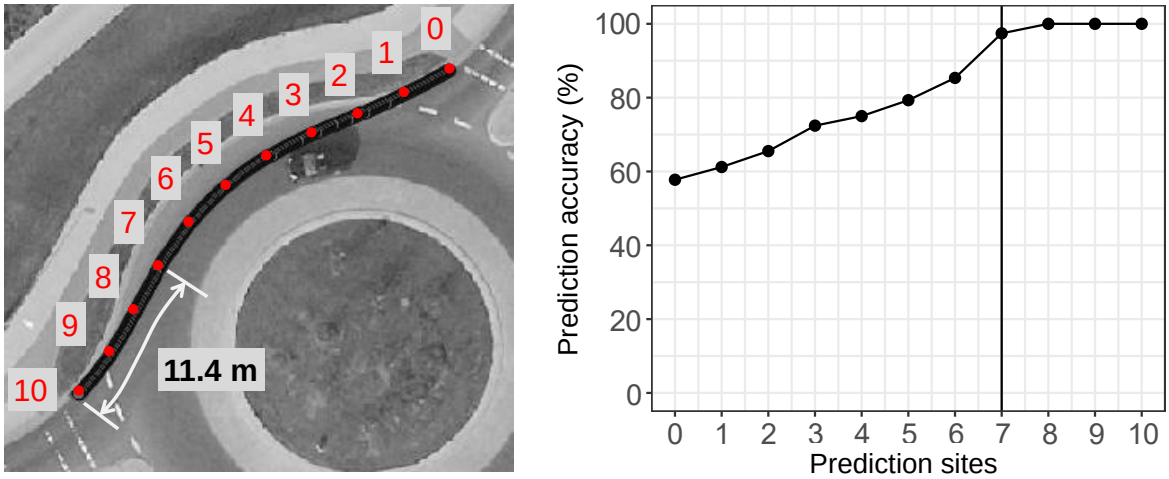

(b) Prediction sites and accuracies for Scenario 2.

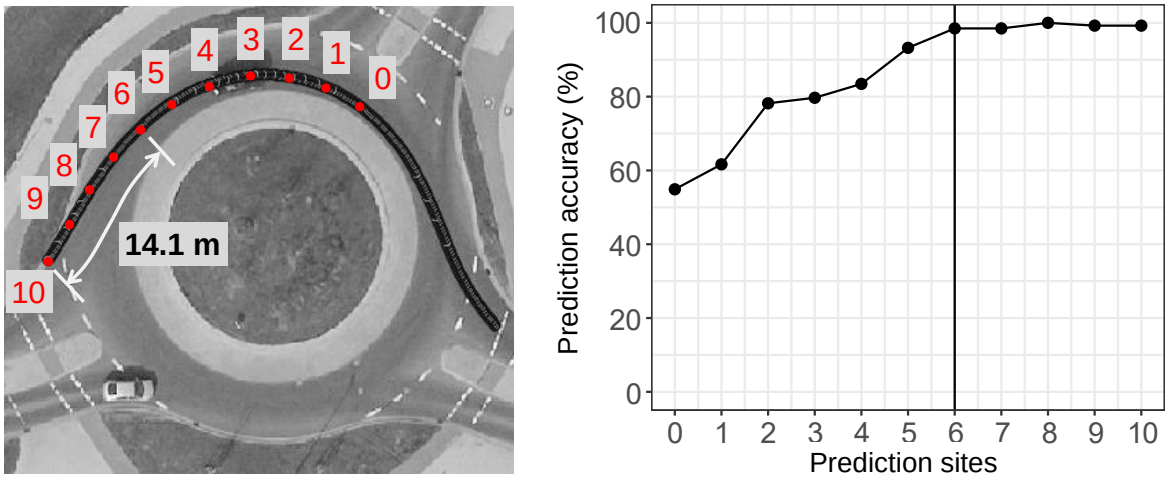

(c) Prediction sites and accuracies for Scenario 3.

Figure 3-9: Prediction sites and accuracies for three scenarios.

- Question 2: What driving behavior and what algorithms are effective in developing a model to predict driver maneuvers in generic roundabouts?
- Question 3: Is the model still effective when there are surrounding cyclists that affect driving behavior?

A simulator study was conducted to answer these three questions. The study was split into two sessions. These two sessions were designed with different settings to address the different questions. The details of the sessions are as follows.

Session 1: Tracks with Systematically Varied Roundabout Radius and Entry-exit Angles

The objectives of Session 1 were:

- To identify the quantitative relationship between driving behavior and geometric features for generic roundabouts, which can be used to propose scenario categorization method. This objective addressed Question 1.
- To develop a model to predict driver maneuvers using the driving behavior acquired from this session. This objective addressed Question 2.

These objectives were achieved by analyzing driving behavior at roundabouts with different geometric features. The two most important geometric features for roundabout layout design, *radius* and *entry-exit angle*, were used as independent variables related to roundabout design in Session 1. The *radius* had two levels, 13 m and 20 m. These values were selected because road design standards in Germany [Hof14] indicate that compact single-lane roundabouts have a radius between 13 and 20 m. Roundabouts with a radius outside this range are not the focus of this study. The *entry-exit angle* had seven levels: 90°, 120°, 150°, 180°, 210°, 240° and 270° (see Figure 3-10). These values were selected because a test drive showed that an angle smaller than 90° made turning very difficult and an angle larger than 270° no longer caused behavioral changes. The resulting 14 roundabouts (seven levels of *entry-exit angle* and two levels of *radius*) were then connected in random order to form two tracks (see Figure 3-11) (a) and (b), so that all roundabouts with 7×2 factor combinations were tested. There was no surrounding traffic on these two tracks because the factor of surrounding traffic should be eliminated when investigating the relationship between driving behavior and the geometric features of roundabouts.

Session 2: Tracks with Systematically Varied Position of Surrounding Traffic

The objective of Session 2 was to evaluate the predictability of the model for the scenario with surrounding traffic. This addressed Question 3 and the answer is presented in Chapter 6. In this session, surrounding cyclists were placed at or near roundabouts to affect the participants' driving behavior as they drove though the roundabouts [ZKS+17].

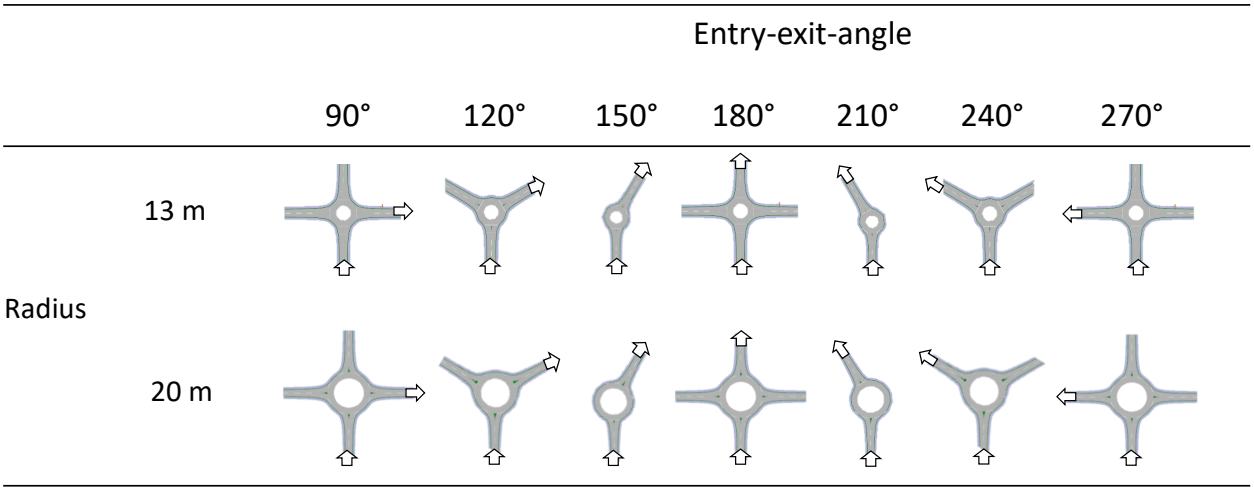

Figure 3-10: Fourteen roundabouts with different radii and entry-exit angles.

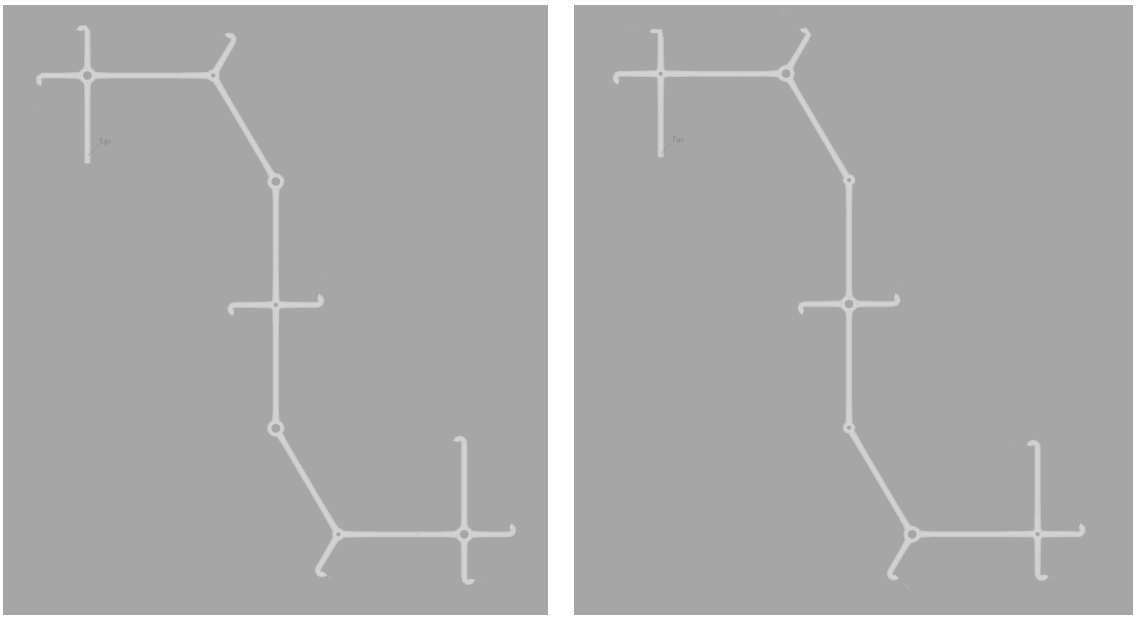

(a) **(b)**

Figure 3-11: Simulation tracks for Session 1.

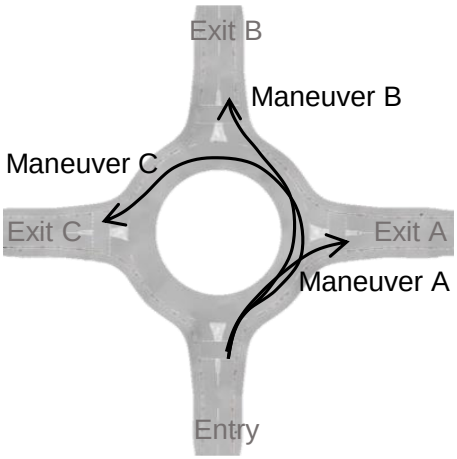

Figure 3-12: Three driver maneuvers at the roundabout.

Three possible driver maneuvers at a four-arm roundabout were investigated in this session (see the three black lines in Figure 3-12): Maneuver A was to leave the roundabout at Exit A, Maneuver B was to leave the roundabout at Exit B, and Maneuver C was to leave the roundabout at Exit C. Two types of driving pattern recognition had to be performed to predict driver maneuvers at these roundabouts: the recognition of Maneuver A and B and the recognition of Maneuver B and C. Three racing cyclists with a constant speed of 6 m/s were designed to move along different tracks in order to see how they affected these two driving pattern recognitions:

- The cyclists entered the roundabout at Exit C and exited at Exit B (see the blue dashed line in Figure 3-13 (a)). This setting allowed the impact of the cyclists on the recognition of Maneuver A and Maneuver B (yellow solid lines) to be investigated. This cyclist setting was named *Traffic 1*.

- The cyclists entered the roundabout at entry* and exited at Exit B (see the green dashed line in Figure 3-13 (b)). This setting allowed the impact of the cyclists on the recognition of Maneuver A and Maneuver B (yellow solid lines) to be investigated. This cyclist setting was named *Traffic 2*.

- The cyclists entered the roundabout at Exit A and exited at Exit C (see the red dashed line in Figure 3-13 (c)). This setting allowed the impact of the cyclists on the recognition of Maneuver B and Maneuver C (yellow solid lines) to be investigated. This cyclist setting was named *Traffic 3*.

- The cyclists entered the roundabout at entry* and exited at Exit C (see the dark grey dashed line in Figure 3-13 (d)). This setting allowed the impact of the cyclists on the recognition of Maneuver B and Maneuver C (yellow solid lines) to be investigated. This cyclist setting was named *Traffic 4*.

Participants drove through two tracks produced from fourteen roundabouts, see Figure 3-14. Eight of these roundabouts resulted from a combination of the four types of cyclist tracks with the two pairs of driver maneuvers. At the remaining six roundabouts, either no traffic was present, or other cars were placed randomly as “distractor vehicles" to lower the scenarios’

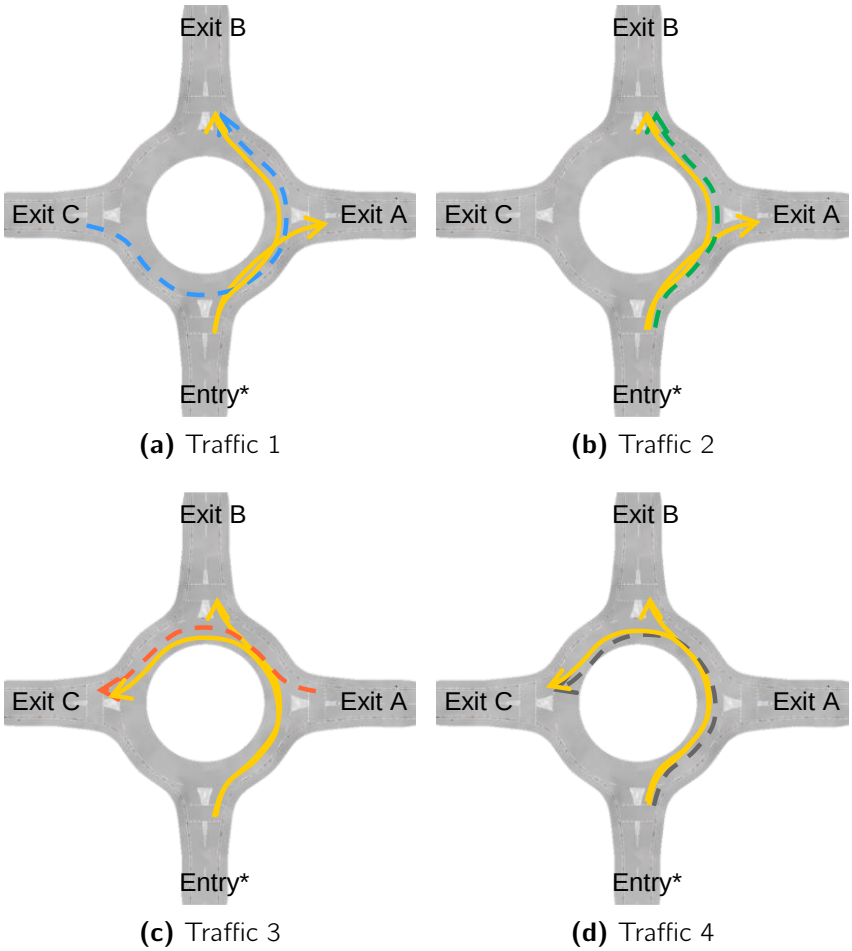

(a) Traffic 1 **(b)** Traffic 2

(c) Traffic 3 **(d)** Traffic 4

Figure 3-13: Scenarios with different cyclist tracks.

predictability for participants. On these two tracks, the 14 roundabouts were connected in a random order.

3.3.2 Data Acquisition

The study was executed in a simulator at the German Aerospace Center in Braunschweig. This simulator uses a complete vehicle mock-up which is implemented in a capsule with a visualization system. The visualization system enables a full view to the front and both sides, as well as a partial rear view (270°×40°). An eye-tracking system was implemented in the mock-up to obtain the data on participants' head direction and gaze direction. Four eye-tracking cameras were distributed at the left window, frontal window, and right window to obtain eye and head information from different perspectives (see Fig. 3-15).

Thirteen participants (three females and ten males) drove through each of the four tracks in the simulator. Their age ranged from 22 to 33 years (M = 27.8, SD = 6.4). Each participant had at least one year of driving experience and drove more than 1000 km per year. They were paid 10 Euro per hour to participate in this study. When the participants approached each roundabout, text instructions appeared on the screen informing them which exit they should

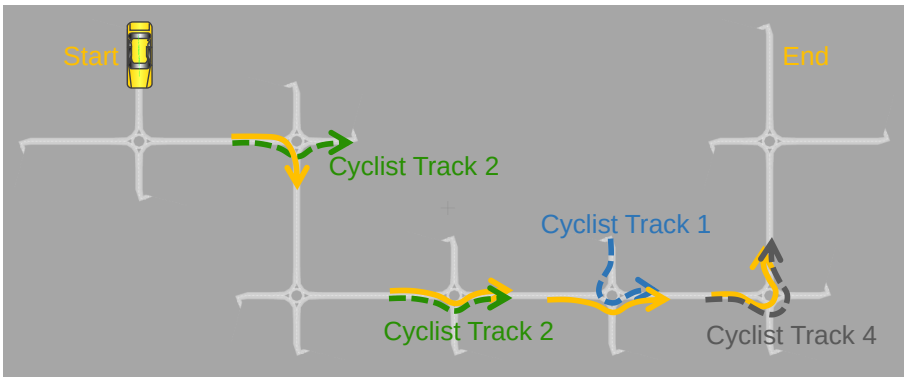

(a)

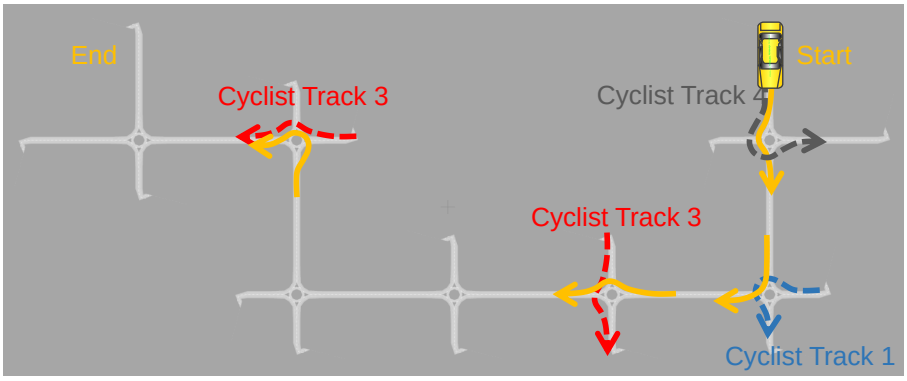

(b)

Figure 3-14: Simulation tracks for Session 2.

take, see Figure 3-16 (a), and the same information appeared again on a white sign when the participants were in front of the exit, see Figure 3-16 (b). At the end of the tracks, the participants were instructed to stop and take a break.

A within-subject design was applied in these two sessions, meaning that the same group of participants drove all tracks. In this case, variance related to the participants (e.g., due to gender and driving skills) could be eliminated statistically [CGK12]. The following variables were recorded during the two sessions with a logging frequency of 20 Hz:

- Steering angle
- Steering angle velocity
- Acceleration
- Velocity
- Position

Furthermore, information of participants' gaze direction and head motion was obtained with the eye-tracking system with a logging frequency of 120 Hz. The simulator study lasted 1.5 hours for each participant because test drives showed that driving on the tracks for longer than 1.5 hours causes simulator sickness for many people. During the 1.5 h, 39 drives were acquired for each combination of two radius values and seven entry-exit angle values, and other 39 drives for

Figure 3-15: Four cameras of the eye tracking system.

each combination of cyclist tracks and car driving directions.

3.3.3 Data Pre-processing

The acquired driving data were pre-processed using a filter criterion, which was a circle whose radius was 30 m larger than the roundabout's radius. Data outside of this range were disregarded for the purpose of the present work. The value of 30 m was large enough to guarantee that relevant data were not excluded. Then, the car position data for all drives were moved and rotated so that all drives had the same entry of the same roundabout (see the drives selected by the dashed circle and located on one roundabout in Figure 3-17). Afterwards, the eye-tracking data were sampled at 20 Hz, the same frequency as the driving data. The data were then ready for driving behavior analysis.

3.3.4 Summary

A simulator study was designed and conducted to achieve the goal of proposing a scenario categorization method for generic roundabouts and then developing an effective model to predict driver maneuvers. In the simulator study, information on participants' driving behavior was acquired as they drove through tracks with systematically varied roundabout geometric features and systematically varied surrounding traffic position. The position data were used as a filter criterion to select the driving data relevant to the research questions. The driving behavior data were then ready to be analyzed to answer the research questions. The answer to Question 1 is presented in the next chapter. The answers to Question 2 and Question 3 are presented in Chapter 5.1 and Chapter 5.2 respectively.

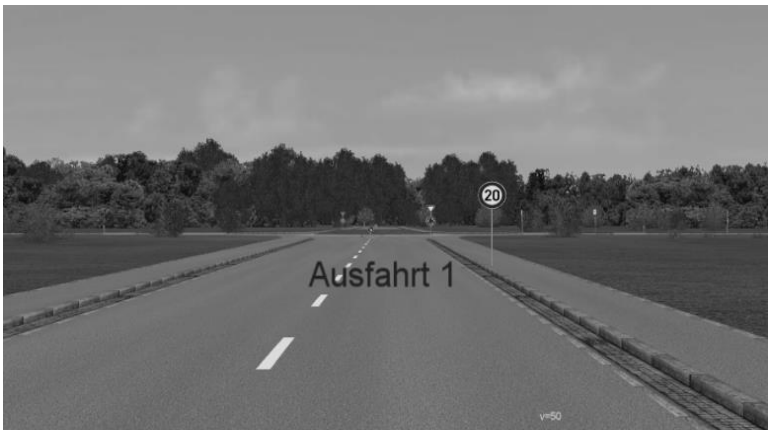

(a) Information on the screen ("Ausfahrt" means "exit" in German).

(b) Information on the sign ("Ausfahrt" means "exit" in German).

Figure 3-16: Information for the exit that the participants should take.

3.4 Method of Scenario Categorization

3.4.1 Steering Wheel Status and Geometric Features of Roundabouts

A scenario categorization method for generic roundabouts was specified on the basis of the simulator study. The method derived from the simulator study had two advantages compared to the approach based on the relationship between the steering wheel turning direction and the entry-exit angle: (1) it was effective for generic roundabouts rather than only the specifically investigated roundabouts, and (2) it was more precise. These advantages were achieved by applying the following techniques:

- A quantitative term for the local extremum of the steering angle (θ_e) was used to characterize steering wheel information, rather than the steering wheel turning direction used in the approach derived from the field study.
- A term for the integrated geometric feature (Geo) was used to integrate information about a roundabout's entry-exit angle and radius, instead of the entry-exit angle used in the approach derived from the field study.

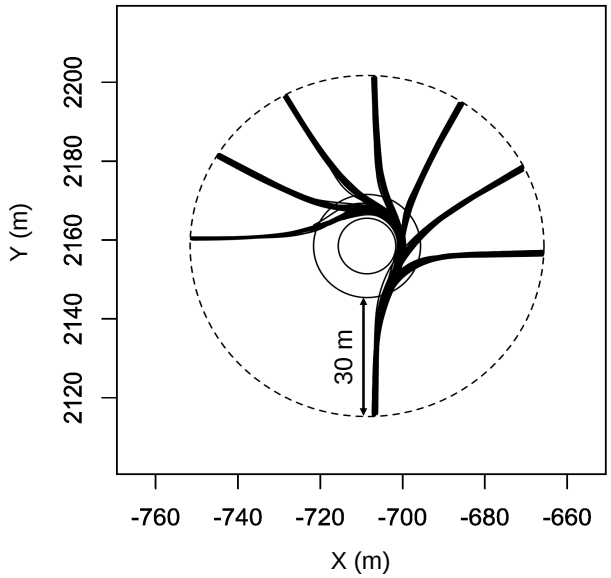

Figure 3-17: Data selection with dashed circle.

- The mathematical correlation between θ_e and Geo was calculated to explain the relationship between steering wheel information and the geometric features of roundabouts in a quantitative way.

Definition of the Local Extremum of the Steering Angle

The local extremum of the steering angle was defined as the steering wheel rotation angle when the steering wheel was turned to its leftmost point during driving through roundabouts. To analyze all participants' steering behavior at the same position of the roundabouts, the driving behavior data were mapped from a time line with 0.05 s intervals to a distance line with 0.5 m intervals via interpolation. The origin of the distance lines was the first point of a given drive that was intercepted by the filter circle. Then, the mean value of the steering angle over all participants was calculated along the distance line for each of the 14 roundabouts in Session 1 of the simulator study. Figure 3-18 (a) presents the mean values for the roundabouts with a radius of 13 m and entry-exit angles of 90°, 120°, 150°, 180°, 210°, 240° and 270°. Figure 3-18 (b) presents the mean values for the roundabouts with a radius of 20 m and entry-exit angles of 90°, 120°, 150°, 180°, 210°, 240° and 270°. The x-axis denotes the distance from the investigated point of the drive to the first point of the drive. Values less than zero mean that the steering wheel was at a right position, and vice versa. Different steering wheel turning patterns were apparent for the drives through different roundabouts:

- For the drives through roundabouts with a 13 m radius and 90° entry-exit angle, the steering wheel had three movement processes:
  - First, moving to the right to enter the roundabouts
  - Then, staying right to leave the roundabouts

  - Last, moving to the middle to drive straight

  Therefore, there is a local minimum of the steering angle in the middle of the drive, see the orange line in Figure 3-18 (a).

- For the other thirteen drives, the steering wheel had four movement processes:
  - First, moving to the right to enter the roundabouts
  - Then, moving to the left to follow the roundabouts
  - Then, moving to the right to leave the roundabouts
  - Last, moving to the middle to drive straight

  Therefore, there is a local maximum value of the steering angle in the middle of these drives, see the other six colored lines in Figure 3-18 (a) and all lines in Figure 3-18 (b).

These local minima or maxima of the steering angle were generated when the steering wheel is turned to its leftmost position during driving through roundabouts. The values were defined as the local extremum of steering angle θ_e.

Definition of the Integrated Geometric Feature

A variable that characterized the geometric features of a given roundabout was defined as the integrated geometric feature

$$Geo = \varphi^2 \cdot r, \tag{3.4.1}$$

where Geo is the integrated geometric feature, φ is the entry-exit angle, and r is the roundabout radius.

Correlation between the Local Extremum of the Steering Angle and the Integrated Geometric Feature

A quantitative relationship between the local extremum of the steering angle θ_e and the integrated geometric feature Geo was investigated via a regression analysis. The correlation was

when $Geo \leq 137.08 \ \ \mathrm{rad}^2 \cdot \mathrm{m}$,

$$\theta_e = 3.68 \cdot \log(Geo) - 15.44, \tag{3.4.2}$$

and when $Geo > 137.08 \ \ \mathrm{rad}^2 \cdot \mathrm{m}$,

$$1.75 \ \mathrm{rad} < \theta_e < 5.75 \ \mathrm{rad}, \tag{3.4.3}$$

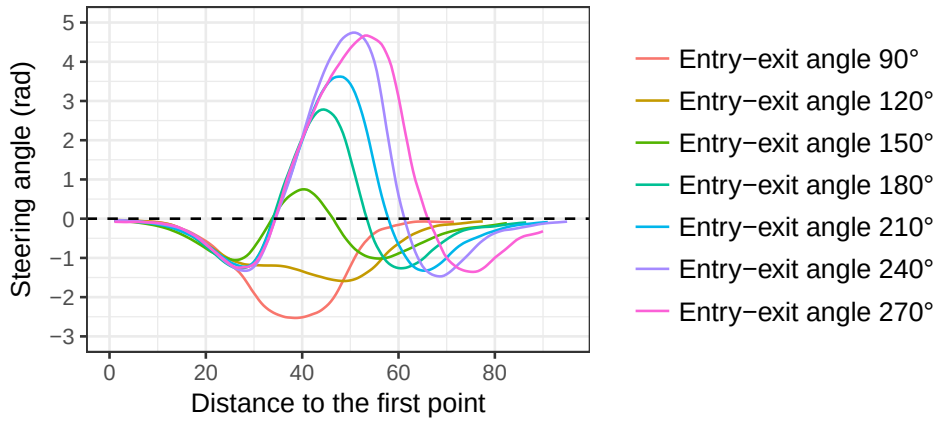

(a) Mean values of steering angle for the drives through the roundabouts with 13 m radius.

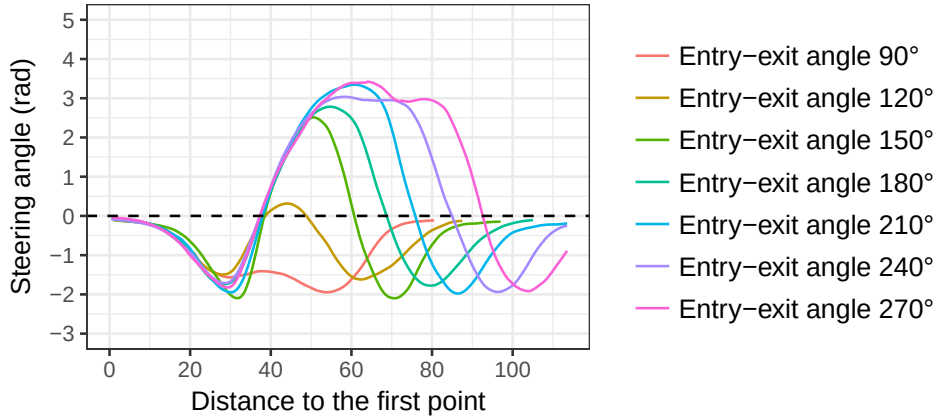

(b) Mean values of steering angle for the drives through the roundabouts with 20 m radius.

Figure 3-18: Mean values of steering angles for the drives through the roundabouts.

where Geo is the integrated geometric feature, and θ_e is the local extremum of the steering angle. The results revealed that the local extremum of the steering angle θ_e is logarithmically related to Geo when the integrated geometric feature Geo is smaller than 137.08 $\mathrm{rad}^2 \cdot \mathrm{m}$, θ_e. The coefficient of determination R^2 is as high as 0.9168. When Geo is larger than 137.08 $\mathrm{rad}^2 \cdot \mathrm{m}$, θ_e randomly oscillates between 1.75 rad and 5.75 rad. The correlation is also illustrated in Figure 3-19. θ_e has four ranges corresponding to the four ranges of Geo (see Figure 3-20):

- $-4\ \mathrm{rad} \leq \theta_e \leq -1.75\ \mathrm{rad}$ when $0\ \mathrm{rad}^2 \cdot \mathrm{m} \leq Geo \leq 40.7\ \mathrm{rad}^2 \cdot \mathrm{m}$;
- $-1.75\ \mathrm{rad} \leq \theta_e \leq -0.25\ \mathrm{rad}$ when $40.7\ \mathrm{rad}^2 \cdot \mathrm{m} \leq Geo \leq 72.4\ \mathrm{rad}^2 \cdot \mathrm{m}$;
- $-0.25\ \mathrm{rad} \leq \theta_e \leq 2\ \mathrm{rad}$ when $72.4\ \mathrm{rad}^2 \cdot \mathrm{m} \leq Geo \leq 108.7\ \mathrm{rad}^2 \cdot \mathrm{m}$;
- $1.75\ \mathrm{rad} \leq \theta_e \leq 5.75\ \mathrm{rad}$ when $Geo \geq 108.7\ \mathrm{rad}^2 \cdot \mathrm{m}$.

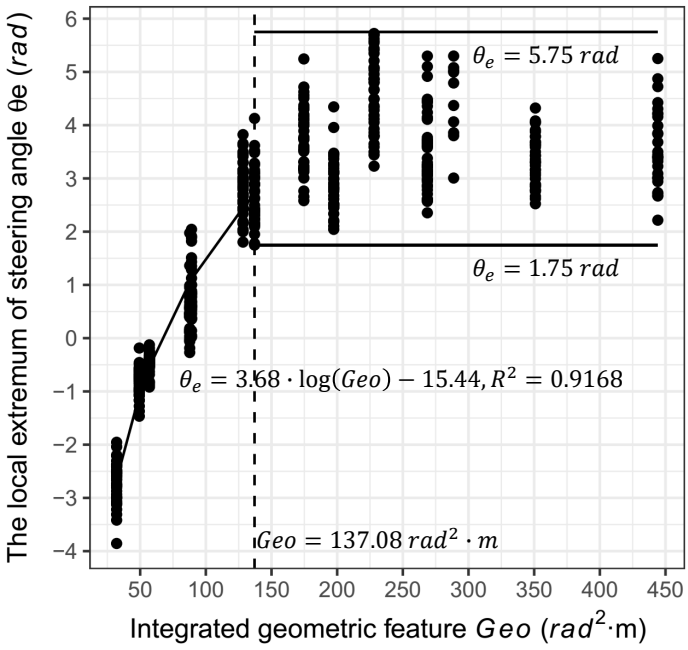

Figure 3-19: Correlation between the local extremum of steering angle and the integrated geometric feature.

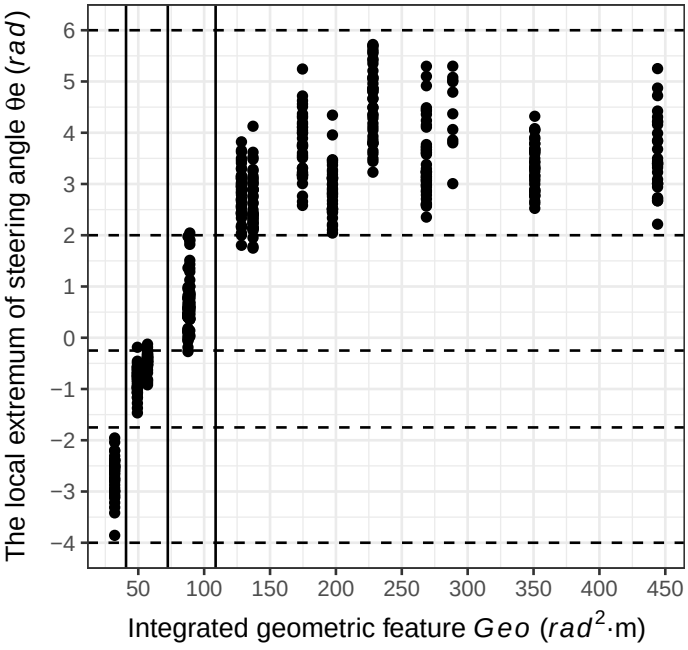

Figure 3-20: Four ranges for the local extremum of steering angle and the integrated geometric feature.

3.4.2 Scenario Categorization

The correlation between θ_e and Geo was used to categorize generic roundabouts as follows:

- Scenarios with $0\ \mathrm{rad}^2 \cdot \mathrm{m} \leq Geo \leq 40.7\ \mathrm{rad}^2 \cdot \mathrm{m}$ are defined as Scenario 1 (see the pink area in Figure 3-21 (a)). In the simulator study, the roundabout with 26 m diameter and 90° entry-exit angle belonged to Scenario 1 (see the roundabout in the pink area of Figure 3-21 (b));
- Scenarios with $40.7\ \mathrm{rad}^2 \cdot \mathrm{m} \leq Geo \leq 72.4\ \mathrm{rad}^2 \cdot \mathrm{m}$ are defined as Scenario 2 (see the yellow area in Figure 3-21 (a)). In the simulator study, the roundabout with 40 m diameter and 90° entry-exit angle and the roundabout with 26 m diameter and 120° entry-exit angle belonged to Scenario 2 (see the roundabouts in the yellow area of Figure 3-21 (b));
- Scenarios with $72.4\ \mathrm{rad}^2 \cdot \mathrm{m} \leq Geo \leq 108.7\ \mathrm{rad}^2 \cdot \mathrm{m}$ are defined as Scenario 3 (see the green area in Figure 3-21 (a)). In the simulator study, the roundabout with 40 m diameter and 120° entry-exit angle and the roundabouts with 26 m and 150° entry-exit angle belonged to Scenario 3 (see the roundabouts in the green area of Figure 3-21 (b));
- Scenarios with $Geo \geq 108.7\ \mathrm{rad}^2 \cdot \mathrm{m}$ are defined as Scenario 4 (see the orange area in Figure 3-21 (a)). In the simulator study, the rest of the roundabouts in the simulator study belonged to Scenario 4 (see the roundabouts in the orange area of Figure 3-21 (b)).

3.4.3 Summary

In this section, a scenario categorization method for generic roundabouts was specified. The local extremum of the steering angles (θ_e) and the integrated geometric feature (Geo) were defined to represent the steering wheel information and roundabout geometric features respectively. The mathematical correlation of these two variables was calculated. This correlation was used to categorize the scenarios into four classes. On this basis, a model can be developed to predict driver maneuvers in each of these four scenarios.

3.5 Summary

This chapter describes two studies that captured driving behavior data, which were then used to develop a scenario categorization method. This method allows any drive through roundabouts to be classified into a scenario category. In each scenario category, the effect of geometric features of roundabouts on driving behavior is eliminated, thus increasing the driving behavior's ability to predict the driver maneuver of exiting/staying in roundabouts.

A field study was conducted in a real driving environment. The study acquired participants' driving behavior data as they drove through a track that included three roundabouts. This study

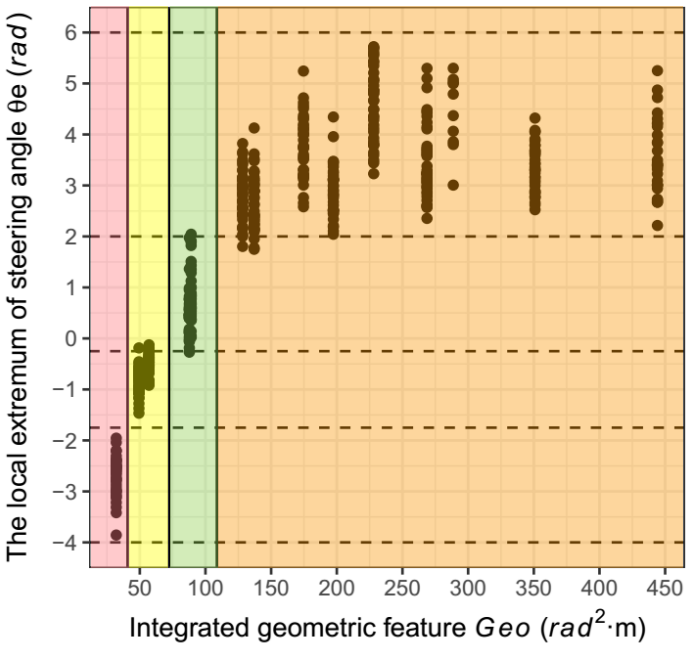

(a)

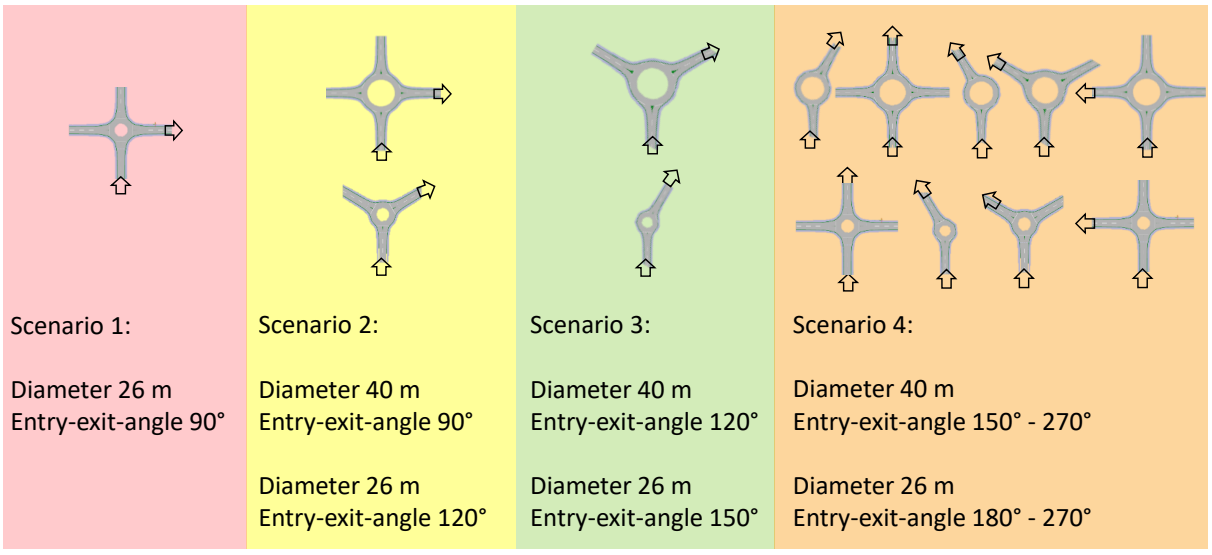

(b)

Figure 3-21: Scenario categorization of the roundabouts.

formed the basis of a proposed approach to scenario categorization for the three investigated roundabouts. Afterwards, the scenarios were categorized into three classes and a sub-model for each was developed with SVM to predict driver maneuvers. The prediction results showed that 1) the scenario categorization approach is effective at predicting driver maneuvers in the investigated roundabouts, 2) the steering angle and steering angle velocity provide important information for driver maneuver prediction, and their predictability increases as the prediction site gets closer to the exit, and 3) SVM effectively predicts driver maneuvers by classifying the data for the exiting maneuver and the data for the staying maneuver. However, the field study was only applicable to three roundabouts.

Subsequently, a simulator study was designed and conducted in a laboratory. This allowed the experimental conditions to be controlled in order to complement the limitations of the field study. The simulator study collected driving behavior data from thirteen participants as they drove through tracks that included fourteen roundabouts with controlled geometric features and traffic situations. In this study, the local extremum of steering angles (θ_e) and the integrated geometric feature (Geo) were defined to represent the steering wheel information and the geometric features of roundabouts respectively. The mathematical correlation between these two variables was calculated, which is Contribution 1 presented in Chapter 1.4. Subsequently, a scenario categorization method for generic roundabouts was proposed, on the basis of which all roundabout scenarios were categorized into four classes. This is Contribution 2 presented in Chapter 1.4. On this basis, a model can now be developed on the basis of driving behavior and a machine-learning algorithm to predict driver maneuvers in each of these four scenarios. The model's development is presented in Chapter 4.

4 Developing a Model for Driver Maneuver Prediction

This chapter explains the development of the driver maneuver predictive model. This model was developed to predict whether or not a driver will exit a roundabout in front of each exit. The model has universality regarding both roundabouts and drivers, i.e., the model can make predictions about the maneuver of drivers with any driving style at roundabouts with any type of layout.

The driver maneuver predictive model consists of four sub-models for the four scenarios identified using the scenario categorization method proposed in Chapter 3.4. Each sub-model consists of a series of classifiers that correspond to a series of prediction sites. The prediction sites are the locations where the prediction is made along the route between the entry and the exit. The details of the model structure and the prediction process can be found in Chapter 4.1. The structure achieves Contribution 3 presented in Chapter 1.4.

The classifiers were trained using machine-learning algorithms with the driving behavior information acquired at the corresponding prediction sites. All driving behavior information acquired in the simulator study and multiple machine-learning algorithms were used for classifier training in order to identify the most effective driving behavior information and algorithms. More details on the classifier training can be found in Chapter 4.2.

In addition, a method for developing a personalized predictive model was also proposed because each driver has her/his personal driving style and should thus also has her/his own personal predictive model. More details on the development of the personalized predictive model can be found in Chapter 4.3.

The important definitions used in this chapter are as follows:

- The driver maneuver predictive model is a model that can predict whether or not a driver will exit a roundabout in front of each exit of the roundabout.
- Sub-models are components of the driver maneuver predictive model. The driver maneuver predictive model consists of four sub-models for the four scenarios identified by the scenario categorization method.
- Classifiers are components of the sub-models. Each sub-model consists of a series of classifiers.
- Prediction sites are the locations where the predictions are made along the route between the entry and the exit.
- Features are driving variables and combinations of driving variables. The driving variables include steering angle, steering angle velocity, speed, acceleration, head direction, and

gaze direction.

- Soft-decision outputs are the outputs of the soft classifiers, which are continuous values of the likelihood of "Exiting" or "Staying".

4.1 Classifier-Based Model

4.1.1 Structure of the Model

The driver maneuver predictive model includes four sub-models that were developed for the four scenarios, one sub-model for each scenario. Each sub-model consists of a series of classifiers corresponding to a series of prediction sites. Prediction sites are the locations where the prediction is made along the route between the entry and the exit. Driving behavior information for all participants at each prediction site were clustered to train the corresponding classifier. The classifiers classified the driving behavior information for two driver maneuvers at each of the prediction sites.

In this thesis, two types of prediction sites were defined: the sites on the entry arm of a roundabout were defined as approaching sites, whereas the sites on the circulating lane of a roundabout were defined as circulating sites. More specifically, the definitions can be interpreted as follows:

- The approaching sites were locations that divided the entry arm of the roundabouts into specific sections until the inscribed circle of the roundabout was reached (see Figure 4-1). The distances to the inscribed circle were 2 m, 4 m, 6 m, 8 m, 10 m, 12 m, 14 m, 16 m, 18 m, and 20 m. Thus, there were ten approaching sites at the entry arm of the roundabouts. The intervals between adjacent approaching sites were 2 m.

- The circulating sites were locations that evenly divided the sections between entries and exits on the circulating lane of the roundabouts. This even distribution made the sites relevant to both the entry position and the exit position. The number of circulating sites were different for different scenarios, because the number varied with the length of the section. The longer a given section, the more circulating sites existed on it. The number of circulating sites for each of the four scenarios are as follows:

  - In Scenario 1, there were five circulating sites evenly dividing the circulating lanes into four parts.

  - In Scenario 2, there were ten circulating sites evenly dividing the circulating lanes into nine parts.

  - In Scenario 3, there were 15 circulating sites evenly dividing the circulating lanes into 14 parts.

– In Scenario 4, there were 20 circulating sites evenly dividing the circulating lanes into 19 parts.

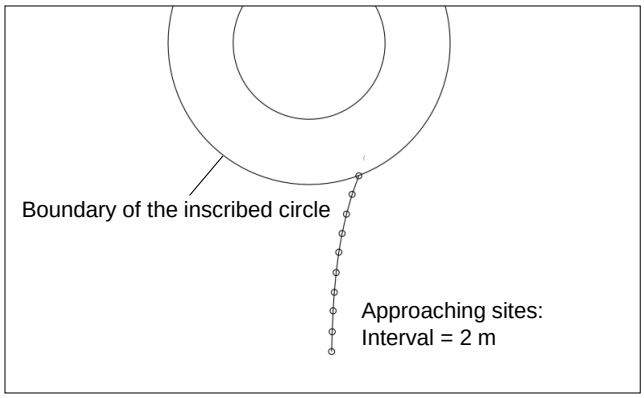

Figure 4-1: Positions of the approaching sites.

Figure 4-2 illustrates the approaching sites and the circulating sites for the four scenarios: The approaching sites are denoted with the small blue circles outside the inscribed circle of the roundabout and the circulating sites are denoted with the small blue circles inside the inscribed circle. The structure of the model was determined according to the number of prediction sites:

- Sub-model 1 consisted of 15 predictors corresponding to 15 prediction sites in Scenario 1;
- Sub-model 2 consisted of 20 predictors corresponding to 20 prediction sites in Scenario 2;
- Sub-model 3 consisted of 25 predictors corresponding to 25 prediction sites in Scenario 3;
- Sub-model 4 consisted of 30 predictors corresponding to 30 prediction sites in Scenario 4.

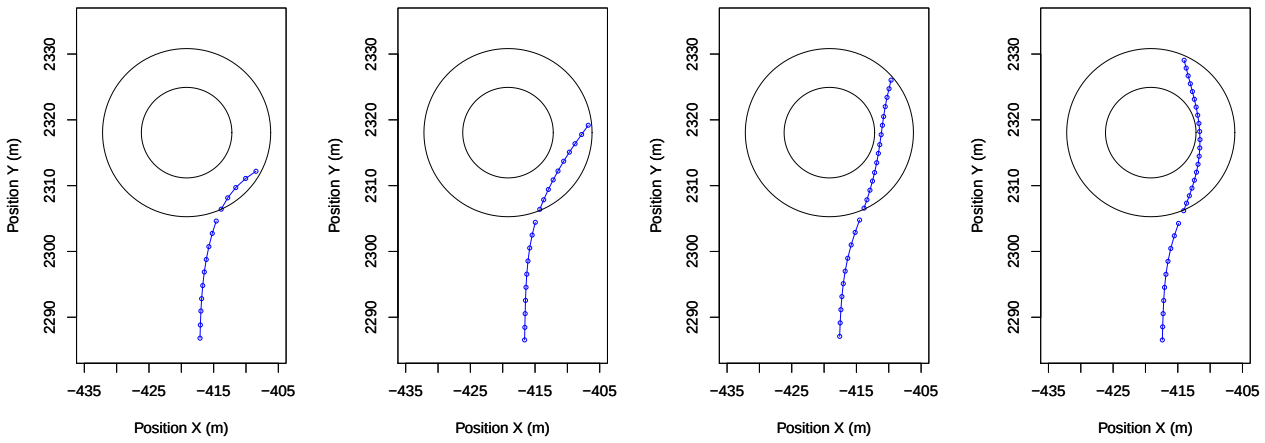

(a) For Scenario 1 **(b)** For Scenario 2 **(c)** For Scenario 3 **(d)** For Scenario 4

Figure 4-2: Prediction sites for four scenarios.

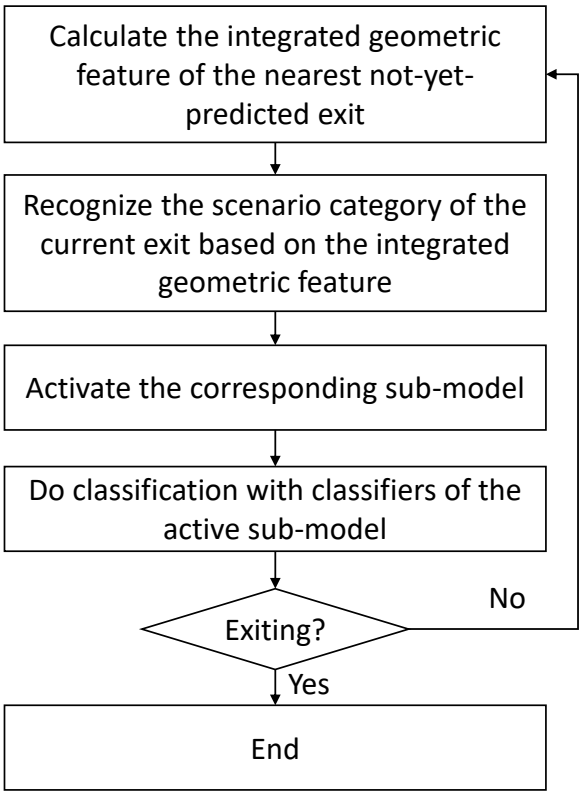

Figure 4-3: Work flow of the driver maneuver predictive model.

4.1.2 Model Prediction Procedure

The procedure for developing the predictive model consisted of five steps:

- Step 1: Calculate the integrated geometric feature (Geo) of the nearest not-yet-predicted exit on the basis of the roundabout layout when a car is approaching the exit. The calculation equation is Equ. 3.4.1.
- Step 2: Recognize which scenario the current exit falls under on the basis of the integrated geometric feature (Geo).
- Step 3: Activate the corresponding sub-model.
- Step 4: Start the classification from the first prediction site until a prediction result of "Exiting" or "Staying" is obtained.
- Step 5: End the prediction procedure if the prediction result is "Exiting". Otherwise, repeat Step 1 to Step 4 until the result of "Exiting" is given.

The procedure is illustrated as a work flow in Figure 4-3.

The details of the procedure are explained with the example of a car driving through a roundabout that has a radius of 15 m and entry-exit angles of 85°, 145°, 215°, and 280° for the four exits. As the driver approaches the roundabout (see Figure 4-4(a)), the integrated geometric feature (Geo) of the first exit is calculated as 33.0 $\mathrm{rad}^2 \cdot \mathrm{m}$. Thus, the route between the entry and

the first exit is categorized in Scenario 1 because 0 $\mathrm{rad}^2 \cdot \mathrm{m} \leq Geo \leq 40.7\ \mathrm{rad}^2 \cdot \mathrm{m}$. Then, the sub-model for Scenario 1 is activated to work, beginning with Prediction Site 1. At Prediction Site 11, the prediction result of "Staying" is obtained, that is to say, the driver is approaching the second exit (see the Figure 4-4(b)). Then, *Geo* of the second exit is calculated as 96.1 $\mathrm{rad}^2 \cdot \mathrm{m}$, thus, the route between the entry and the second exit is categorized in Scenario 3 because 72.4 $\mathrm{rad}^2 \cdot \mathrm{m} \leq Geo \leq 108.7\ \mathrm{rad}^2 \cdot \mathrm{m}$. Then, the sub-model for Scenario 3 is activated to work, starting from the prediction site next to the Prediction Site 11 of Scenario 1. At Prediction Site 22, the prediction result of "Staying" is obtained. This means the driver is approaching the third exit (see the Figure 4-4(c)). Then, *Geo* of the third exit is calculated as 211.2 $\mathrm{rad}^2 \cdot \mathrm{m}$. Thus, the route between the entry and the third exit is categorized in Scenario 4 because $Geo \geq 108.7\ \mathrm{rad}^2 \cdot \mathrm{m}$. Then, the sub-model for Scenario 4 is activated to work, starting from the prediction site which is next to the Prediction Site 22 of Scenario 3. At Prediction Site 27, the prediction result of "Exiting" is obtained. The driver maneuver of exiting the roundabout has been detected, so the prediction process ends. In this process, the classifiers of the sub-model for Scenario 1, the sub-model for Scenario 3, and the sub-model for Scenario 4 are activated in the order shown in Figure 4-5 (The activated sub-model is illustrated in yellow.).

4.1.3 Summary

This section described the structure of the driver maneuver predictive model: it consists of four sub-models for each of the four scenarios, and each sub-model consists of a series of classifiers that correspond to a series of prediction sites for that scenario. By following the proposed prediction procedure, the model can predict driver maneuvers by classifying the driving behavior information. The next section discusses the training of the classifiers with machine-learning algorithms and the driving behavior information.

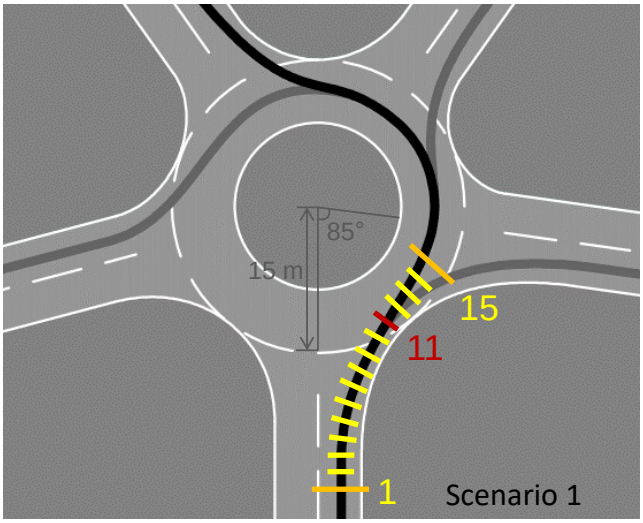

(a) Prediction for the first exit.

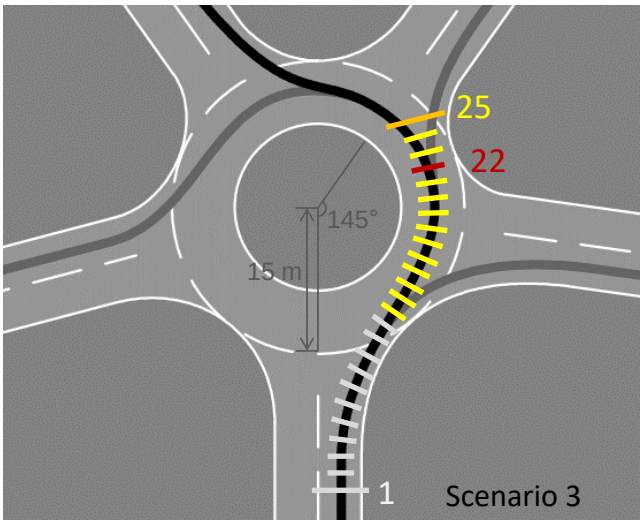

(b) Prediction for the second exit.

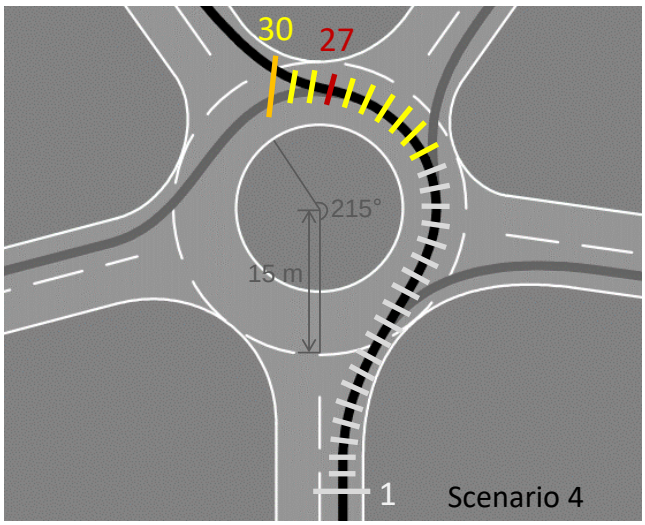

(c) Prediction for the third exit.

Figure 4-4: Prediction procedure when a driver drives through a roundabout.

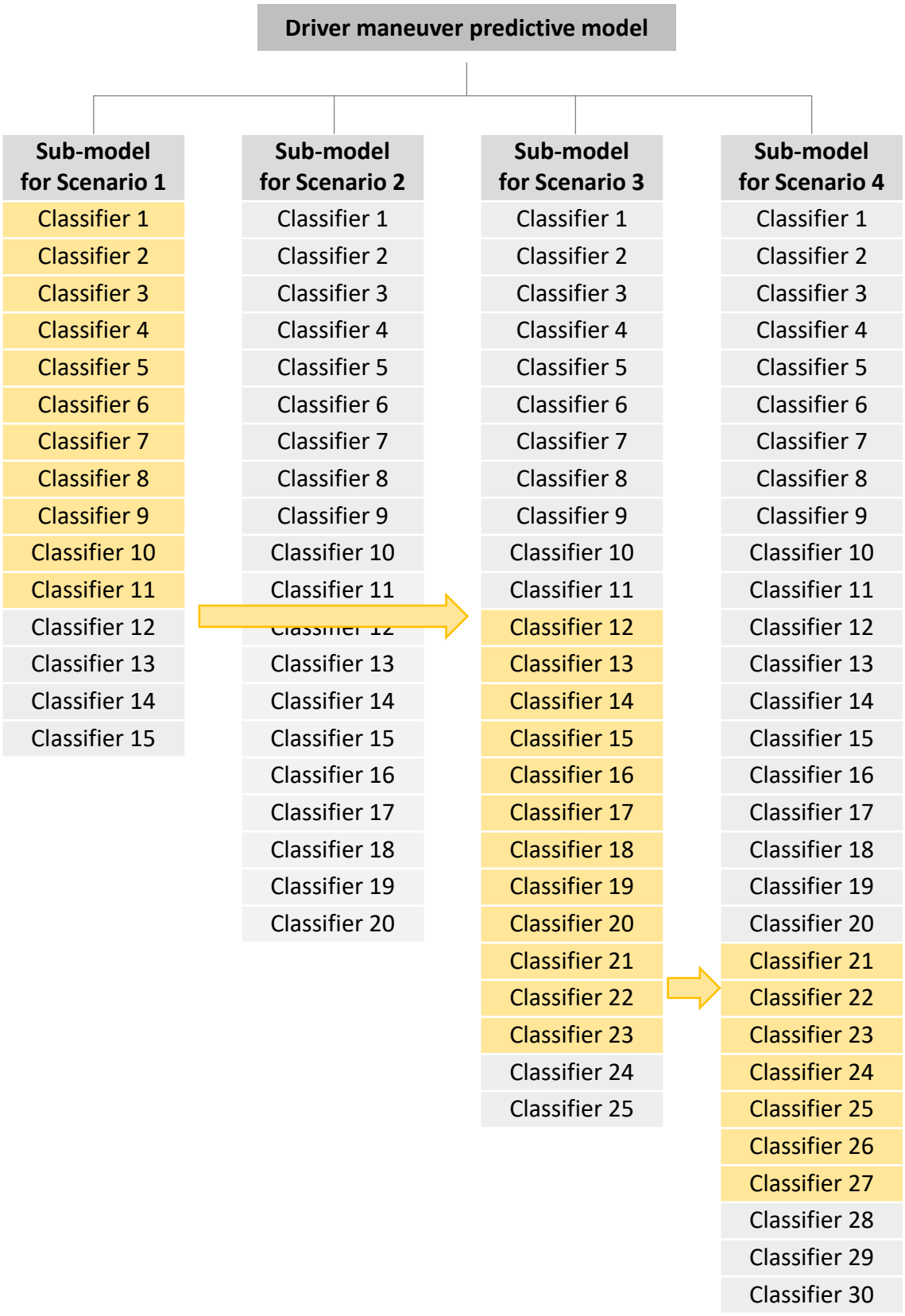

Figure 4-5: Activated sub-models in the example.

4.2 Classifier Training

4.2.1 Features for Classification

The classifiers included in the four sub-models were trained with the driving behavior information from the simulator study. The field study showed that steering angle and steering angle velocity are important features for predicting driver maneuvers. Nevertheless, the other driving behavior information was also used here as features for training the classifiers. All features were prepared for modeling with a three-step procedure:

- Step 1: Feature extraction. The values of the eight variables (steering angle, steering angle velocity, speed, acceleration, heading direction, and gaze direction) at each prediction site were extracted as features for training the classifier.

- Step 2: Feature scaling. All features were scaled to the range [-1, 1] to avoid having features with large ranges dominate those with smaller ranges [HL02].

- Step 3: Feature combination. Different features provide different predictabilities, and different combinations of features can also provide different predictabilities. Thus, all combinations of features were tested as inputs to train the classifiers. The four different basic features are as follows:

  - *Steering* was defined as the combination of steering angle and steering angle velocity.

  - *Motion* was defined as the combination of speed and acceleration.

  - *Head* was defined as the combination of head heading and head pitch. Head heading is the left/right rotation of the driver's head (also known as "no" rotation). Head pitch is the up/down rotation of the head (also known as "yes" rotation).

  - *Gaze* was defined as the combination of gaze heading and gaze pitch. Gaze heading is the left/right angle of the gaze direction. Gaze pitch is the up/down angle of the gaze direction.

  The 15 possible combinations of these four features are presented in Table 4-1: The star (*) means that the basic features in the corresponding column are included in the feature combination in the corresponding row.

This three-step process was applied at each prediction site for each scenario to prepare the features for classifier training.

Next, the following training procedure was applied to the prepared feature data:

- Step 1: Nested cross validation. As shown in Figure 4-6, an outer 5-fold cross-validation loop was used to split the feature data into training folds and test folds. The training folds were used to train the classifiers and the testing folds were used to evaluate the

Table 4-1: Fifteen possible feature combinations.

	Steering angle and steering angle velocity	Speed and acceleration	Head heading and head pitch	Gaze heading and gaze pitch
Steering	*			
Motion		*		
Head			*	
Gaze				*
Steering-Motion	*	*		
Steering-Head	*		*	
Steering-Gaze	*			*
Steering-Motion-Head	*	*	*	
Steeing-Motion-Gaze	*	*		*
Steering-Head-Gaze	*		*	*
Steering-Motion-Head-Gaze	*	*	*	*
Motion-Head		*	*	
Motion-Gaze		*		*
Motion-Head-Gaze		*	*	*
Head-Gaze			*	*

model's performance. The inner 5-fold cross-validation loop was used to identify the best parameters for the classifiers. The best parameters are the ones that can minimize the loss functions for the classifiers and generate the best prediction result, which was achieved in this way [Alb18]:

  - Sub-step 1: Set the parameters to some values.
  - Sub-step 2: Split the data in the training fold into five sub-folds.
  - Sub-step 3: Train the model with four of the five sub-folds using the parameter values.
  - Sub-step 4: Test the model on the remaining sub-fold.
  - Sub-step 5: Repeat sub-steps 3 and 4 so that each sub-fold is the test data once.
  - Sub-step 6: Repeat sub-steps 1 to 5 for all possible values of the parameters.
  - Sub-step 7: Retrieve the parameters that generate the best result.

- Step 2: Balancing the training data sets of the two classes. Oversampling was used for the class with less data.
- Step 3: Training the classifiers using machine-learning algorithms. The classifiers were trained with soft-classification algorithms, see Chapter 2. In this thesis, two types of soft-classification algorithms were investigated: simple algorithms and complex algorithms. The details of the algorithms are presented in the next two subsections.

Soft classifiers were trained using soft-classification algorithms. After being fed the inputs of the feature data, the soft classifiers output continuous values of the likelihood of "Exiting" or "Staying" [LZW11]. The output is named soft-decision output. This soft classifiers decided whether or not to report the results for "Exiting" or "Staying" with an output threshold of 95%: If the soft-decision outputs were larger than 95%, the drives were labeled as "Exiting", whereas if the outputs were smaller than 5%, the drives were labeled as "Staying". Drives with soft-decision outputs between 5% and 95% were labeled NA (No result available), meaning that, the classifiers could not offer results for these drives because they were uncertain about the decision. The value of 95% was decided upon because output that is larger than 95% can be considered as reliable prediction. Hence, the prediction results had three possible stati: Correct, wrong, or not available.

4.2.2 Classifier Training Based on Simple Algorithms

The following simple classification algorithms were used to train the classifiers:

- Linear SVM

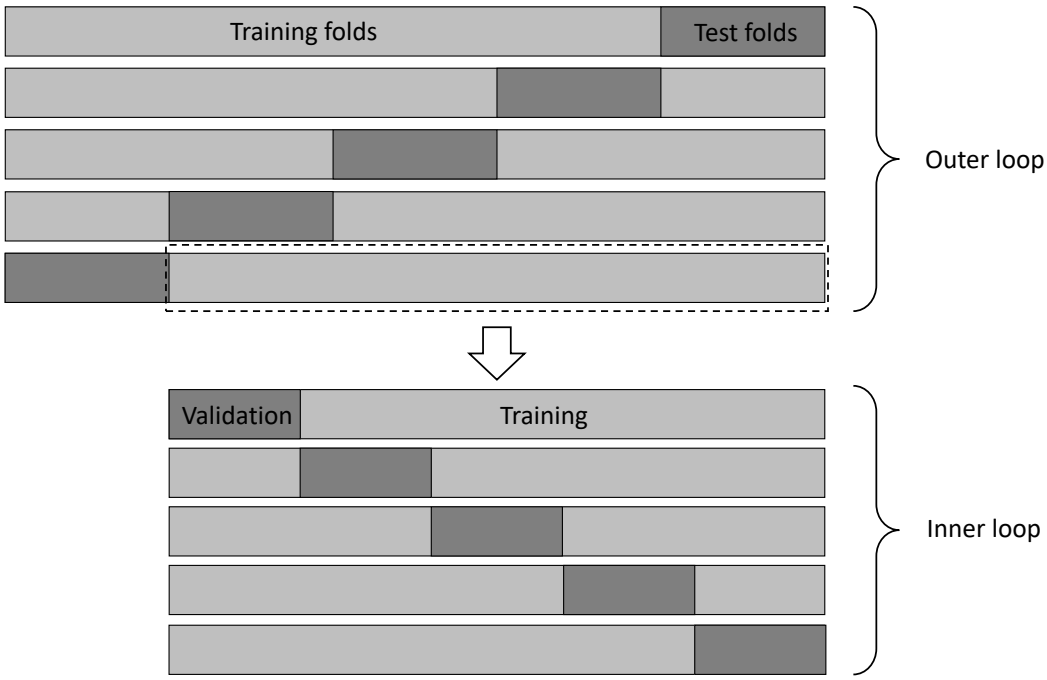

Figure 4-6: Nested 5-fold cross validation.

- Gaussian SVM
- Polynomial SVM
- RF
- AdaBoost
- logistic regression

These algorithms are described as effective methods of predicting driver behavior in Chapter 2.2. The algorithms were used in their typical format, so they were named simple algorithms. The development of complex algorithms is discussed in the next subsection. The parameters of the simple algorithms were determined by the training data set. The parameters are presented as follows:

- Linear SVM: Kernel funcion = linear kernel function and cost C = 1.
- Gaussian SVM: Kernel funcion = radial basis (Gaussian) kernel function, cost C = 1, and sigma = 0.117321976626512.
- Polynomial SVM: Kernel funcion = polynomial kernel function, cost C = 1, degree = 1, scale = 1, and offset = 1.
- Random Forest (RF): Number of trees = 500.
- AdaBoost: Number of predictors = 10.
- Logistic regression: RMSE = 0.4901843 and R^2 = 0.08812054.

The simple algorithms trained a series of classifiers independently, meaning that the outputs of these classifiers were also independent, i.e., when the present classifier makes a judgment of exiting or staying at the present prediction site, it does not consider the judgment of the previous classifier, but considers only what the driving behavior at the present site suggests. Thus, complex algorithms were developed to overcome this disadvantage of simple algorithms.

4.2.3 Classifier Training Based on Complex Algorithms

This subsection describes the development of complex algorithms, which integrate HMM and the simple algorithms. The following complex algorithms were developed:

- Linear SVM-based quasi-HMM
- Gaussian SVM-based quasi-HMM
- Polynomial SVM-based quasi-HMM
- RF-based quasi-HMM
- Adaboost-based quasi-HMM
- Logistic-based quasi-HMM

The quasi-HMM algorithms treat the series of classifiers included in each sub-model as a Markov chain. Thus, the output of the present classifier partly depends on the output of the previous classifier, i.e., when the present classifier makes a decision about exiting or staying at the present prediction site, it considers not only current driving behavior information but also the previous classifier's suggestion. This theoretically improves the predictability of the quasi-HMM algorithms. The structure of the quasi-HMM was developed to represent driver maneuvers and driving behavior at roundabouts, as depicted in Fig. 4-7. The length of the Markov chain is the number of prediction sites, denoted as K. The hidden state at prediction site k is denoted as S_k, which has two possibilities denoted as $X = \{x_1 = \text{Exit}, x_2 = \text{Stay}\}$. The observation at each prediction site is a vector of one of the features proposed above. This is the structure of the quasi-HMM.

The quasi-HMM was obtained by optimizing its parameters, which are the initial probability, the transition-probability matrix, and the emission probabilities (definitions of these parameters are given in Chapter 2.2). The Baum-Welch algorithm is often used to train the parameters for an HMM [RJ86]. However, the Baum-Welch algorithm works only when the transition-probability matrix on the chain is constant [RJ86]. For the driver maneuver prediction in this thesis, the transition-probability matrix varies on the chain. At the very beginning of the chain, the driver is still far away from the on-coming exit, so she/he is able to change her/his maneuver freely. Therefore, the probability $p(S_{i+1} = x_1|S_i = x_1)$ can be equal to the probability $p(S_{i+1} = x_2|S_i = x_1)$. A matrix A can be used to describe the transition-probability matrix at one prediction site, where the element a_{mn} in row m and column n is $p(S_{i+1} = m|S_i = n)$. The transition probability

matrix at the first prediction site is then

$$A = \begin{bmatrix} 0.5 & 0.5 \\ 0.5 & 0.5 \end{bmatrix}. \tag{4.2.1}$$

However, at the end the chain, when the driver is close to the exit, the maneuver can hardly be changed, so, the transition probability matrix at the last prediction site is

$$A = \begin{bmatrix} 1 & 0 \\ 0 & 1 \end{bmatrix}. \tag{4.2.2}$$

Therefore, the transition-probability matrix varies at different prediction sites on the chain: The closer the prediction site is to the exit, the larger the transition probabilities $p(S_{i+1} = x_1|S_i = x_1)$ and $p(S_{i+1} = x_2|S_i = x_2)$ and the smaller the transition probabilities $p(S_{i+1} = x_1|S_i = x_2)$ and $p(S_{i+1} = x_2|S_i = x_1)$. This suggests that 1) the HMM with a constant transition-probability matrix is not suitable in this case, which is the reason why the algorithm is named a "quasi" hidden Markov model (quasi-HMM) and, 2) the initial probability, the transition-probability matrix, and the emission probabilities can not be trained with the Baum-Welch algorithm [RJ86]. In the following paragraphs, the methods that were used to determine these three types of parameters are introduced.

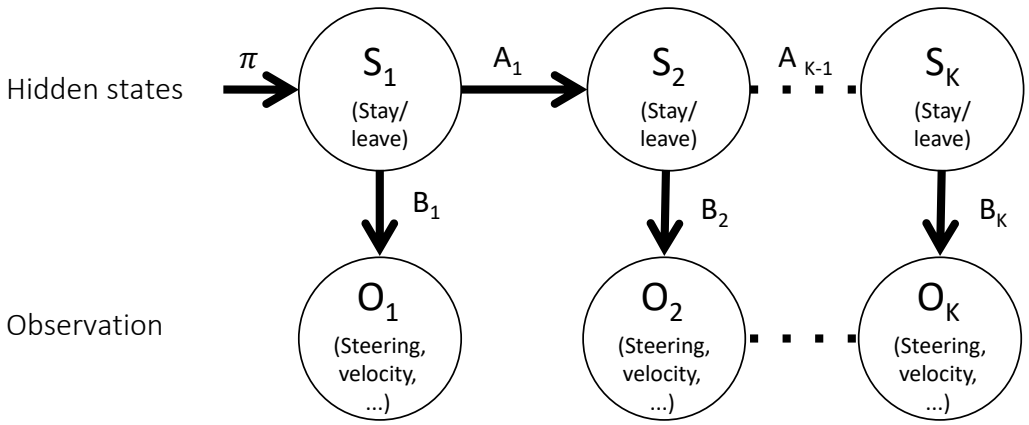

Figure 4-7: Quasi-HMM structure.

Initial Probability

The initial probability vector π was defined as $\pi = [0.5, 0.5]$ for two reasons:

- From the perspective of the individual driver, at the first prediction site, there were almost no clues as to the driving direction, so the probabilities of the two states were equal.
- From a statistical perspective, there were equal numbers of training data for the two different states. Therefore, the initial probabilities of the two different states must be

equal, otherwise the prediction at the beginning of drives would be biased towards the state with a higher initial probability. However, it should be noted that, in real-world driving, the initial probability can be determined according to the traffic volume, i.e., a higher initial probability can be assigned to the exit with heavier traffic through it.

Emission Probability

The emission probability $p(O_i|S_i = x)$ at each prediction site was determined using the soft-decision output of the corresponding simple algorithms. However, the output was in the form $p(S_i = x|O_i)$, where x was the hidden state and O_i was the observation. To convert the conditional probability, the Bayesian rule was applied as

$$p(O_i|S_i = x) = \frac{p(O_i, S_i = x)}{p(S_i = x)} = p(x|O_i) \cdot \frac{p(O_i)}{p(S_i = x)} \tag{4.2.3}$$

where $\frac{p(O_i)}{p(S_i=x)}$ is a constant because both, $p(O_i)$ and $p(S_i = x)$ are prior probabilities that have no influence on each other. This constant can be obtained by normalization, i.e.,

$$\sum_x p(S_i = x|O_i) \cdot \frac{p(O_i)}{p(S_i = x)} = 1 \tag{4.2.4}$$

where x takes all possible states. In practice, normalization can be executed later for the posterior probabilities calculated in equation (2.2.7) to ensure that the sum of the posterior probabilities of all possible states equals 1. Therefore, the soft-decision outputs of the simple algorithms were used to calculate the emission probabilities of the six complex algorithms.

Transition probability

The transition probability matrices vary at different prediction sites along the routes. The above analysis considered that, at the beginning of each drive, the transition probability $p(S_{i+1} = x_1|S_i = x_1) = p(S_{i+1} = x_2|S_i = x_2) = 0.5$, whereas at the end of each drive, the transition probability $p(S_{i+1} = x_1|S_i = x_1) = p(S_{i+1} = x_2|S_i = x_2) = 1$. These numbers should increase over the course of the drive. Therefore, the distribution of the transition probability $p(S_{i+1} = x_1|S_i = x_1)$ along each drive was assumed to take the form of an S-shape. A typical S-shaped function, a logistic function, was used to define this distribution. The parameters of the logistic function were empirically determined for the four scenarios as follows:

- For Scenario 1:

$$P = p(S_{i+1} = x_1|S_i = x_1) = \frac{0.5}{1 + e^{-3.11\cdot(x-10)}} + 0.5 \tag{4.2.5}$$

- For Scenario 2:

$$P = p(S_{i+1} = x_1|S_i = x_1) = \frac{0.5}{1 + e^{-6.21\cdot(x-14)}} + 0.5 \tag{4.2.6}$$

- For Scenario 3:

$$P = p(S_{i+1} = x_1 | S_i = x_1) = \frac{0.5}{1 + e^{-3.11 \cdot (x-18)}} + 0.5 \tag{4.2.7}$$

- For Scenario 4:

$$P = p(S_{i+1} = x_1 | S_i = x_1) = \frac{0.5}{1 + e^{-6.21 \cdot (x-24)}} + 0.5 \tag{4.2.8}$$

where x is the distance from the entry of the roundabout to the prediction site. The transition-probability matrix at a given prediction site is

$$A = \begin{bmatrix} P & 1-P \\ 1-P & P \end{bmatrix}. \tag{4.2.9}$$

Six complex algorithms were obtained by optimizing the initial probabilities, the transition-probability matrices, and the emission probabilities.

4.2.4 Summary

This subsection introduced the feature extraction method for training classifiers. Moreover, simple and complex algorithms were used to train the classifiers. The simple algorithms were SVM, logistic regression, RF, and Adaboost. The complex algorithms were developed by integrating an HMM chain with these simple algorithms. In Chapter 5.1, the features and the algorithms with the best predictive performance will be selected with model evaluation.

4.3 Reinforcement Learning for a Personalized Model

4.3.1 Different Driving Styles for Different Drivers

Sometimes, drivers behave differently even in the same roundabout scenario due to their different driving styles. This is easily visible in Figure 4-8. It depicts the mean values of steering angle for each participant in the field study as the participants exited a roundabout. It can be observed that the steering angle of all participants increases at the beginning and then starts decreasing in the middle until the end. In other words, all participants first steered the steering wheel left to follow the roundabout for a short time and then steered right to take the exit. However, Participant 2 and Participant 4 steered with different angles and different angle speeds: They turned the steering wheel left heavily, while the others steered left much more slightly to follow the roundabout before taking the exit. The reason may be that they have less driving experience or a cautious personality. It can thus be assumed that a driver maneuver predictive model that is trained with generic driving behavior data will not succeed for such drivers whose personal driving styles are very different from generic drivers. To solve this problem, it is necessary to develop personalized predictive models.

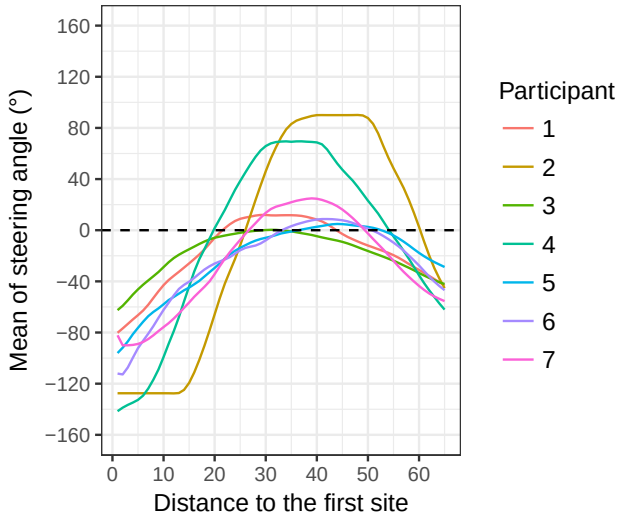

Figure 4-8: Mean values of steering angle from each participant.

4.3.2 The Development of Personalized Predictive Models

A personalized predictive model is defined as a model that is trained specifically for an individual driver. The model is obtained by updating an original predictive model. The original model was developed using the method presented in Chapter 4.1 and Chapter 4.2. The training data for the original model were acquired from generic drivers. The model can be updated by solving a reinforcement learning problem, which is the problem faced by a model that learns behavior through trial-and-error interactions with a dynamic environment [KLM96][SB98]. In this thesis, the environment is dynamic because driving behavior differs among drivers. These trial-and-error-interactions allow the model to be self-adaptive to the feedback of the output generated

Table 4-2: Driving experience of participants in the field study.

No.	Age in 2015	Gender	Year of driver's license acquisition	Driving regularly since	Driving mileage in 2014 (km)
1	22	female	2010	2010	4000
2	29	male	2014	2014	100
3	33	male	2004	/	1000
4	24	female	2009	2009	5000
5	23	female	2008	2008	5000
6	23	male	2010	2010	10000
7	23	male	2010	2010	1000

by the model. When a driver approaches the exit of a roundabout, the original model equipped in her/his car is updated via a process of reinforcement learning with the following procedure:

- Step 1: Feed the model with the driver's driving behavior data as an input to get the prediction result of the model - the maneuver of staying or exiting.
- Step 2: Make a judgment about whether or not the result is correct after the driver executes the staying or exiting maneuver.
- Step 3: Apply this feedback to update the training data set of the model. There are two types of feedbacks depending on whether the result is correct or incorrect: positive feedback when the result is correct and negative feedback when the result is incorrect. Positive feedback is integrating the input data and prediction result into the model's training data set, whereas negative feedback is integrating the input data and the *opposite* of the result into the training data set.
- Step 4: Train the model with the updated training data set.

This procedure is executed to optimize the driver maneuver predictive model for an individual driver by integrating that driver's driving behavior data into the training data set. The more personal data are integrated, the more specialized the model becomes for this specific driver. Figure 4-9 illustrates the work flow of the reinforcement learning-based model developed with the above procedure.

4.3.3 Summary

This subsection discussed the need for personalized models. In addition, a method for updating a general model for an individual driver was proposed. This method can improve the predictability of the driver maneuver predictive model. The updating can be achieved using a reinforcement learning method that can integrate real-time behavior data into the training data set. Integrating

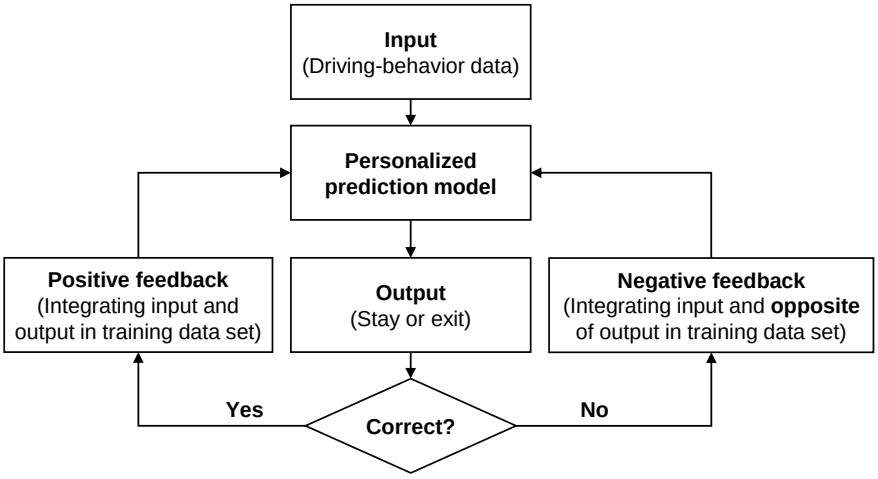

Figure 4-9: Work flow of the reinforcement learning-based predictive model.

the individual driver's behavior data allows a personalized predictive model for that driver to be obtained. A performance evaluation of the personalized model is presented in Chapter 5.3.

4.4 Summary

This chapter explained the development of a driver maneuver predictive model. The model can predict the maneuvers of a driver with any type of driving style at a roundabout with any type of layout. The presented driver maneuver predictive model consists of four sub-models for the four scenarios. Each sub-model consists of a series of classifiers that correspond to a series of prediction sites. This model structure is presented as Contribution 3 in Chapter 1.4. When a driver approaches a roundabout exit, the relevant scenario is determined using the scenario categorization method, and the corresponding sub-model is activated. The classifiers included in the sub-model make the classification of "Exiting" or "Staying" from the first prediction site until a reliable result of "Exiting" or "Staying" is obtained. This process predicts the future driver maneuver using the model. The classifiers were trained by machine-learning algorithms with the driving behavior information acquired at the corresponding prediction sites. Fifteen combinations of the acquired variables, namely steering angle, steering angle velocity, speed, acceleration, heading direction, and gaze direction, were used as classification features to train the classifiers. Simple algorithms (SVM, RF, Adaboost, and logistic regression) and complex algorithms (SVM-based quasi-HMM, RF-based quasi-HMM, Adaboost-based quasi-HMM, and logistic-based quasi-HMM) were applied to train the classifiers. Finally, a method to update the model into a personalized predictive model for each driver was proposed. This method allows the model to learn an individual driver's driving style on-line when it is activated to predict the driver's maneuvers. The models are then evaluated in different scenarios in Chapter 5.

5 Evaluation and Discussion

This chapter evaluates the driver maneuver predictive model that was developed using the method described in Chapter 4. First, the most informative feature and the algorithm with the best predictive performance were selected and the sites where reliable prediction results can be obtained were investigated. Second, the impact of cyclists at or near a roundabout on driver maneuver prediction was analyzed. Last, the personalized model was evaluated. One participant in the field study who has a significantly different driving style from the other participants was selected as the test driver. A personalized model that was trained specifically for this participant was evaluated and compared with a generalized model.

In this chapter, the following contributions are made:

- Contribution 4: A grading system for evaluating the model. This grading system rewards correct predictions, punishes incorrect predictions, and ignores unavailable results.
- Contribution 5: Identification of the information that can be captured automatically and be used to best predict future behavior. This information includes steering wheel information and car motion parameters. The advantage of this information is that it can be acquired at a low cost and without violating drivers' privacy.
- Contribution 6: The complex algorithm that integrates the HMM and logistic regression is well suited for predicting driver behavior.
- Contribution 7: A driver maneuver predictive model that succeeds in the scenarios with and without surrounding traffic.
- Contribution 8: Empirical proof that human behavior depends not only on the geometric features of roundabouts but also on person-specific parameters such as driving style. This knowledge was used to develop a personalized predictive model.

The important definitions used in this chapter are listed as follows:

- Soft-decision outputs are the outputs of the soft classifiers. These outputs are continuous values of the likelihood of "Exiting" or "Staying".
- A performance score is defined as an evaluation score for soft classifiers.
- Given rate is the ratio between the number of samples that are classified as "Exiting" or "Staying" and the total number of samples available in the test data set.
- Given accuracy is the ratio between the number of samples correctly classified and the number of samples that are classified as "Exiting" or "Staying".
- Reliable sites are defined as the prediction sites with a performance score higher than 85.

5.1 Model Evaluation for Feature and Algorithm Selection

5.1.1 Algorithm-Feature Combinations

This subsection evaluates the driver maneuver predictive model that can be developed with multiple machine-learning algorithms and multiple driving behavior features. Twelve possible algorithms, including six simple algorithms and six complex algorithms, are as follows (see Chapter 2):

- Linear SVM
- Gaussian SVM
- Polynomial SVM
- Random Forest
- Adaboost
- Logistic regression
- Linear SVM-based quasi-HMM
- Gaussian SVM-based quasi-HMM
- Polynomial SVM-based quasi-HMM
- RF-based quasi-HMM
- Adaboost-based quasi-HMM
- Logistic-based quasi-HMM

And fifteen possible features included:

- Steering
- Motion
- Head
- Gaze
- Steering-Motion
- Steering-Head
- Steering-Gaze

- Motion-Head
- Motion-Gaze
- Head-Gaze
- Steering-Motion-Head
- Steering-Motion-Gaze
- Steering-Head-Gaze
- Motion-Head-Gaze
- Steering-Motion-Head-Gaze

There were 180 ways to combine these algorithms and features. Thus, 180 driver maneuver predictive models were trained with these combinations using the method introduced in Chapter 4. These models were evaluated and compared with one another in this chapter, allowing for the selection of the algorithm-feature combination with the best performance.

5.1.2 Evaluation of the Algorithm-Feature Combinations

Test data for evaluating the models were defined using the nested cross validation presented in Chapter 4.2. As shown in Figure 4-6, an outer 5-fold cross-validation loop was used to split the data into training and test folds. The data in the training folds were used to train models, whereas the data in the test folds were used for model evaluation.

The test data set contained driving samples with exiting maneuvers and samples with staying maneuvers. During model testing, the models labeled these samples as "Exiting", "Staying", or "NA (no result available)" on the basis of the soft-decision outputs of the models and the output threshold of 95%. In this case, traditional evaluation scores for hard classification such as accuracy, F1 score, detection rate, and false alarm rate [Pow11] are not appropriate because these scores would treat "no result available" as an incorrect result. Therefore, a grading system was proposed to calculate evaluation scores for the soft-decision based models. This grading system is based on the principle that a correct prediction is the best situation, an incorrect prediction is the worst situation, and "no result available" is neutral. Following this principle, the models were scored in this way:

- The models received one positive point when they offered a correct prediction result for a given test drive.
- The models received zero points when they didn't offer a result for a given test drive.
- The models received one negative point when they offered an incorrect prediction result for a given test drive.

However, the scores the models acquired in this way depended not only on the prediction results but also on the number of test drives. For this reason, the points were converted into percentages so that the scores for all scenarios varied within the same range, from -100 (incorrectly predicting all test drives) to 100 (correctly predicting all test drives). This score is called the *performance score*.

The performance scores for all combinations of the twelve algorithms and 15 features at each prediction site for each of the four scenarios were calculated and presented in Figure A-1-A-12 in Appendix A. These figures show that scores at the beginning of the drives were as low as 0-20, then increased in the middle up to 100, and were as high as 100 at the end of the drives. It was assumed that a better model would reach 100 at an earlier prediction site. Thus the sites in which the scores were near 100 were selected as *key sites*. The key sites for the four scenarios were as follows:

- For Scenario 1, the key sites were Prediction Site 9, Prediction Site 10, Prediction Site 11, and Prediction Site 12.
- For Scenario 2, the key sites were Prediction Site 12, Prediction Site 13, Prediction Site 14, and Prediction Site 15.
- For Scenario 3, the key sites were Prediction Site 17, Prediction Site 18, Prediction Site 19, and Prediction Site 20.
- For Scenario 4, the key sites were Prediction Site 25, Prediction Site 26, Prediction Site 27, and Prediction Site 28.

At these key sites, the performance score of one algorithm-feature combination, "Gaze with Adaboost (Ada)", was compared to every other algorithm-feature combination by calculating Cohen's *d* between them [Lak13]. Cohen's *d* is an effect size and measures the difference between the performance of "Gaze with Ada" and the algorithm-feature combination under comparison: When Cohen's *d* is positive, the compared algorithm-feature combination performs better than "Gaze with Ada", and the larger the value, the better this algorithm-feature combination performs compared to "Gaze with Ada". On the contrary, when Cohen's *d* is negative, the compared algorithm-feature combination performs worse than "Gaze with Ada", and the smaller the value, the worse this algorithm-feature combination performs compared to "Gaze with Ada". Cohen's *d* thus allows the algorithm-feature combinations to be ranked at each key site for each scenario. "Gaze with Ada" was selected by random. The baseline selected does not affect the ranking of the performances of all algorithm-feature combinations. The ranking at the first key site for Scenario 1 is presented in Appendix B as an illustrative example. The top several algorithm-feature combinations across all key sites are presented in Table 5-1 and Tables B-2-B-16.

Table 5-1-B-16 show that the best algorithm-feature combination at each key site are as follows:

- For Scenario 1:
  - At Prediction Site 9: The best algorithm-feature combination is Steering-Motion-

Table 5-1: Top algorithm-feature combinations at Prediction Site 9 in Scenario 1.

Features	Cohen's d	Rank
Steering-Motion-Head_with_logistic	9.633974	1
Steering-Motion-Head-Gaze_with_HMMLogistic	9.25089	2
Steering-Motion-Head-Gaze_with_logistic	9.25089	2
Steering-Motion-Head_with_HMMLogistic	9.031955	4
Steering-Motion-Gaze_with_HMMSVMlinear	8.635495	5

Head with logistic regression (See Table 5-1).

- At Prediction Site 10: The best algorithm-feature combinations are Steering-Motion-Head with logistic-based quasi-HMM and with logistic regression (See Table B-2).
- At Prediction Site 11: The best algorithm-feature combinations are Steering-Motion with logistic-based quasi-HMM and with logistic regression (See Table B-3).
- At Prediction Site 12: There were fifteen algorithm-feature combinations performing equally good (See Table B-4).

- For Scenario 2:
  - At Prediction Site 12: The best algorithm-feature combinations are Steering-Gaze with RF-based quasi-HMM and with Random Forest (See Table B-5).
  - At Prediction Site 13: The best algorithm-feature combinations are Steering–Motion-Head-Gaze with logistic-based quasi-HMM and with logistic regression (See Table B-5).
  - At Prediction Site 14: There were fourteen algorithm-feature combinations performing equally good (See Table B-5).
  - At Prediction Site 15: There were fourteen algorithm-feature combinations performing equally good (See Table B-5).

- For Scenario 3:
  - At Prediction Site 17: The best algorithm-feature combination is Steering-Motion with logistic-based quasi-HMM (See Table B-9).
  - At Prediction Site 18: The best algorithm-feature combination is Steering-Motion-Head with logistic regression (See Table B-10).
  - At Prediction Site 19: The best algorithm-feature combination is Steering-Motion-Head with logistic regression (See Table B-11).
  - At Prediction Site 20: There were seven algorithm-feature combinations performing

equally good (See Table B-12).

- For Scenario 4:
  - At Prediction Site 25: The best algorithm-feature combination is Steering-Motion with logistic-based quasi-HMM (See Table B-13).
  - At Prediction Site 26: The best algorithm-feature combination is Steering with AdaBoost-based quasi-HMM (See Table B-14).
  - At Prediction Site 27: The best algorithm-feature combination is Steering-Motion with RF-based quasi-HMM (See Table B-15).
  - At Prediction Site 28: There were four algorithm-feature combinations performing equally good (See Table B-16).

The predictive power of the different features were then analyzed. Figures A-1-A-12 in Appendix A show that the features can be clustered into three groups on the basis of their performance scores: features including Head-Gaze, features including Motion, and features including Steering. The average performance scores for these three clusters were calculated and are illustrated in Figure 5-1. It shows that the features including Steering (steering angle and steering angle velocity) provide the most valuable information and the features including Head-Gaze (only Head or Gaze information) provide the least information. The predictability of the different features was analyzed further with box plots [SWRT14] of the features over different algorithms, see Figure C-1-C-4. These figures show that 1) the Cohen's d values of the features including Steering are significantly larger than the features that exclude Steering and 2) the Cohen's d values of the features including Motion are slightly larger than the features that exclude Motion. That is to say, the predictability order of the features is Steering-Motion $\approx$ Steering-Motion-Gaze $\approx$ Steering-Motion-Head $\approx$ Steering-Motion-Gaze-Head $>$ Steering $\approx$ Steering-Gaze $\approx$ Steering-Head $\approx$ Steering-Gaze-Head $>>$ Motion-Gaze $\approx$ Motion-Head $\approx$ Motion-Gaze-Head $>$ Gaze $\approx$ Head $\approx$ Gaze-Head. This analysis makes clear that the steering wheel information and motion information are most important for predicting driver maneuvers.

The algorithms' performance were analyzed with box plots [SWRT14] of the complex algorithms and the simple algorithms over different features, see Figure C-5-C-8. These figures show that the complex algorithms (quasi-HMMs) performed better than the simple algorithms. The soft-decision outputs of the twelve soft-classification algorithms are the likelihood of the results of "Exiting". For example, an output of 95% means that the model is 95% sure about the result of Exiting and 5% sure about the result of Staying. Contrast, an output of 5% means that the model is 5% sure about the result of Exiting and 95% sure about the result of Staying. Figures D-1-D-12 in Appendix C show the soft-decision outputs generated by the twelve algorithms for all test drives. The outputs of the logistic regression were compared to those of the logistic-based quasi-HMM as an example comparing the outputs of the simple and complex algorithms: Figure D-11 shows the outputs of the simple logistic regression algorithm at all prediction sites on the test drives that were categorized in the four scenarios. The blue lines denote the routes exiting the roundabout and the red lines denote the routes staying in the roundabout.

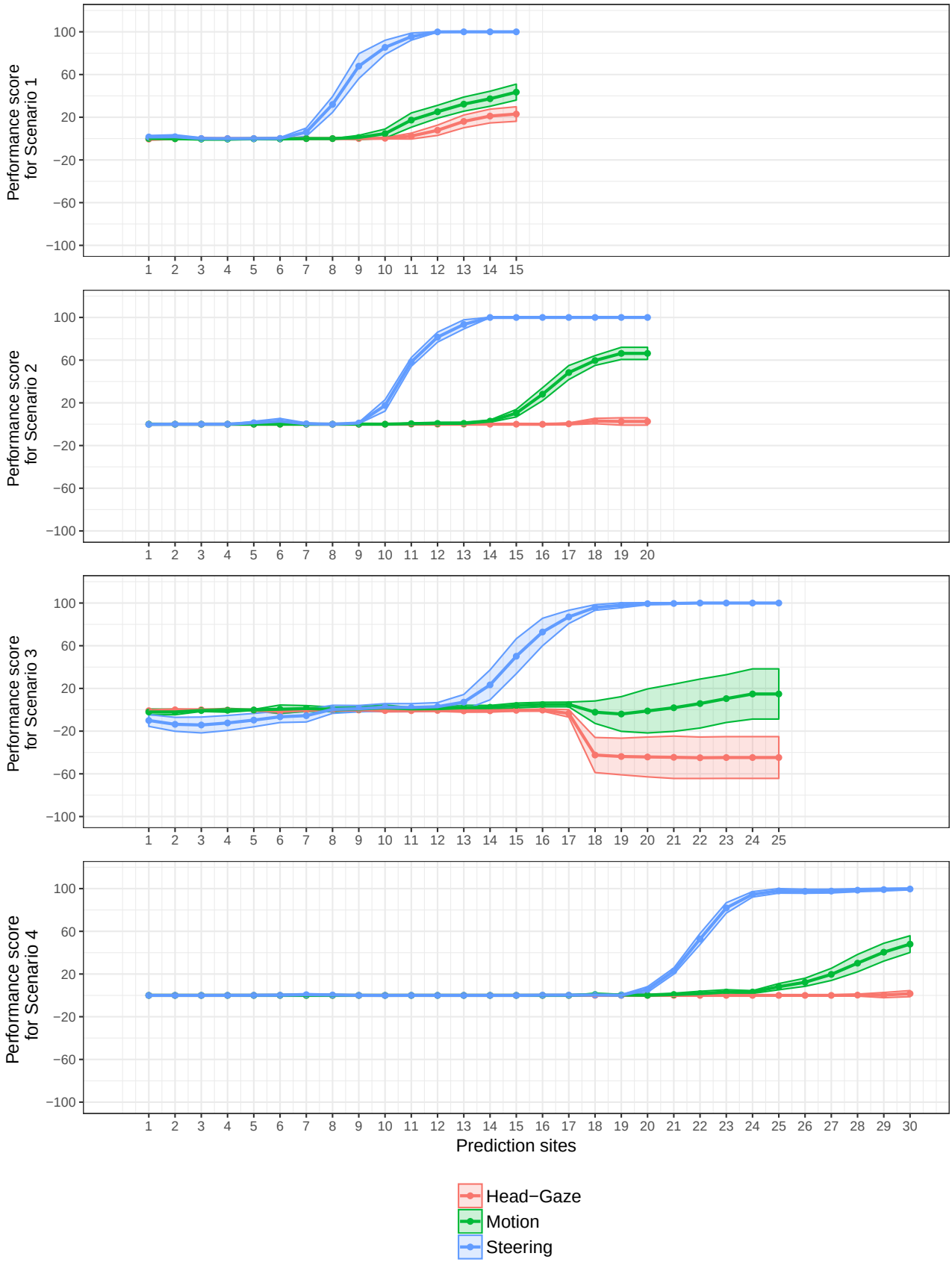

Figure 5-1: Average performance scores of three clusters of features.

It can be observed that, for the first two-thirds of drives, the outputs for the drives with two different maneuvers can not be easily distinguished. However, for the last one-third, the blue lines become close to 100% and the red lines become close to 0%, allowing the drives with two maneuvers to be distinguished from one another. Similarly, Figure D-12 shows the outputs of the logistic-based quasi-HMM. It can be observed that more green lines reach 100% and more red lines reach 0% over the last one-third in Figure D-12 than in Figure D-11. That is to say, the outputs of the logistic-based quasi-HMM are more stable in the last phase of each drive than logistic regression, and thus the logistic-based quasi-HMM offers more reliable judgments. This is why the logistic-based quasi-HMM was considered to perform better than the logistic regression. Similarly, the other five quasi-HMMs also performed better than their corresponding simple algorithms.

In summary, the best features varied at different prediction sites in different scenarios, but steering information is always integrated into the best features, and motion information is integrated into most of the best features. Thus, steering wheel information (steering angle and steering angle speed) turns out to be the most important information and the motion status (velocity and acceleration) turns out to be the second important information. Moreover, the best algorithms are always complex ones, and the logistic-based quasi-HMM performed best at most of the prediction sites. For this reason, Steering-Motion with logistic-based quasi-HMM was considered the best algorithm-feature combination for developing the driver maneuver predictive model. The performance scores of the model developed with Steering-Motion and logistic-based quasi-HMM for all prediction sites over the four scenarios are presented in Figure 5-2.

Two constructs, defined below, were used to identify how many maneuvers the model that was trained with Steering-Motion and logistic-based quasi-HMM predicted correctly in test drives:

- Given rate is defined as the ratio between the number of samples that were classified as "Exiting" or "Staying" and the total number of samples available in the test data set. Its mathematical expression is

$$Give\ rate = (P + N - NA)/(P + N) \tag{5.1.1}$$

  where P (Positive) is defined as the number of exiting maneuver samples in the test data set, N (Negative) is defined as the number of staying maneuver samples in the test data set, and NA (Not available) is defined as the number of samples that were not providing a prediction result.

- Given accuracy is defined as the ratio between the number of samples correctly classified and the number of samples classified as "Exiting" or "Staying". Its mathematical expression is

$$Give\ accuracy = (TP + TN)/(P + N - NA) \tag{5.1.2}$$

  where P (Positive) is defined as the number of exiting maneuver samples in the test data set, N (Negative) is defined as the number of staying maneuver samples in the test data set, NA (Not available) is defined as the number of samples that were not providing a prediction result, TP (True positive) is defined as the number of samples that were correctly identified

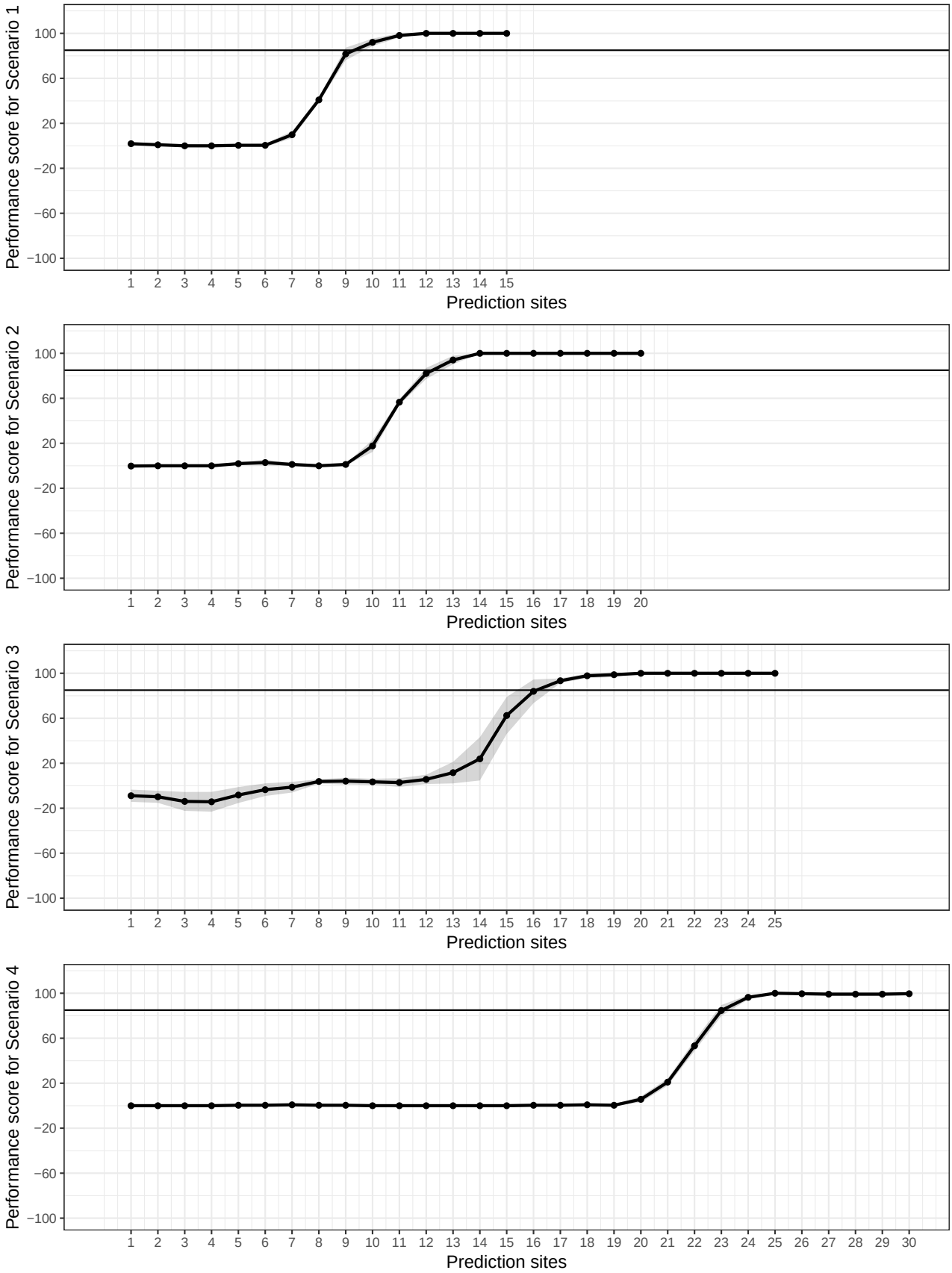

Figure 5-2: Performance scores of the model trained with logistic-based quasi-HMM and Steering-Motion (The gray areas denote the 95% confidence intervals).

as exiting maneuvers (the exiting maneuver samples were labeled as "Exiting"), and TN (True negative) is defined as the number of samples that were correctly recognized as staying maneuvers (the staying maneuver samples were labeled as "Staying").

The given rates and given accuracies of the model trained with Steering-Motion and logistic-based quasi-HMM for all prediction sites in the four scenarios are presented in Figure 5-3. It can be observed that the given rate increases with prediction sites, while the given accuracy is quite stable over the prediction sites.

5.1.3 Performance of the Predictive Model at Reliable Sites

"Reliable sites" were previously defined prediction sites with performance scores higher than 85 (85 was used as an example value because it represents quite high prediction performance). The earlier the first reliable site, the better the model' performance. Thus, the first reliable sites in the four scenarios and the prediction performance associated with them were investigated (also see Table 5-2):

- In Scenario 1, the first reliable site was Prediction Site 10 (see the position in Figure 5-4 (a)). At this prediction site, the model's average performance score was 92.0, the average given rate was 97.67%, and the given accuracy was 97.15%. In the simulator study, only roundabouts with a 13 m radius belonged to Scenario 1 (see Figure 3-21 (b)). At these roundabouts, the distance from Prediction Site 10 to the oncoming exit is about 10.0 m.

- In Scenario 2, the first reliable site was Prediction Site 13 (see the position in Figure 5-4 (b)). At this prediction site, the model's average performance score was 94.0, the average given rate was 99.76%, and the given accuracy was 97.14%. In the simulator study, roundabouts with both a 13 m and 20 m radius belonged to Scenario 2 (see Figure 3-21 (b)). At the smaller roundabouts, the distance from Prediction Site 13 to the oncoming exit is about 10.0 m. At the larger roundabouts, the distance from Prediction Site 13 to the oncoming exit is about 14.0 m.

- In Scenario 3, the first reliable site was Prediction Site 17 (see the position in Figure 5-4 (c)). At this prediction site, the model's average performance score was 93.4, the average given rate was 99.06%, and the given accuracy was 97.13%. In the simulator study, roundabouts with both a 13 m and 20 m radius belonged to Scenario 3 (see Figure 3-21 (b)). At the smaller roundabouts, the distance from Prediction Site 17 to the oncoming exit is about 12.0 m. At the larger roundabouts, the distance from Prediction Site 17 to the oncoming exit is also about 12.0 m.

- In Scenario 4, the first reliable site was Prediction Site 24 (see the position in Figure 5-4 (d)). At this prediction site, the model's average performance score was 96.4, the given rate was 97.99%, and the given accuracy was 99.18%. In the simulator study, roundabouts with both a 13 m and 20 m radius belonged to Scenario 4 (see Figure 3-21 (b)). At the smaller roundabouts, the distance from Prediction Site 24 to the oncoming exit is about

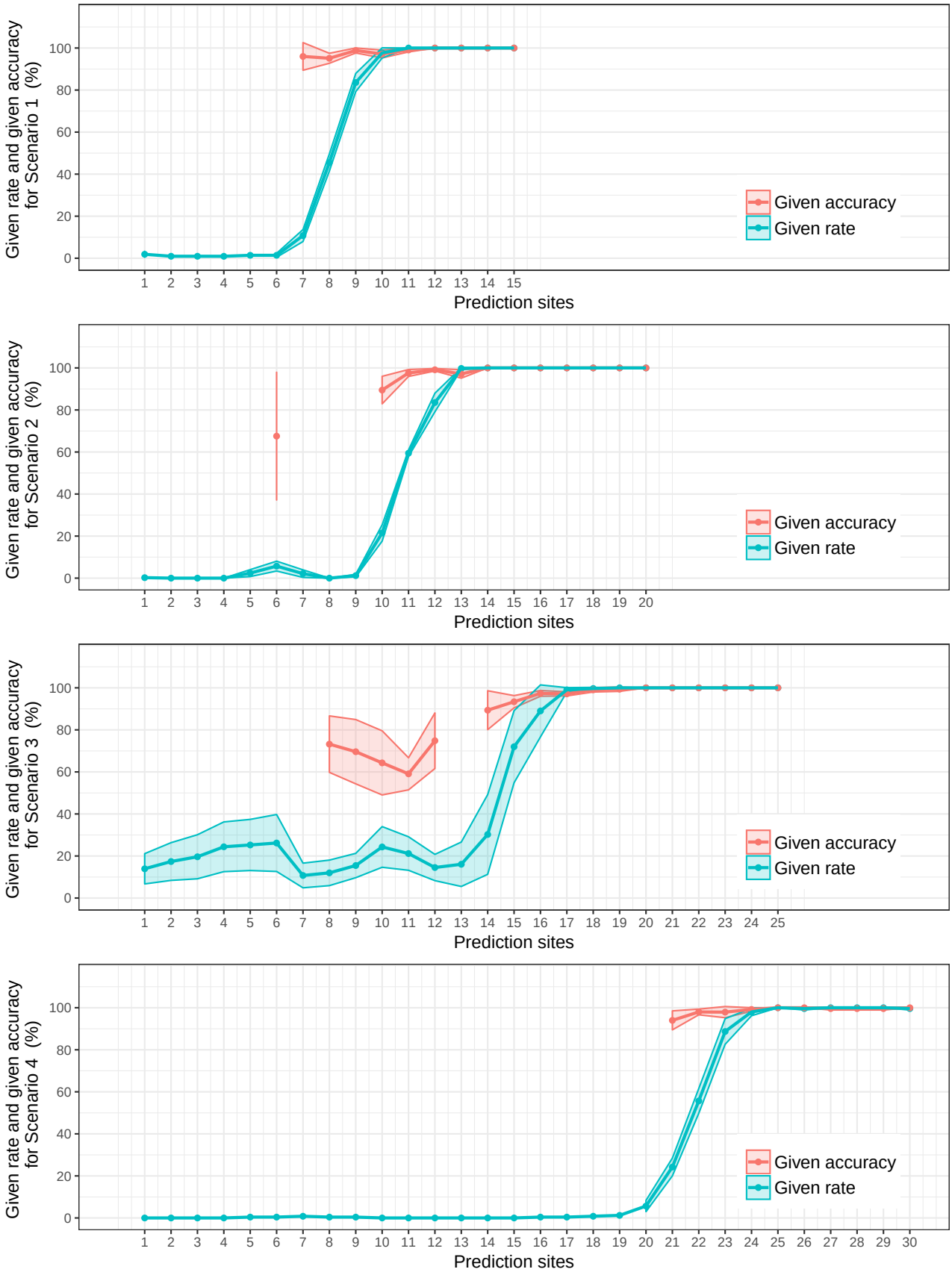

Figure 5-3: Given rate and given accuracy of the model trained with logistic-based quasi-HMM and Steering-Motion.

7.5 m. At the larger roundabouts, the distance from Prediction Site 24 to the oncoming exit is about 10.5 m.

Table 5-2: Prediction results in the four different scenarios.

	Performance score	Given rate	Given accuracy	Distance to the exit
Scenario 1	92	97.67%	97.15%	10.0 m
Scenario 2	94	99.76%	97.14%	10.0-14.0 m
Scenario 3	93.4	99.06%	97.13%	12.0 m
Scenario 4	96.4	97.99%	99.18%	7.5-10.5 m

The prediction accuracy is promising: The upcoming maneuver could be predicted with a high given rate and given accuracy (both larger than 97%) at a distance of approximately 10 m (about 2 seconds) before the exit.

5.1.4 Conclusion and Discussion

Conclusion 1: Steering-Motion is the most important feature.

The rankings of the algorithm-feature combinations (see Chapter 5.1.2) show that Steering-Motion is the most important feature for driver maneuver prediction at all key sites. The predictability order of the features is Steering-Motion $\approx$ Steering-Motion-Gaze $\approx$ Steering-Motion-Head $\approx$ Steering-Motion-Gaze-Head $>$ Steering $\approx$ Steering-Gaze $\approx$ Steering-Head $\approx$ Steering-Gaze-Head $>>$ Motion-Gaze $\approx$ Motion-Head $\approx$ Motion-Gaze-Head $>$ Gaze $\approx$ Head $\approx$ Gaze-Head. Thus, the steering wheel information and motion information are most important for predicting driver maneuvers. One reason why the steering information is significantly better than the other information could be that the scenario categorization method takes differences in steering behavior across the different scenarios into account. Previous studies on predicting driver maneuvers at intersections [NMI+08, SH14, GJW+16, TMF16, TKG15, PWK17]have frequently considered motion and turning signal information, but have only rarely considered steering wheel information and have never attempted to predict maneuvers at roundabouts. This work shows that steering wheel and motion information is more informative for maneuver prediction at roundabouts.

Steering wheel and motion information from drivers makes the model application feasible for commercial use. It is easy to acquire and analyze steering wheel and motion information by reading out steering wheel sensor data and CAN bus data. This equipment is easy to install in cars. Furthermore, unlike gaze information and head information, which are acquired by cameras, steering wheel information and motion information can be acquired with fewer challenges regarding privacy. These are the advantages of steering wheel and motion information as predictive features.

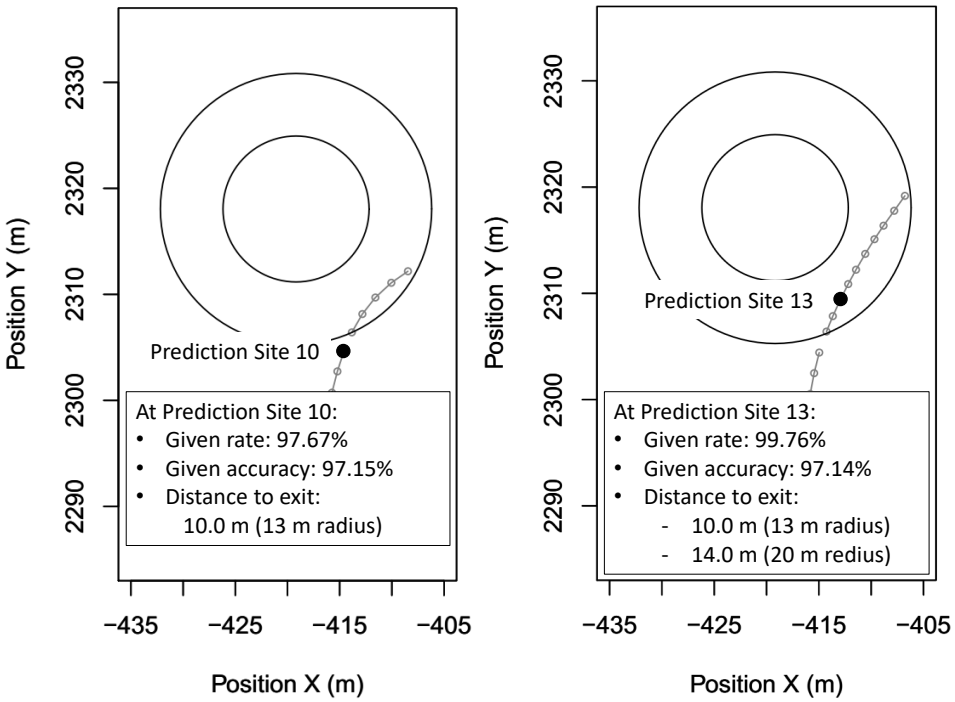

(a) For Scenario 1.

(b) For Scenario 2.

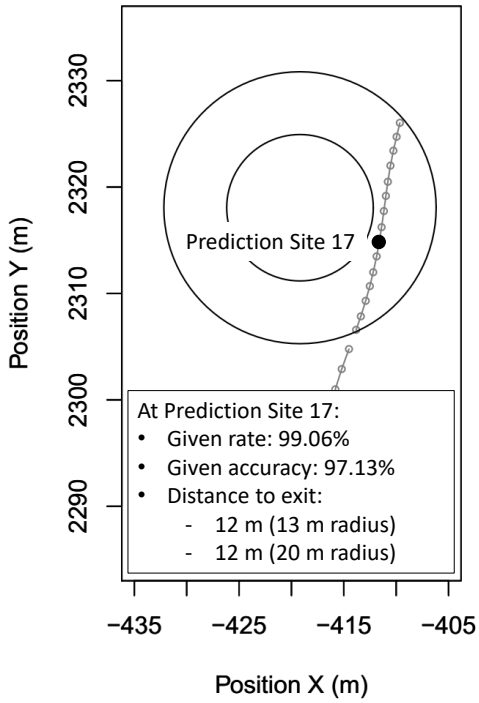

(c) For Scenario 3.

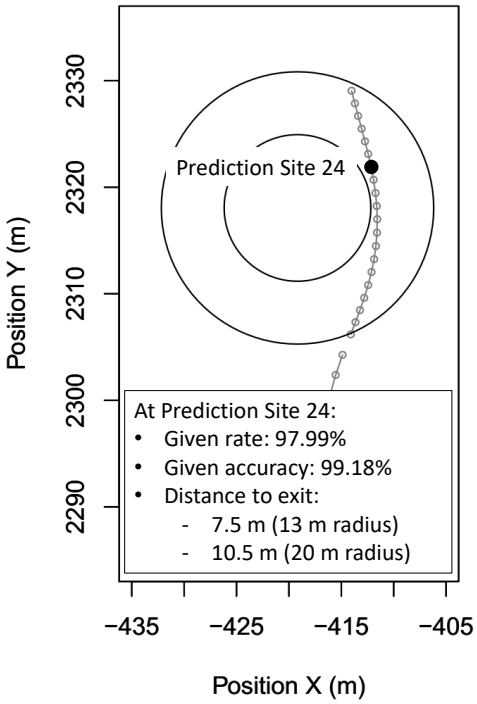

(d) For Scenario 4.

Figure 5-4: Prediction results of the best algorithm-feature combination.

Conclusion 2: The complex algorithms perform better than the simple algorithms.

The rankings of the algorithm-feature combinations (see Chapter 5.1.2) show that the complex algorithms (quasi-HMMs) perform best at all key sites, and that the logistic-based quasi-HMM specifically performs best for most key sites.

There is a theoretical reason for why the complex algorithms performed better: The simple algorithms [CV95][BSB+96][PLI02][FHT+00][LWWL13][RJ86] trained the classifiers at different prediction sites independently, i.e., when the present classifier makes a judgment of exiting or staying at the present prediction site, it only considers driving behavior at the present prediction site. On the other hand, the complex algorithms treat the classifiers included in each sub-model as a Markov chain, i.e., when the present classifier makes a decision about exiting or staying at the present prediction site, it considers not only current driving behavior information but also the previous classifier's suggestion. Therefore, the complex algorithms for driver maneuver prediction developed in this work are more effective than the simple algorithms.

Conclusion 3: Only the classifiers at the reliable sites are activated for the maneuver prediction.

The driver behavior predictive model's prediction results before the reliable sites have a quite low given accuracy (in some cases even below 90%), see Figure 5-3. These results could weaken user's trust in the model. Therefore, it is recommended that only the classifiers at the reliable sites are activated for maneuver prediction. That is to say, the model should offer prediction results of "Staying", "Leaving", or "NA (No result available)" from the first prediction site until the first full-score site. Full-score sites are defined as prediction sites where the performance score is 100, i.e., the given rate and the given accuracy are also 100%. This means that the classifiers will be activated at following prediction sites:

- In Scenario 1, the classifiers should offer results from Prediction Site 10 (the first reliable prediction site) to Prediction Site 12 (the first full-score prediction site).
- In Scenario 2, the classifiers should offer results from Prediction Site 13 (the first reliable prediction site) to Prediction Site 14 (the first full-score prediction site).
- In Scenario 3, the classifiers should offer results from Prediction Site 17 (the first reliable prediction site) to Prediction Site 20 (the first full-score prediction site).
- In Scenario 4, the classifiers should offer results from Prediction Site 24 (the first reliable prediction site) to Prediction Site 25 (the first full-score prediction site).

Previous studies on driver maneuver prediction at intersections [NMI+08, SH14, GJW+16, TMF16, TKG15, PWK17] did not use the term *prediction site* to describe the distance to the research object, such as an intersections or a roundabout. This definition makes it easier to know the predictabilities of the features and algorithms at different positions. However, effective use of the *prediction site* construct requires accurate position data.

5.1.5 Summary

In this section, the models trained with 180 possible combinations of algorithms and features were evaluated. The model's performances were scored using a proposed grading system. Then, the models were ranked in order to compare their performances. It was found that the features integrating steering wheel information and motion information were better than the other features, and complex algorithms were better than simple algorithms. Taking into consideration for all key sites within each of the four scenarios, Steering-Motion with logistic-based quasi-HMM was selected as the best algorithm-feature combination for training the driver maneuver predictive model. This conclusion answers Question 2 proposed in Chapter 3.3.1.

In addition, recommended prediction sites where the classifiers included in the model should offer results have been given. At these recommended prediction sites, the prediction results offered by the model are always reliable, and the model is guaranteed to be trustworthy for users.

5.2 Model Evaluation for Traffic Scenarios

5.2.1 Without-Traffic Model and With-Traffic Model

This subsection investigates the impact of cyclists at or near a roundabout on the driver maneuver predictive model. It was to be determined whether the algorithms and features that were earlier found to be predictive of driver maneuvers remain highly predictive even when other traffic participants are present. Thus, the impact of the four traffic scenarios introduced in Chapter 3.3.1 were investigated. The details of the cyclist settings and the affected driver maneuvers are illustrated in Figure 3-13. The scenarios with the four types of traffic were categorized using the scenario categorization method (see Chapter 3). The scenario categories and their corresponding sub-models are as follows:

- The scenario with Traffic 1 fell under Scenario 2; thus, sub-model 2 of the driver maneuver predictive model was activated to predict driver maneuvers under the impact of Traffic 1.
- The scenario with Traffic 2 also fell under Scenario 2; thus, sub-model 2 of the driver maneuver predictive model was activated to predict driver maneuvers under the impact of Traffic 2.
- The scenario with Traffic 3 fell under Scenario 4; thus, sub-model 4 of the driver maneuver predictive model was activated to predict driver maneuvers under the impact of Traffic 3.
- The scenario with Traffic 4 also fell under Scenario 4; thus, sub-model 4 of the driver maneuver predictive model was activated to predict driver maneuvers under the impact of Traffic 4.

Two different driver maneuver predictive models were evaluated for the traffic scenarios. The difference between them was that their training data were acquired from different sessions of the simulator study: The data from Session 1 were driving behavior data without cyclist effects, whereas the data from Session 2 were driving behavior data with cyclist effects. The model trained with the data from Session 1 was named the *without-traffic model* and the model trained with the data from Session 2 was named the *with-traffic model*. To investigate how well these models performed under the impact of traffic, the test data set was always drawn from Session 2. These two models were trained with the best feature-algorithm combination: Steering-Motion and logistic-based quasi-HMM.

The performance scores of the without-traffic model and the with-traffic model for the four traffic scenarios are depicted in Fig. 5-5. It can be observed that the performance scores of the with-traffic model were larger than those of the without-traffic model for all four traffic scenarios, meaning that the with-traffic model performed better in the scenarios with cyclists.

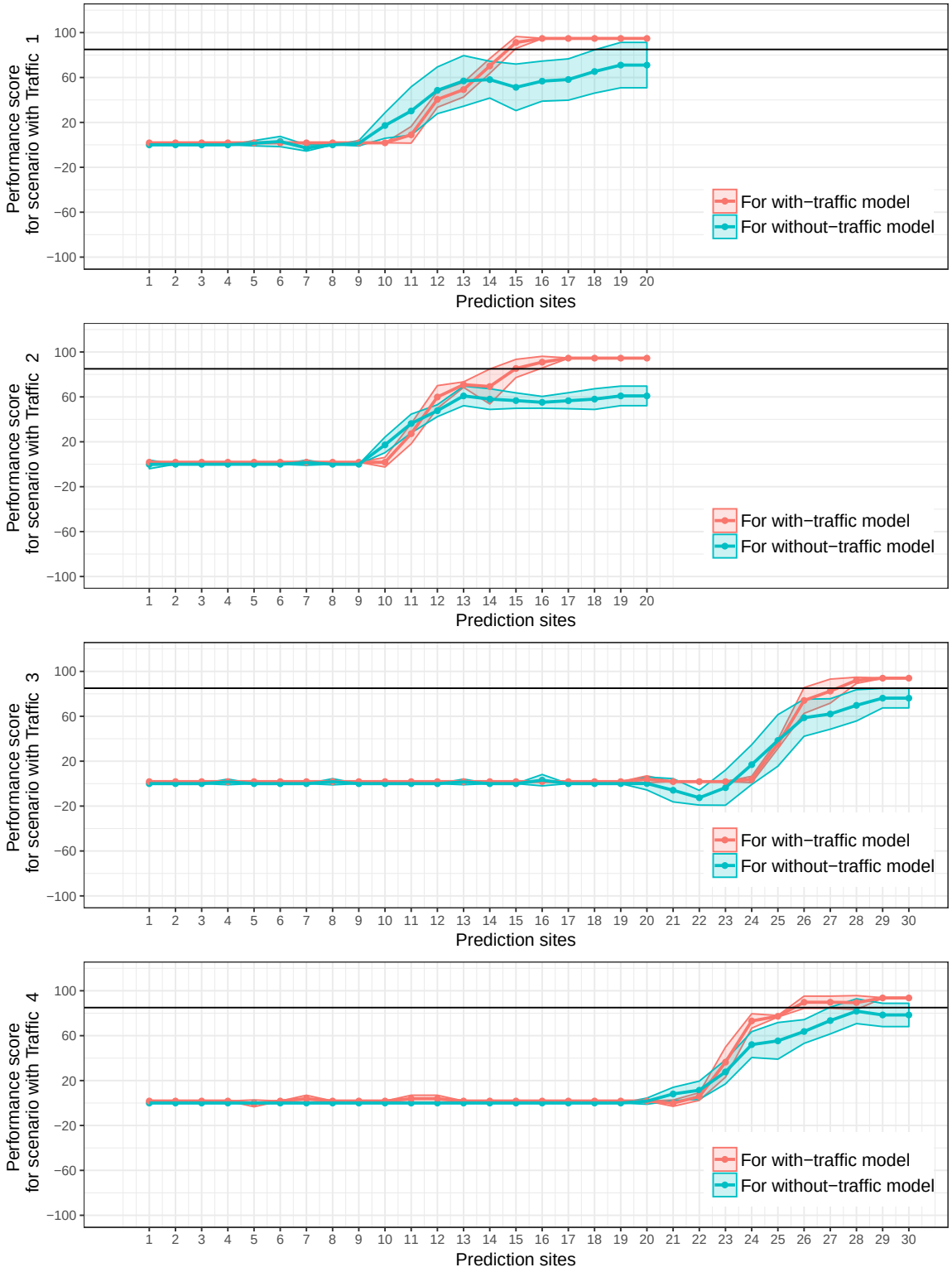

Figure 5-5: Performance score of the without-traffic model and the with-traffic model.

5.2.2 Performance of the With-Traffic Model

The given rate and the given accuracy of the with-traffic model are shown in Fig. 5-6. The given rate and the given accuracy of the first reliable site in the traffic scenarios were also investigated as follows (also see Table 5-3):

- In the scenarios with Traffic 1, the first reliable site is Prediction Site 15 (see the position in Figure 5-7 (a)). At this prediction site, the average performance score is 91.2, the average given rate is 100.00%, and the given accuracy is 93.91%. The distance from Prediction Site 15 to the oncoming exit is about 9.5 m.
- In the scenarios with Traffic 2, the first reliable site is Prediction Site 15 (see the position Figure 5-7 (b)). At this prediction site, the average performance score is 85.3, the average given rate is 98.08%, and the given accuracy is 95.83%. The distance from Prediction Site 15 to the oncoming exit is about 9.5 m.
- In the scenarios with Traffic 3, the first reliable site is Prediction Site 28 (see the position Figure 5-7 (c)). At this prediction site, the average performance score is 92.0, the average given rate is 97.92%, and the given accuracy is 100.00%. The distance from Prediction Site 28 to the oncoming exit is about 4.5 m.
- In the scenarios with Traffic 1, the first reliable site is Prediction Site 26 (see the position Figure 5-7 (d)). At this prediction site, the average performance score is 89.8, the average given rate is 100.00%, and the given accuracy is 97.92%. The distance from Prediction Site 26 to the oncoming exit is about 9.0 m.

Table 5-3: Prediction results in the scenarios with surrounding cyclists.

	Performance score	Given rate	Given accuracy	Distance to the exit
Traffic 1	91.20	100%	93.91%	9.5 m
Traffic 2	85.30	98.08%	95.83%	9.5 m
Traffic 3	92	97.92%	100%	4.5 m
Traffic 4	89.80	100%	97.92%	9.0 m

5.2.3 Conclusion and Discussion

Conclusion 1: The with-traffic model performs better than the without-traffic model in traffic scenarios.

The evaluation results (see Chapter 5.2.1) reveal that the with-traffic model performs better than the without-traffic model in traffic scenarios. The difference between these two models is the source of their training data: The with-traffic model was trained with data acquired from

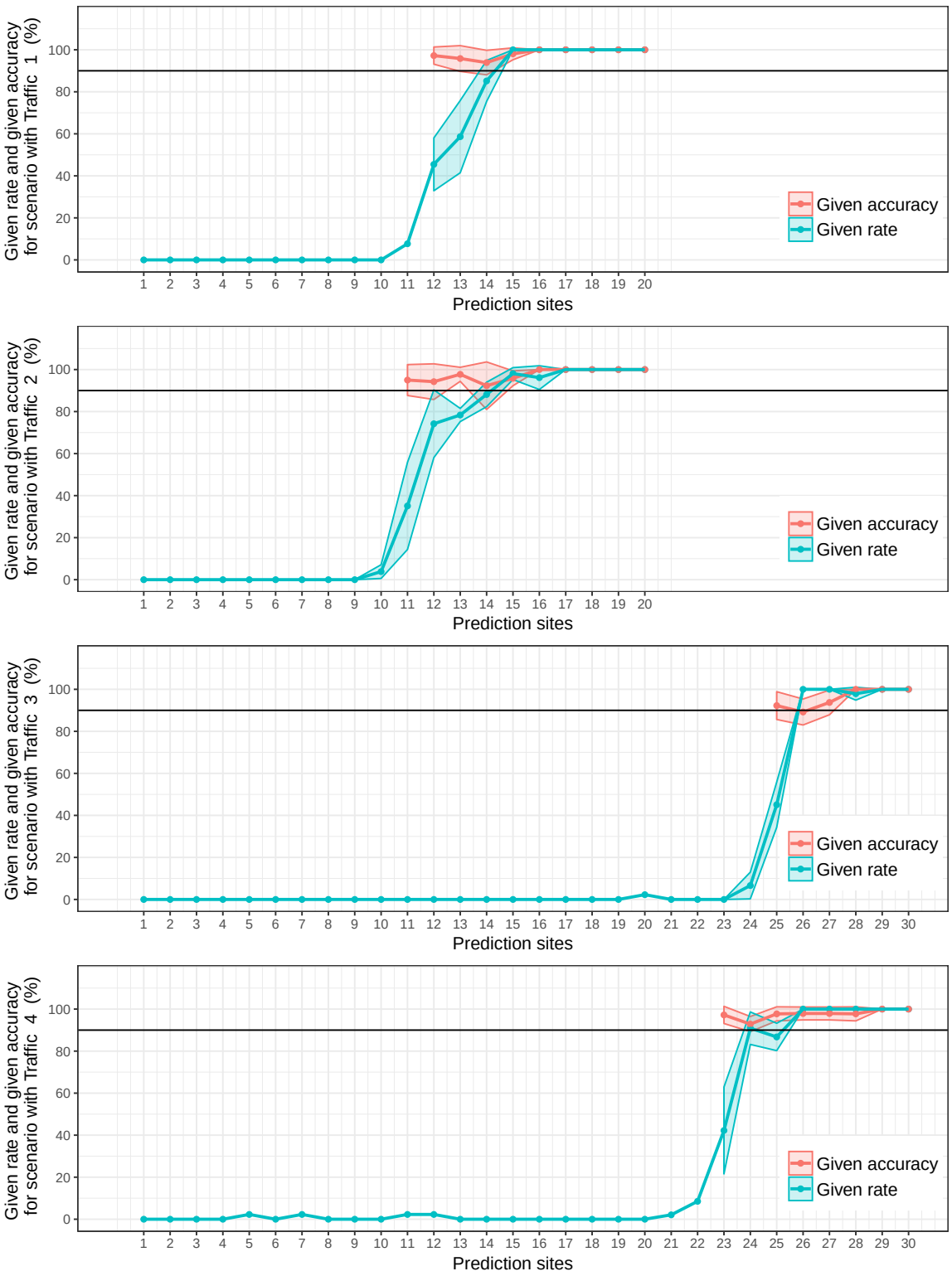

Figure 5-6: Given rate and given accuracy of the with-traffic model.

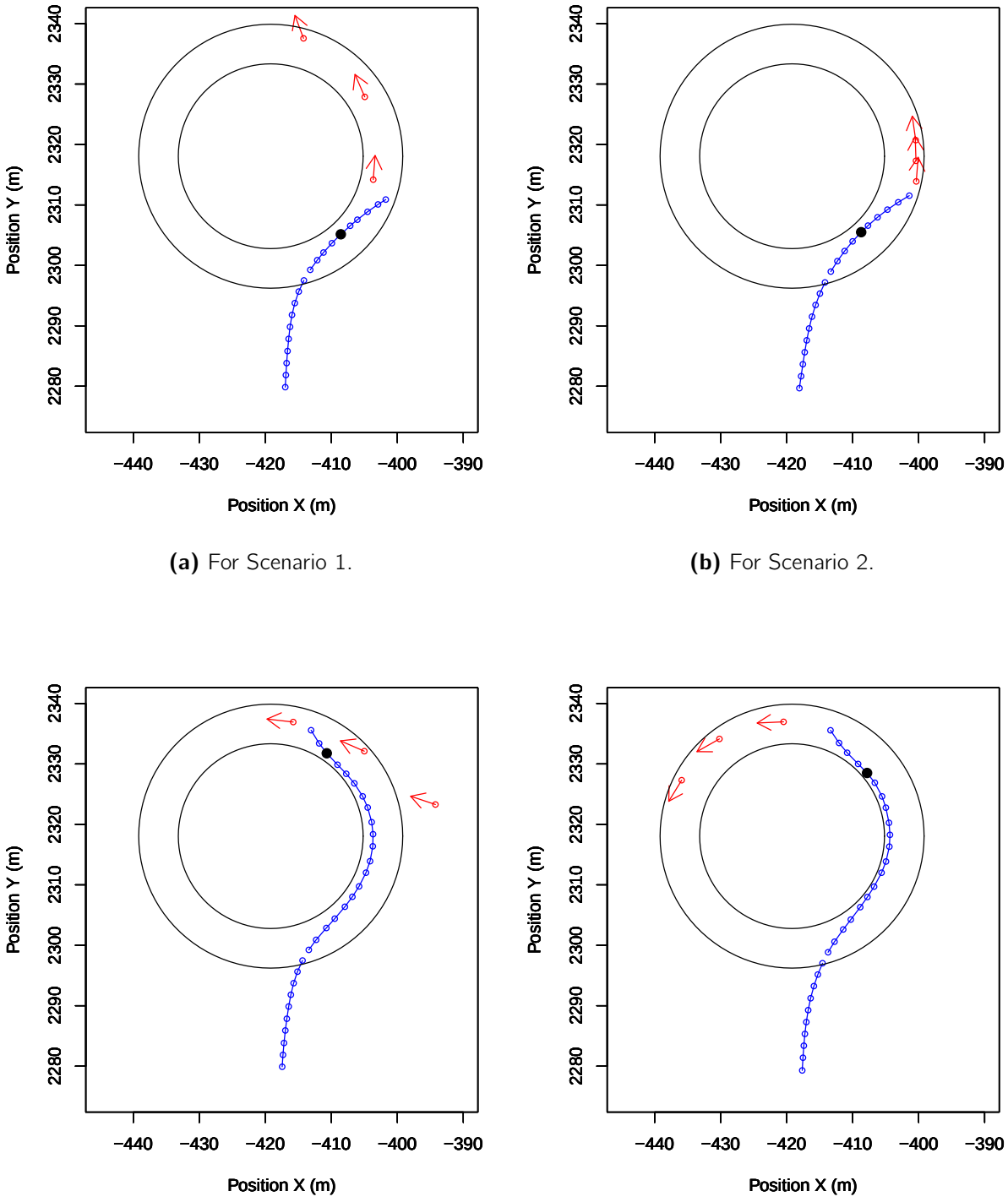

(a) For Scenario 1.

(b) For Scenario 2.

(c) For Scenario 3.

(d) For Scenario 4.

Figure 5-7: Prediction results and the cyclist positions.

the scenarios with cyclists, whereas the without-traffic model was trained with data acquired from the scenarios without traffic. The comparison shows that drivers behave differently in with-traffic scenarios and without-traffic scenarios. As a result, the model trained with data from without-traffic scenarios does not succeed in predicting driver maneuvers in scenarios with traffic, even when these two types of scenarios belong to the same scenario category defined according to roundabout geometric features. For this reason, it will be necessary to define specific sub-models for different types of cyclists or traffic. When the model is applied in cars on the road, sensors equipped in this cars should firstly sense the cyclists and then activate the corresponding sub-model.

Conclusion 2: The driver maneuver prediction model succeeds in most of traffic scenarios.

The evaluation results (see Chatpter 5.2.2) revealed that the model (Steering-Motion and logistic-based quasi-HMM) succeeds in the scenario with Traffic 1, the scenario with Traffic 2, and the scenario with Traffic 4. Only the prediction result for Traffic 3 is not good. The poor model performance in Traffic 3 may be caused by individually varying driver reactions to the cyclists' presence. In Figure 5-8, the three red arrows with small red circles denote the cyclists and their direction when the car is in front of the oncoming exit. The red line and the blue lines denote two types of driving tracks. It can be observed that the driver on the red track steered the car to the left more than the driver on the blue track. The reason for the difference in steering might be that the driver tries to avoid the possible collision with the cyclist coming from right. The different steering behavior makes the prediction difficult. However, for the purpose of warning drivers of a possible collision, the model's lower predictability can be tolerated in Traffic 3 because, the cyclists and the car drivers can always see each other in Traffic 3.

If the Steering and Motion information makes a successful prediction, it means that the driver did not adjust her/his steering behavior and speed due to the presence of the cyclists, which is dangerous and indicates that the model was necessary for driving safety. On the other hand, if the model with Steering and Motion information fails, it means that the driver did adjust his/her behavior due to the presence of surrounding cyclists. The situation is thus safe and the model was not needed. Thus, Steering and Motion is robust to the necessity of driver maneuver prediction in the presence of cyclists. Liebner (2013) [LRKS13, LKB+13] developed a model to predict turning maneuvers at intersections using only velocity information. This model achieved a true positive rate of only 55% when preceding vehicles were present. In comparison, the results presented in Chapter 5.2.2 demonstrate progress as a result of the use of Steering and Motion information.

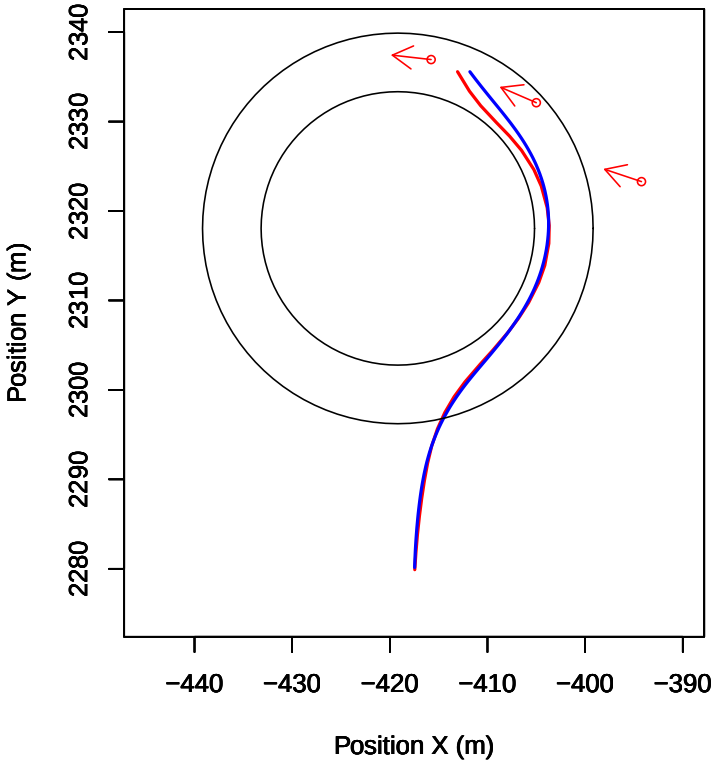

Figure 5-8: Two different types of driving tracks in the scenario with Traffic 3.

5.2.4 Summary

This section evaluated the driver maneuver prediction model in the scenarios with traffic. The conclusions answer Question 3 proposed in Chapter 3.3.1. The impact of the four types of traffic on the prediction results was investigated. The evaluation results show that 1) the with-traffic model performs better than the without-traffic model in the traffic scenarios and, 2) the modeling method with Steering-Motion and logistic-based quasi-HMM succeeds in the scenarios Traffic 1, Traffic 2, and Traffic 4. As the cyclists and car drivers can easily see each other in Traffic 3, the model's lower predictability in this situation can be tolerated.

5.3 Personalized Model Evaluation

This section presents the evaluation of the personalized predictive model. A *personalized predictive model* is defined as a model that is trained specifically for one individual driver. In this thesis, a personalized model was developed for Participant 4 in the field study (see Chapter 4.3.1). From the analysis of all participants' steering behavior in Figure 4-8, it is clear that, Participant 4 steered with a different angle and angle speed compared to the other participants.

5.3.1 Personalized Predictive Model for Participant 4 in the Field Study

The personalized predictive model was obtained by updating the original predictive model with driving behavior data from an individual driver (see Chapter 4.3.2). The original model was developed using the method presented in Chapter 4.1 and Chapter 4.2. The training data for the original model consisted of the data from Participant 1, Participant 3, Participant 5, Participant 6, and Participant 7. Participant 2 and Participant 4 were excluded because they were considered to have individual driving styles. The training data set was then updated for Participant 4 using the reinforcement-learning method introduced in Chapter 4.3. The updated training data consisted of two parts:

- Half of Participants 4's driving data (the other half was used to test the models).
- Half the data from Participant 1, Participant 3, Participant 5, Participant 6, and Participant 7 (the other half was excluded to weaken the effect of these data on the prediction).

The personalized predictive model for Participant 4 was obtained by optimizing the model parameters with the updated training data set.

5.3.2 Evaluation of the Personalized Predictive Model

The personalized predictive model was evaluated with one half of the data set from Participant 4. The given rate and the given accuracy were used to evaluate the original predictive model and the personalized predictive model. Figure 5-9 depicts the given rate and the given accuracy of these two models. It can be observed that both the given rate and the given accuracy of the personalized predictive model are higher than those of the original predictive model. Both the given rate and the given accuracy reach a peak value at Prediction Site 9. It is because the driver behaved quite differently (different steering wheel information and different motion information) at Prediction Site 9 depending on the maneuver he/she was about to execute. At Prediction Site 10, on the other hand, the behaviors for different maneuvers are quite similar. Hence, the steering wheel and motion information is more predictive at Prediction Site 9 than Prediction Site 10.

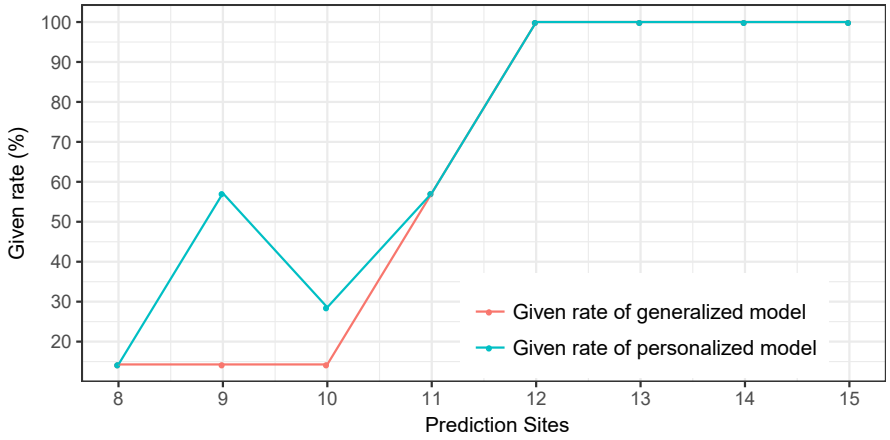

(a) Given rate for two models.

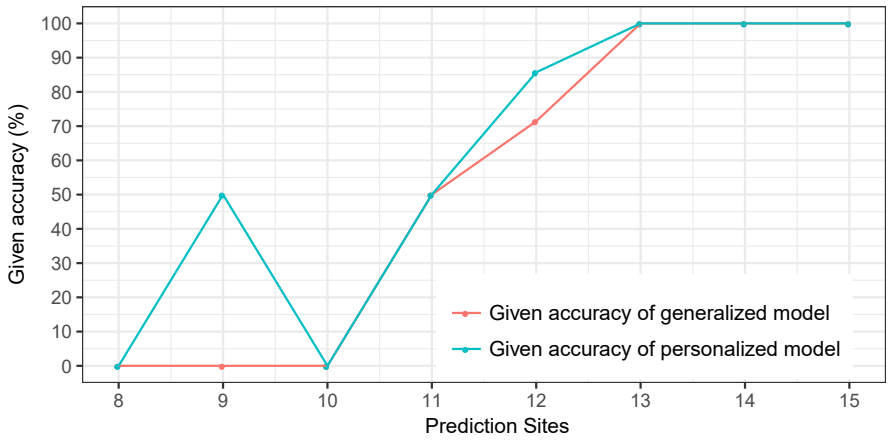

(b) Given accuracy for two models.

Figure 5-9: Given rate and given accuracy for the generalized and the personalized models.

5.3.3 Conclusion and Discussion

Conclusion: Personalized predictive models perform better for an individual driver than non-personalized predictive models

The evaluation revealed that the personalized prediction model exhibited good performance. A personalized predictive model that is updated with an individual driver's driving behavior data can learn that driver's particular driving style. For this reason, personalized predictive models are recommended for predicting driver maneuvers. However, it should be noted that, in this case, Participant 4 has a significantly different driving style than the others, so the performance of the personalized predictive model may be overestimated for an average driver.

5.3.4 Summary

In Chapter 5.3, a personalized prediction model based on a reinforcement-learning method (see Chapter 4.3) was trained and evaluated with one test driver in the field study. The personal-

ized model performed better in a direct comparison to the non-personalized model. Thus, a personalized predictive model is recommended.

5.4 Summary

This chapter evaluated the driver maneuver predictive model that was developed with the method presented in Chapter 4. A grading system was proposed to evaluate the models, which were trained with all combinations of twelve algorithms and 15 features. The grading system is Contribution 4 presented in Chapter 1.4. The model's performances were scored with the grading system and ranked on the basis of these scores. These rankings allow to conclude that 1) the features integrating steering wheel and motion information were better than the other features, 2) the complex algorithms were better than the simple algorithms, 3) the classifiers should be activated for maneuver prediction only at the reliable sites. Therefore, the important driving information and algorithms were identified, achieving Contributions 5 and 6 presented in Chapter 1.4.

The driver maneuver prediction model was evaluated in the scenarios with traffic. This evaluation covered two issues. First, it sought to identify informative features and high-performing algorithms. Second, it sought to identify the effects of other traffic participants. The evaluation showed that 1) the with-traffic model performed better than the without-traffic model in the traffic scenarios, and 2) the modeling method with Steering-Motion and logistic-based quasi-HMM succeeded in predicting driver maneuvers in most with-traffic scenarios. Therefore, the driver maneuver predictive model succeeds in scenarios with and without surrounding traffic and Contribution 7 presented in Chapter 1.4 has been achieved.

Finally, a personalized prediction model based on reinforcement learning was evaluated with a test driver. This personalized predictive model trained with that individual driver's driving behavior data performed better than a generalized predictive model trained with driving behavior data from generic drivers. Thus, Contribution 8 presented in Chapter 1.4 has been achieved.

6 Summary and Outlook

6.1 Summary

In this thesis, a driver maneuver predictive model was developed to predict whether a driver will exit or stay in a roundabout as she/he approaches an exit. To ensure that the model succeeds in predicting driver maneuvers at roundabouts with different layout designs and in different traffic situations, driving behavior data in different scenarios were gathered and investigated. This chapter summarizes the process and the results of the investigation.

First, a scenario categorization method for roundabouts was proposed, see Chapter 3. This eliminated the effects of geometric features of roundabouts on driving behavior in each specific scenario category. Eliminating these confounding variables increases the extent to which driving behavior predicts the driver maneuvers of exiting/staying in roundabouts. Two studies were conducted to propose the scenario categorization method: First, a field study was conducted in a real driving environment. On the basis of this study, a scenario categorization approach for the three investigated roundabouts was proposed. The limitations of the field study are that it only considered the investigated roundabouts and that traffic could not be controlled for. Therefore, a simulator study was designed and conducted in a laboratory under controlled experimental condition to improve upon the limitations of the field study. Driving behavior and roundabout geometric features were further analyzed in the simulator study. The local extremum of the steering angles (θ_e) and the integrated geometric feature (Geo) were defined to represent steering wheel information and the geometric features of roundabouts respectively. Then, the correlations between these two variables was calculated as a basis for categorizing roundabout scenarios. The categorization was as follows:

- Scenarios with $0\ \mathrm{rad}^2 \cdot \mathrm{m} \leq Geo \leq 40.7\ \mathrm{rad}^2 \cdot \mathrm{m}$ were defined as Scenario 1;
- Scenarios with $40.7\ \mathrm{rad}^2 \cdot \mathrm{m} \leq Geo \leq 72.4\ \mathrm{rad}^2 \cdot \mathrm{m}$ were defined as Scenario 2;
- Scenarios with $72.4\ \mathrm{rad}^2 \cdot \mathrm{m} \leq Geo \leq 108.7\ \mathrm{rad}^2 \cdot \mathrm{m}$ were defined as Scenario 3;
- Scenarios with $Geo \geq 108.7\ \mathrm{rad}^2 \cdot \mathrm{m}$ were defined as Scenario 4.

This serves as the basis for developing a driver maneuver predictive model for the four scenarios, see Chapter 4. The driver maneuver predictive model consisted of four sub-models for each of the four scenarios. Each sub-model consisted of a series of classifiers corresponding to a series of prediction sites. When a driver approached a roundabout exit, the scenario for that exit is determined using the scenario categorization method. The corresponding sub-model is then activated. The classifiers included in the sub-model calculate predicted probabilities of "Exiting" or "Staying" from the first prediction site on until a final result of "Exiting" or "Staying" is obtained. This is the process through which the model predicts the driver maneuver. Driving behavior data and machine-learning algorithms were used to train the classifiers. In addition, a

method to update the model into a personalized predictive model was proposed. This method makes it possible for a model to learn an individual driver's driving style on-line. This allows the model to predict the maneuvers of a driver with any type of driving style at a roundabout with any type of layout.

The driver maneuver predictive model was then evaluated to ensure that the model can successfully predict driver maneuvers at roundabouts, see Chapter 5. Models trained with all possible combinations of different algorithms and different features were evaluated [TIS+07, NMI+08, SH14, GJW+16, TMF16]. The models' performances were scored using a proposed grading system: The models receive one positive point when they made a correct prediction for a given test drive, zero points when they provided no result for a given test drive, and one negative point when they made an incorrect prediction result for a given test drive. An effect size analysis of the models' performance allowed the best features *Steering* and *Motion* and the best algorithm *logistic-based quasi-HMM* to be selected. The model's performance was as follows:

- In Scenario 1, the first reliable prediction occurred at the prediction site at a distance of about 10 m from the oncoming exit. At this prediction site, the model's average performance score was 92.0, the average given rate was 97.67%, and the given accuracy was 97.15%.

- In Scenario 2, the first reliable prediction occurred at the prediction site at a distance of 10 - 14 m from the oncoming exit. At this prediction site, the model's average performance score was 94.0, the average given rate was 99.76%, and the given accuracy was 97.14%.

- In Scenario 3, the first reliable prediction occurred at the prediction site at a distance of 12 m from the oncoming exit. At this prediction site, the model's average performance score was 93.4, the average given rate was 99.06%, and the given accuracy was 97.13%.

- In Scenario 4, the first reliable prediction occurred at the prediction site at a distance of 7.5 - 10.5 m from the oncoming exit. At this prediction site, the model's average performance score was 96.4, the given rate was 97.99%, and the given accuracy was 99.18%.

Then, the driver maneuver predictive model was evaluated in the scenarios with traffic to ensure that the model can also predict driver maneuvers at roundabouts with traffic. The four types of traffic scenarios discussed in Chapter 3.3.1 were investigated. In the traffic scenarios, the model's performance was as follows:

- In the scenario of Traffic 1, the first reliable prediction occurred at the prediction site at a distance of about 9.5 m from the oncoming exit. At this prediction site, the average performance score was 91.2, the average given rate was 100.00%, and the given accuracy was 93.91%.

- In the scenario of Traffic 2, the first reliable prediction occurred at the prediction site at a distance of about 10 m from the oncoming exit. At this prediction site, the average performance score was 85.3, the average given rate was 98.08%, and the given accuracy was 95.83%.

- In the scenario of Traffic 3, the first reliable prediction occurred at the prediction site at a distance of about 4.5 m from the oncoming exit. At this prediction site, the average performance score was 92.0, the average given rate was 97.92%, and the given accuracy was 100.00%.

- In the scenario of Traffic 4, the first reliable prediction occurred at the prediction site at a distance of about 9.0 m from the oncoming exit. At this prediction site, the average performance score was 89.8, the average given rate was 100.00%, and the given accuracy was 97.92%.

Drivers may behave differently even in the same roundabout scenario due to their different driving styles. Therefore, a method for developing a personalized predictive model was proposed. The model was evaluated with a test driver. The given rate and the given accuracy of the personalized predictive model were higher than in the original predictive model.

6.2 Conclusions and Contributions

The work related to this thesis can be summarized as follows:

- Human driving behavior in roundabouts is affected by the geometric features of roundabouts, and this impact can be expressed quantitatively (The details are presented in Chapter 3). This finding is Contribution 1 presented in Chapter 1.4.

- Roundabout scenarios can be categorized according to relevant geometric features and the human driving behavior associated with them (The details of this are also presented in Chapter 3). The categorization method is Contribution 2 presented in Chapter 1.4.

- The scenario categorization method can be used to structure the driver maneuver predictive model. The model includes four sub-models corresponding to four scenario categories (The details are presented in Chapter 4). The structure is Contribution 3 presented in Chapter 1.4. This is why information about roundabout layouts is needed for the driver maneuver predictive model.

- Steering-Motion is the most informative feature. Steering (steering angle and steering angle velocity) and Motion (velocity and acceleration) are most important for predicting driver maneuvers. The reason why Steering information is significantly better than other information is that roundabout layouts determine steering behavior (The details are discussed in Chapter 5). Therefore, the information that is needed to predict driver maneuvers at roundabouts can be identified, which is Contribution 5 in Chapter 1.4.

- The complex algorithms perform better than the simple algorithms. The complex algorithms treat the classifiers included in a given sub-model as a Markov chain, i.e., when the present classifier makes a decision at the present prediction site, it considers both the current driving behavior information and the previous classifier's suggestion (The details

of this are also discussed in Chapter 5). Thus, complex algorithms are recommended for predicting driver maneuvers at roundabouts. This finding is Contribution 6 in Chapter 1.4.

- The model's prediction results before the reliable prediction sites have a quite low given accuracy (even lower than 90%). These results could weaken user's trust in the model. Therefore, it is recommended that the classifiers only at the reliable prediction sites are activated. That is to say, the model should start offering prediction results of "Staying", "Leaving", or "NA (No result available)" at the first reliable prediction site and continue until the first full-score prediction site (The details of this are also presented in Chapter 5). This finding makes the driver maneuver predictive model reliable in real driving situations, thus contributing to model development. An accurate positioning system is needed for the maneuver predictive model in order to obtain precise position information about prediction sites.

- The model used in scenarios with traffic needs to be trained with data acquired from scenarios with the same type of traffic. Drivers behave differently in with-traffic scenarios and without-traffic scenarios. As a result, the model trained with driving data from without-traffic scenarios does not make successful predictions in with-traffic scenarios (The details of this are also discussed in Chapter 5). Nevertheless, the driver maneuver predictive model succeeds in most traffic scenarios. This finding is Contribution 7 in Chapter 1.4.

- Personalized predictive models perform better for individual drivers because they can adapt to drivers with different driving styles caused by different driving experience or personalities. A personalized predictive model trained with an individual driver's driving behavior data can learn that particular driver's driving style (The details of this are also presented in Chapter 5). Thus, personalized predictive models are recommended. These findings form Contribution 8 in Chapter 1.4.

The main achievement of this work is that a driver maneuver predictive model was developed for compact roundabouts with all types of layouts and drivers with any driving styles. Therefore, this achievement fills a research gap, namely predicting driver maneuvers in roundabouts on a tactical timescale, see Table 6-1. The given rate and given accuracy of the model are above 97% in the scenarios without traffic and above 93% in the scenario with surrounding cyclists about 10 m before the relevant roundabout exits.

Table 6-1: State of the art and the results of this thesis.

Study	Measure	Algorithm	Evaluation	Result
This work	Steering wheel angle, steering angle velocity, velocity, and acceleration of the ego car	Logistic-based quasi-HMM	Given rate and given accuracy	Above 97% of given rate and given accuracy in the scenario without traffic and above 93% of given rate and given accuracy in the scenario with surrounding cyclists at about 10 m before the relevant exits of roundabouts
Taguchi et al. (2007) [TIS+07]	Ego car velocity, leading-car velocity, and the distance between the ego car and leading cars	Logistic regression	Detection rate	Detection rate of 80.0%
Naito et al. (2008) [NMI+08]	Accelerator throttle, brake, and velocity of the ego car	K-means	Accuracy	95.6% as early as 5 seconds before the intersections
Lefevre et al. (2011) [LIGL11, LLIG11]	Turn signal of the ego car and the information about the entry lanes	Bayesian network	Accuracy	100% approximately 10 m away from the exit of the intersection.
Sathyanaray-ana et al. (2012) [SSH12]	Velocity, steering wheel angle, engine RPM, and gas/brake pedal pressure information	SVM	Accuracy	Accuracy of 89%
Liebner et al. (2013) [LRKS13, LKB+13]	Ego car velocity	Intelligent driver model (IDM)	Detection rate	Detection rate of 95% Without traffic whereas 55% in the presence of preceding vehicles

Continued on next page

Table 6-1 – continued from previous page

Study	Measure	Algorithm	Evaluation	Result
Gadepally et al. (2014) [GKO14]	Velocity, position, and orientation of the ego car	HMM	Number of correct predictions	Correct recognition for 38 of the 40 observation sequences.
Streubel et al. (2014) [SH14]	Velocity, acceleration, and yaw value of ego car	HMM	Accuracy	Above 90% as early as 7 seconds before entering the intersections
Tang et al. (2015) [TKG15]	Position, velocity, acceleration, yaw value of the ego car and lane-level maps	SVM	accuracy	90% as early as 1.6 seconds before the intersection
Gross et al. (2016) [GJW+16]	Position, heading, acceleration, and velocity of the ego car	RF	Recall	76% at 30 m before the relevant intersection center
Tawari et al. (2016) [TMF16]	The information extracted from driver camera, scene camera, and navigation camera	RF	Accuracy	Over 80% 2 seconds before the maneuver event
Barbier et al. (2017) [BLSIG17]	Velocity, position, and heading of the ego car (20% of real driving data and 80% of data from simulated environment)	RF	Accuracy	Accuracy of 80.3%
Phillips et al. (2017) [PWK17]	Ego car velocity and acceleration, the lane-relative heading, the number of lanes, and the headway distance to the preceding vehicle	Recurrent Neural Networks (RNNs)	Accuracy	85% as early as 150 m before the intersection

6.3 Limitations and Outlook

This work has achieved its goal of predicting driver maneuvers at compact roundabouts. However, there are still some limitations. The limitations and possible corresponding solutions are as follows:

- The scenarios with different types of surrounding traffic combined with different roundabout layouts are not investigated. The two simulator study sessions in this research focused on separately different roundabout layouts and surrounding traffic. However, in real driving situations, there can be different types of traffic at roundabouts with different layouts. Thus, future work will need to investigate scenarios with different types of surrounding traffic combined with different roundabout layouts. A simulator study is recommended to design such scenarios because different types of traffic and roundabout layouts can be manipulated in a simulation environment. The roundabouts with different layouts designed for Session 1 of the simulator study can be used to test different types of surrounding traffic in future research.

- Too little personalized data were used to train the predictive model in this work. It is expected that the personalized predictive models can be improved with more training data. Therefore, future work should attempt to demonstrate whether the more data from a given driver are integrated into the training database, the more the model learns about this driver and the better the personalized model will perform.

- A driver with a significantly different driving style was chosen as the test person for personalized predictive model in this work. This significant difference might have caused the performance of the personalized predictive model to be overestimated for an average driver. Therefore, it will be necessary to evaluate the personalized predictive model with more test drivers in future work. These evaluations will reveal for which driving styles, the personalized model can succeed in maneuver prediction.

- Only compact roundabouts were investigated in this thesis. Other types of roundabouts aside from compact roundabouts can become the object of future investigations, such as mini-roundabouts (diameter of 13 and 25 m) with a traversable island, larger roundabouts (40 - 60 m) with two circulating lanes, and turbo-roundabouts [Bri11]. In performing such analyses, it is suggested that investigating driver behavior in the relevant scenarios first and before, exploring the informative features, such as car or driver information, traffic information, or roundabout layout information, that can predict driver maneuvers.

The driver maneuver predictive model can still be improved even though it is already able to successfully predict driver maneuvers at single-lane roundabouts. Further investigations can certainly improve the robustness of the model in different scenarios.

A Evaluation Scores for All Algorithms and Features

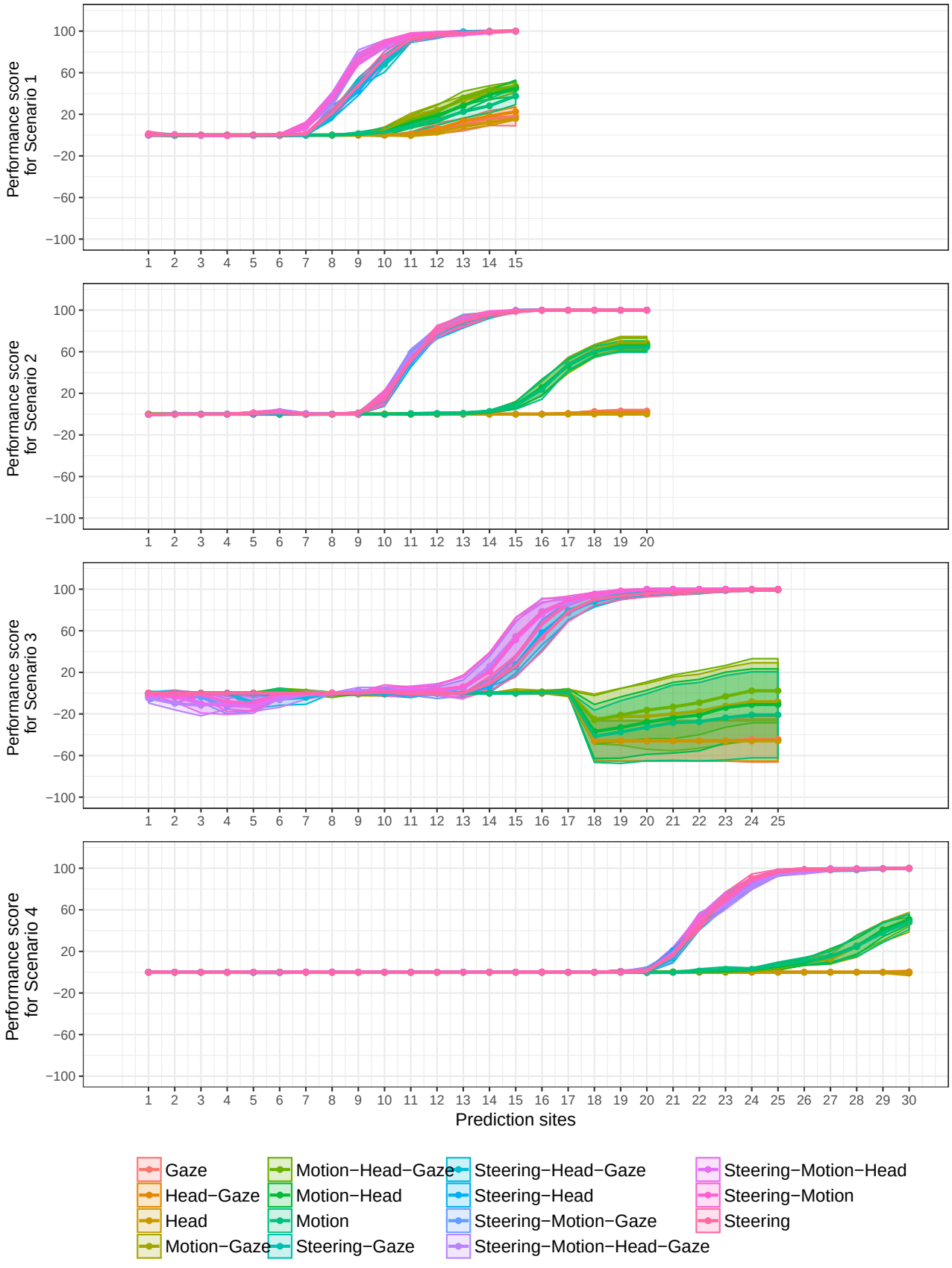

Figure A-1: Performance scores of linear SVM-based quasi-HMM with all features.

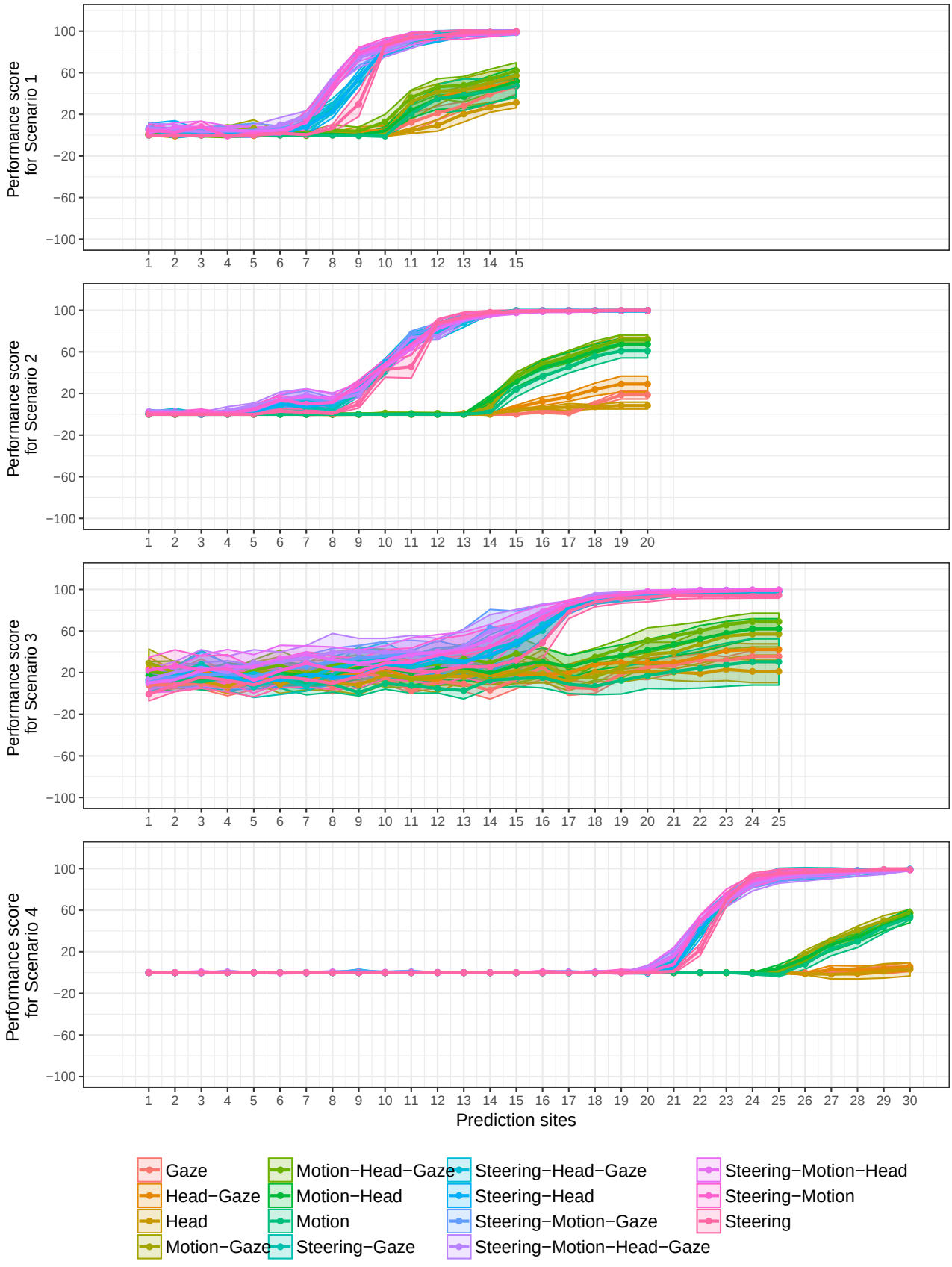

Figure A-2: Performance scores of Gaussian SVM-based quasi-HMM with all features.

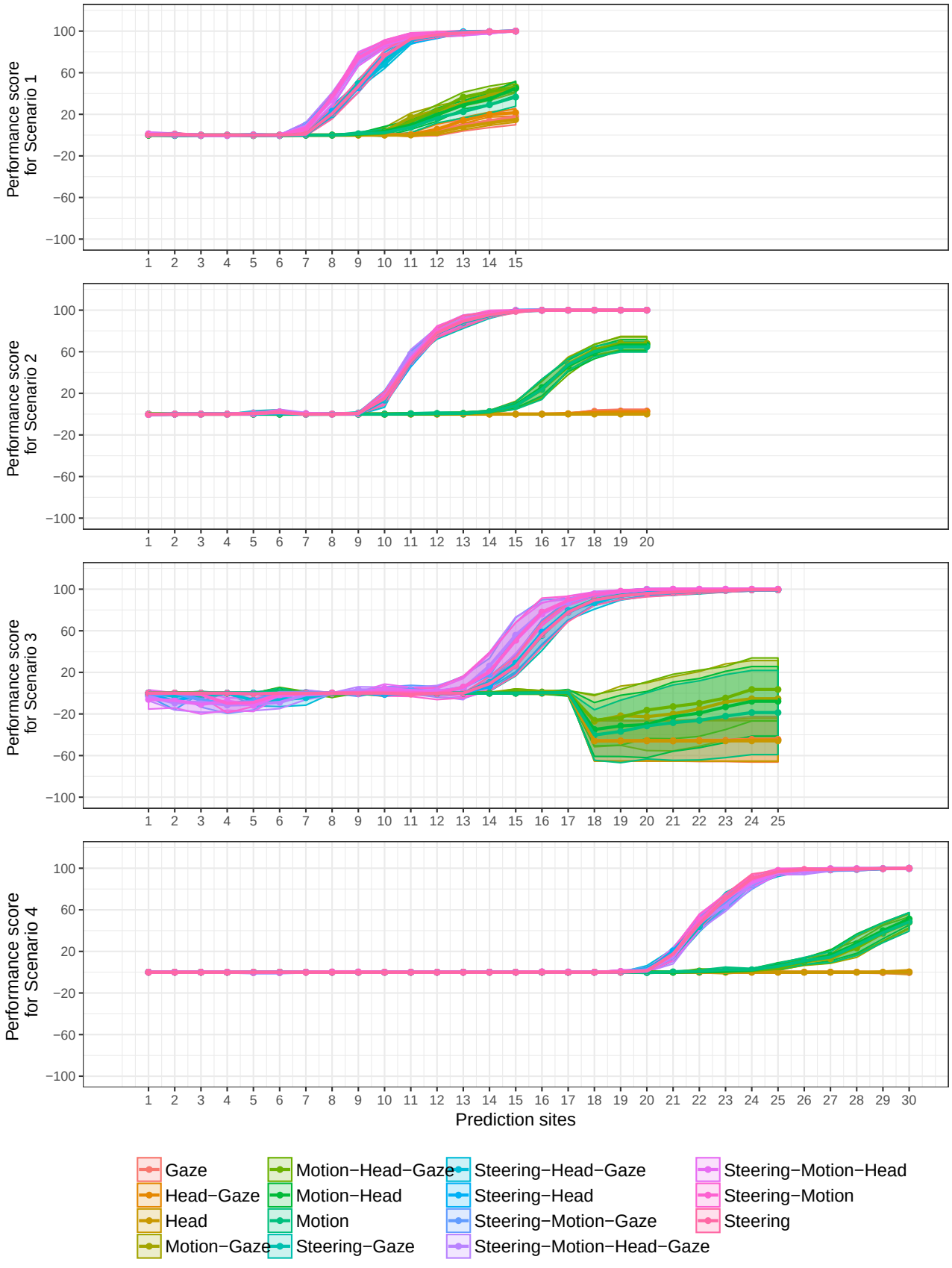

Figure A-3: Performance scores of polynomial SVM-based quasi-HMM with all features.

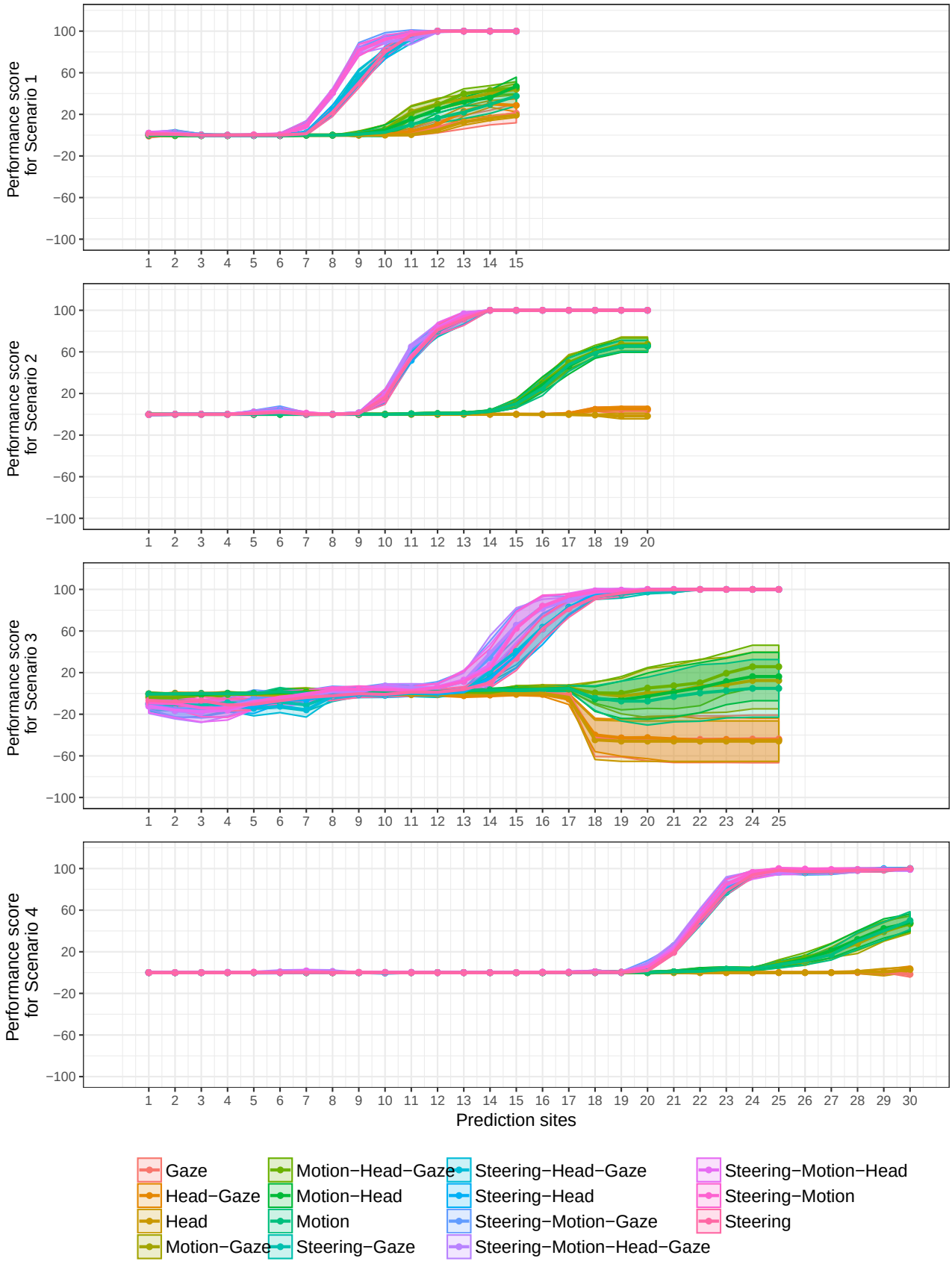

Figure A-4: Performance scores of logistic-based quasi-HMM with all features.

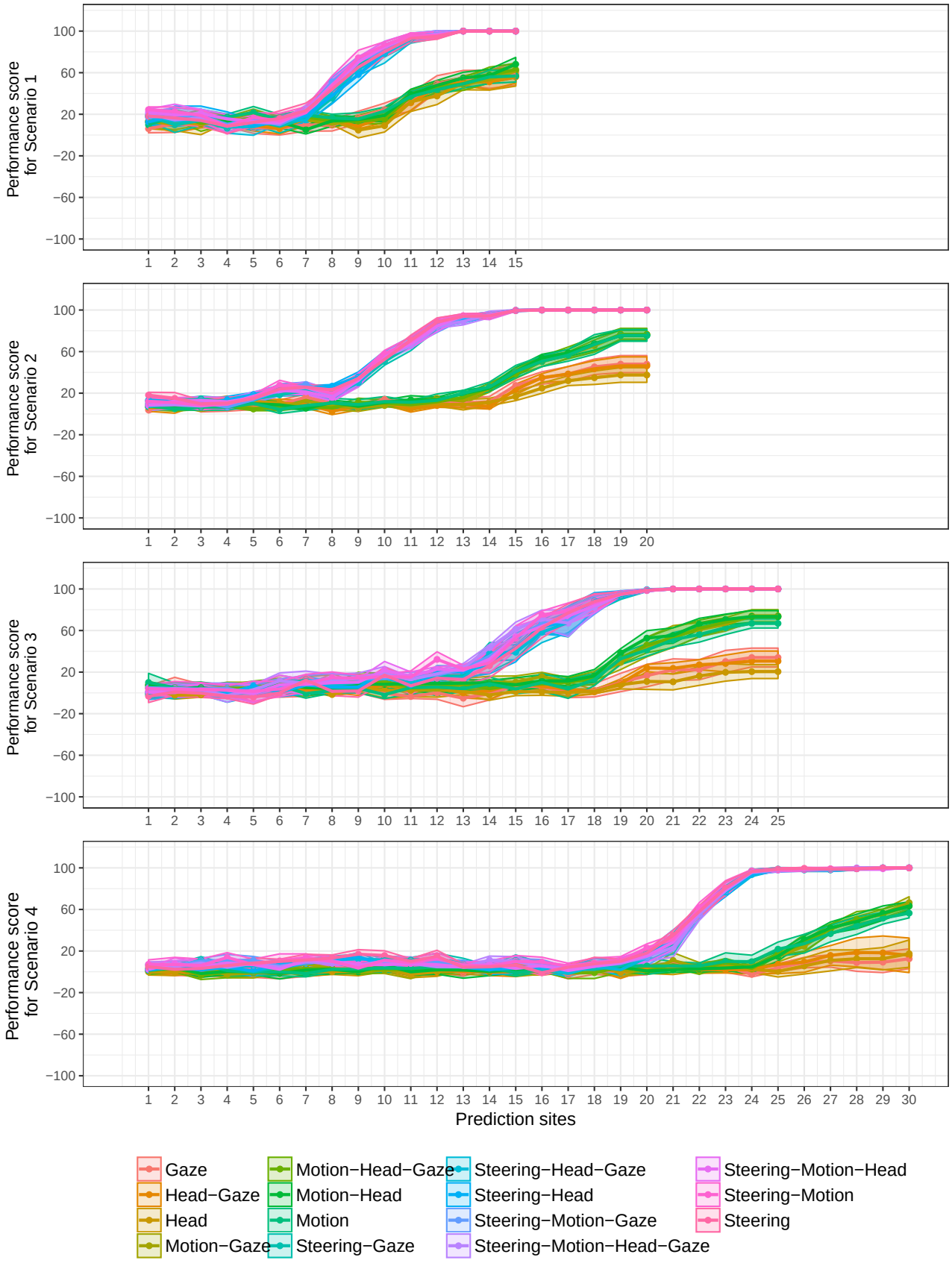

Figure A-5: Performance scores of Ada-based quasi-HMM with all features.

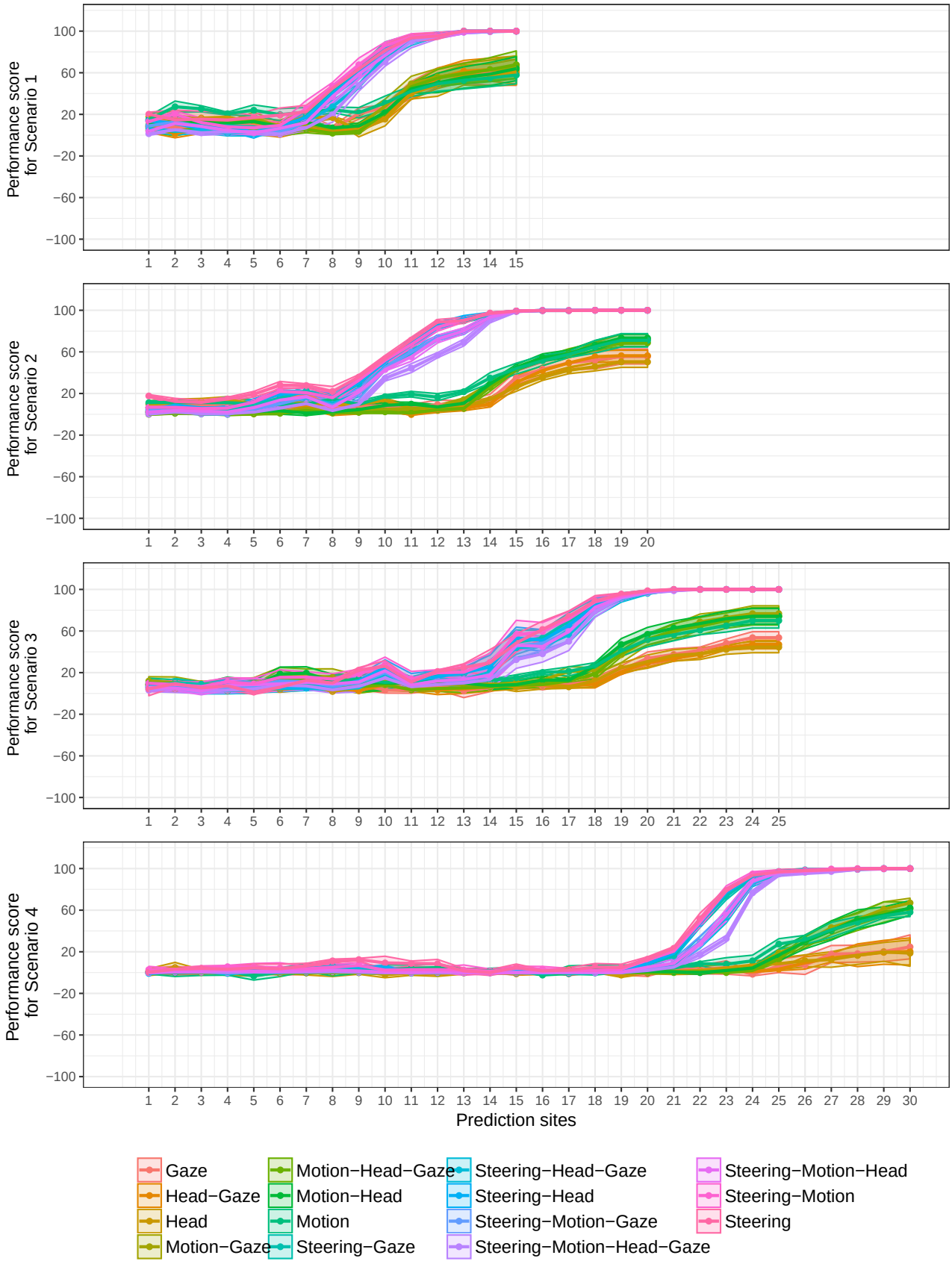

Figure A-6: Performance scores of RF-based quasi-HMM with all features.

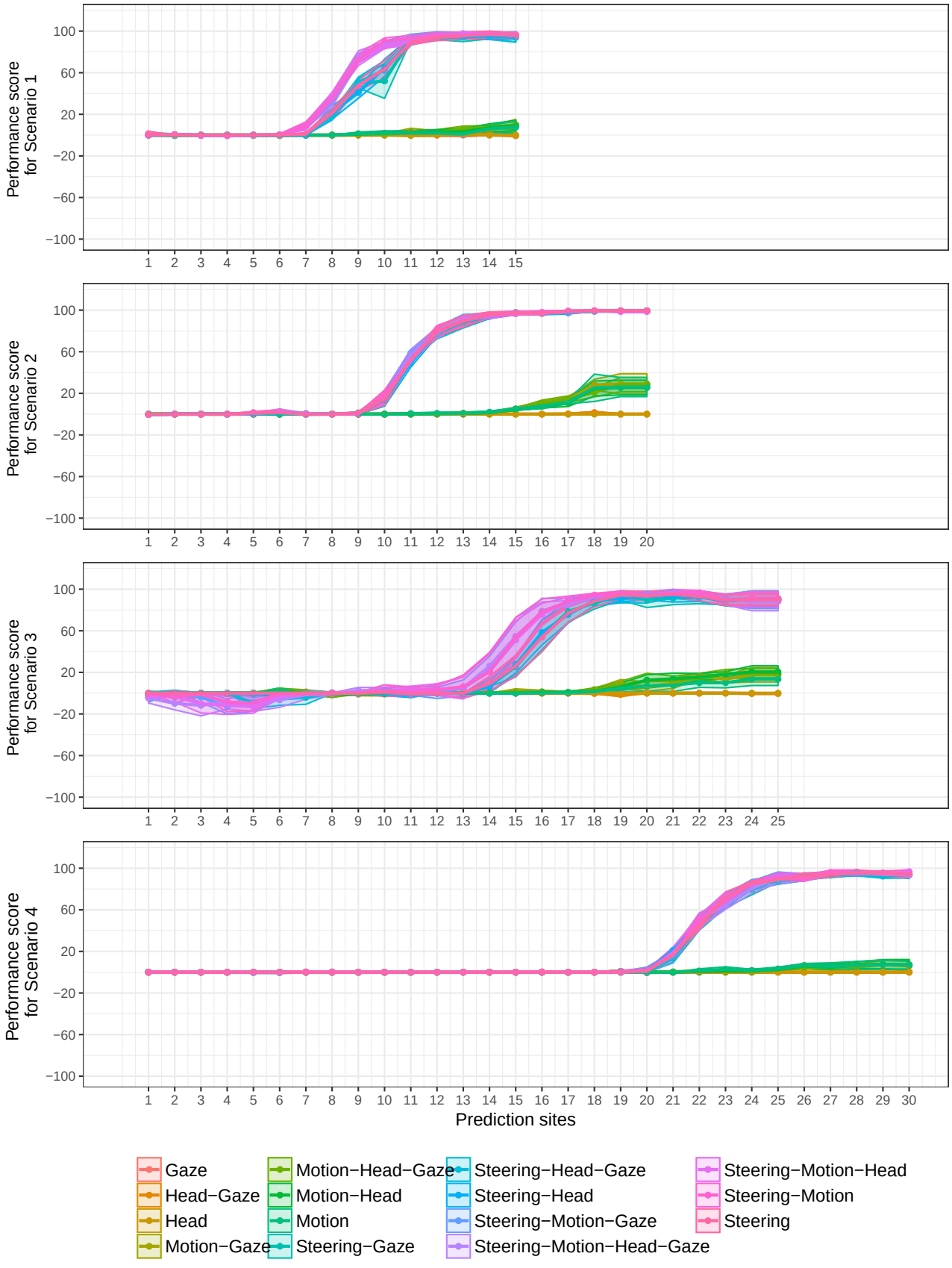

Figure A-7: Performance scores of linear SVM with all features.

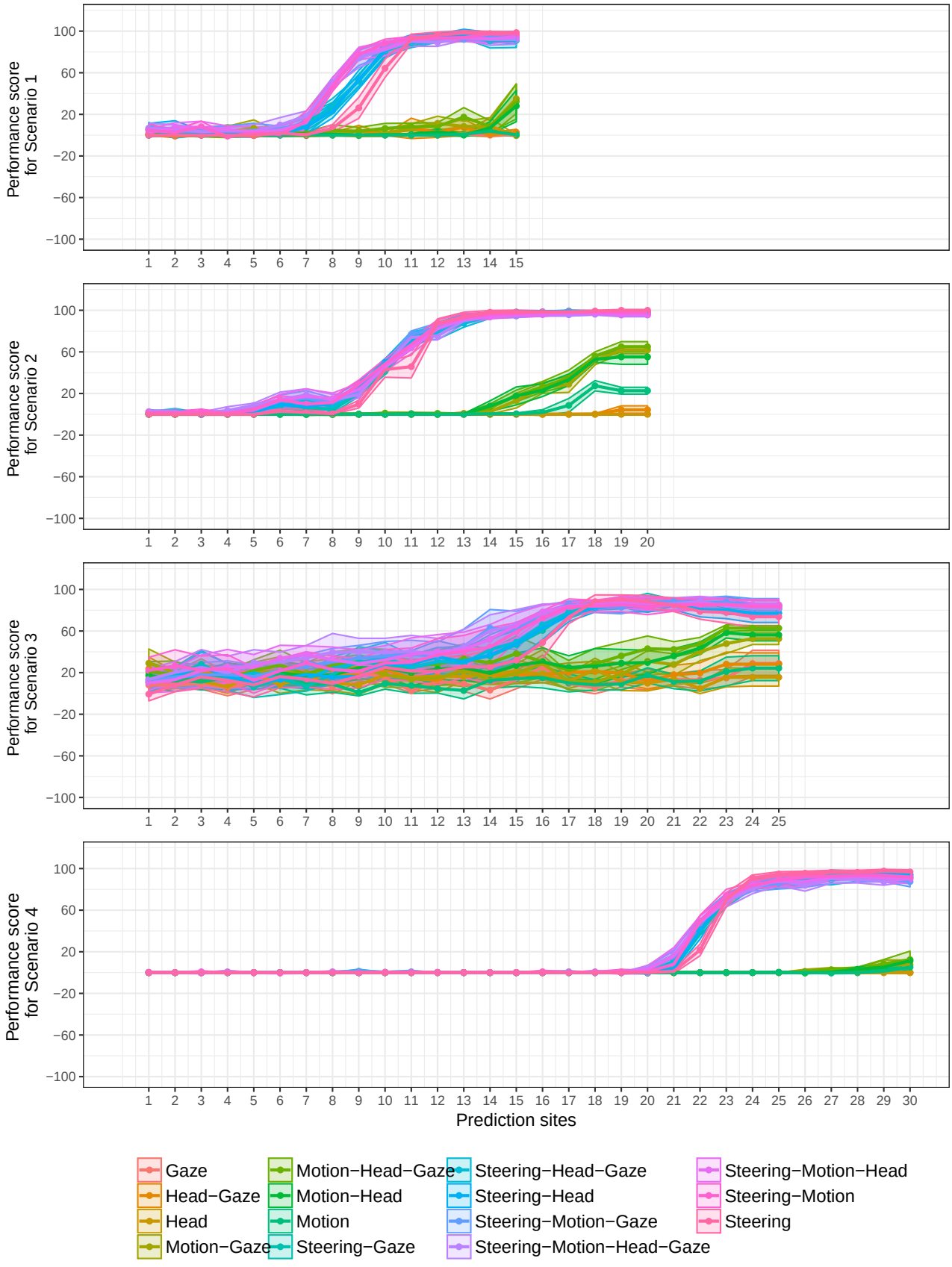

Figure A-8: Performance scores of Gaussian SVM with all features.

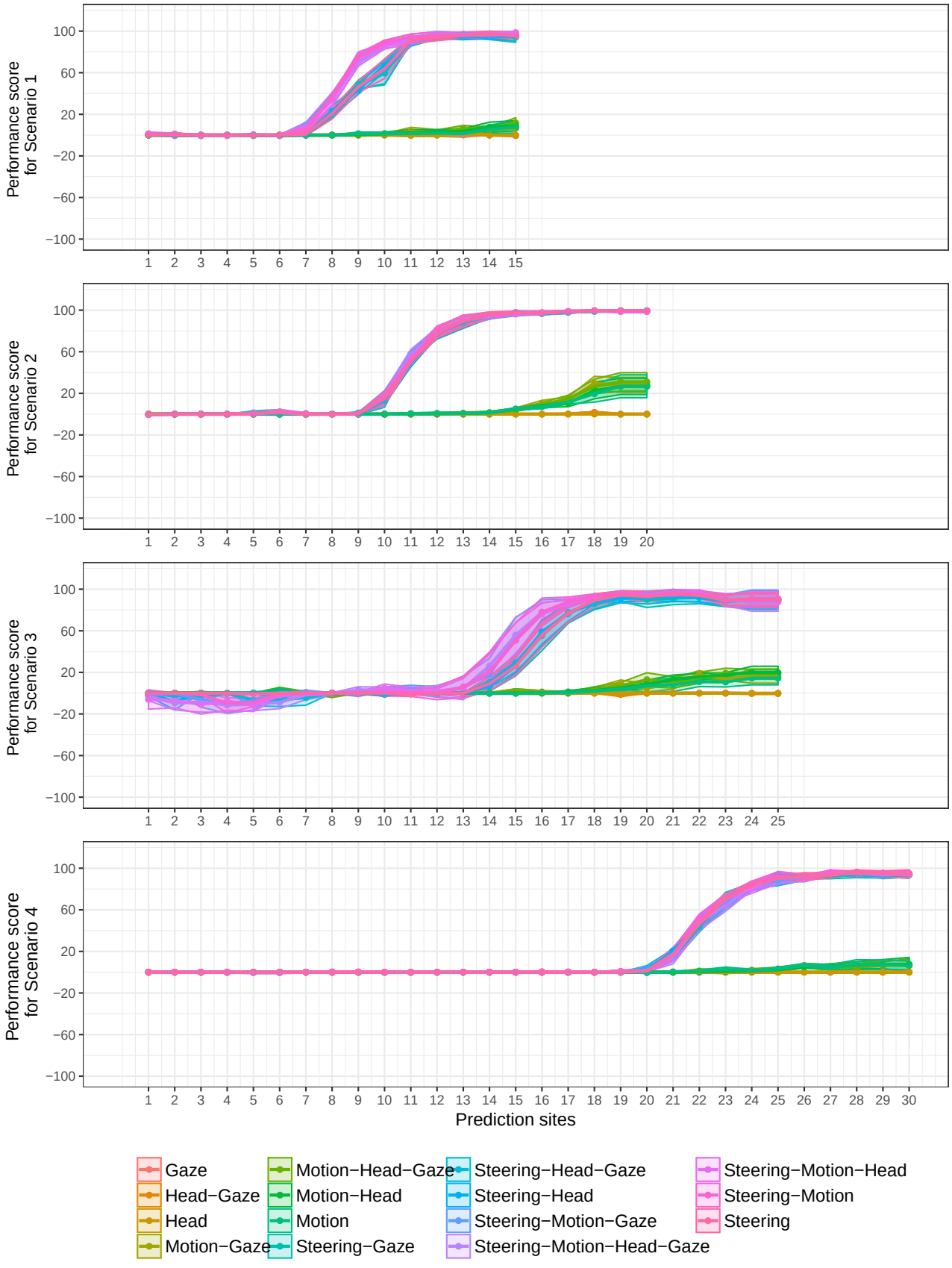

Figure A-9: Performance scores of polynomial SVM with all features.

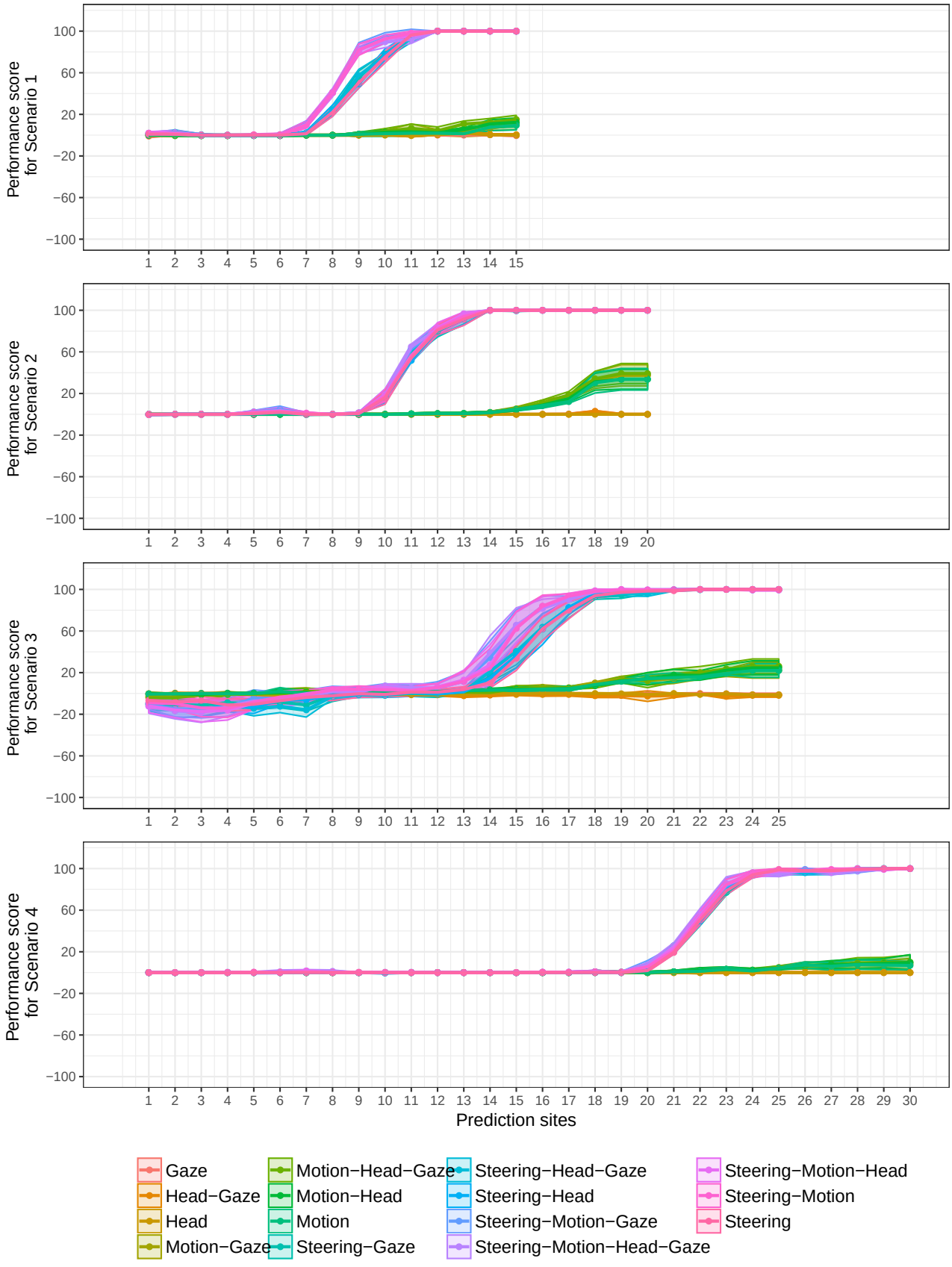

Figure A-10: Performance scores of logistic regression with all features.

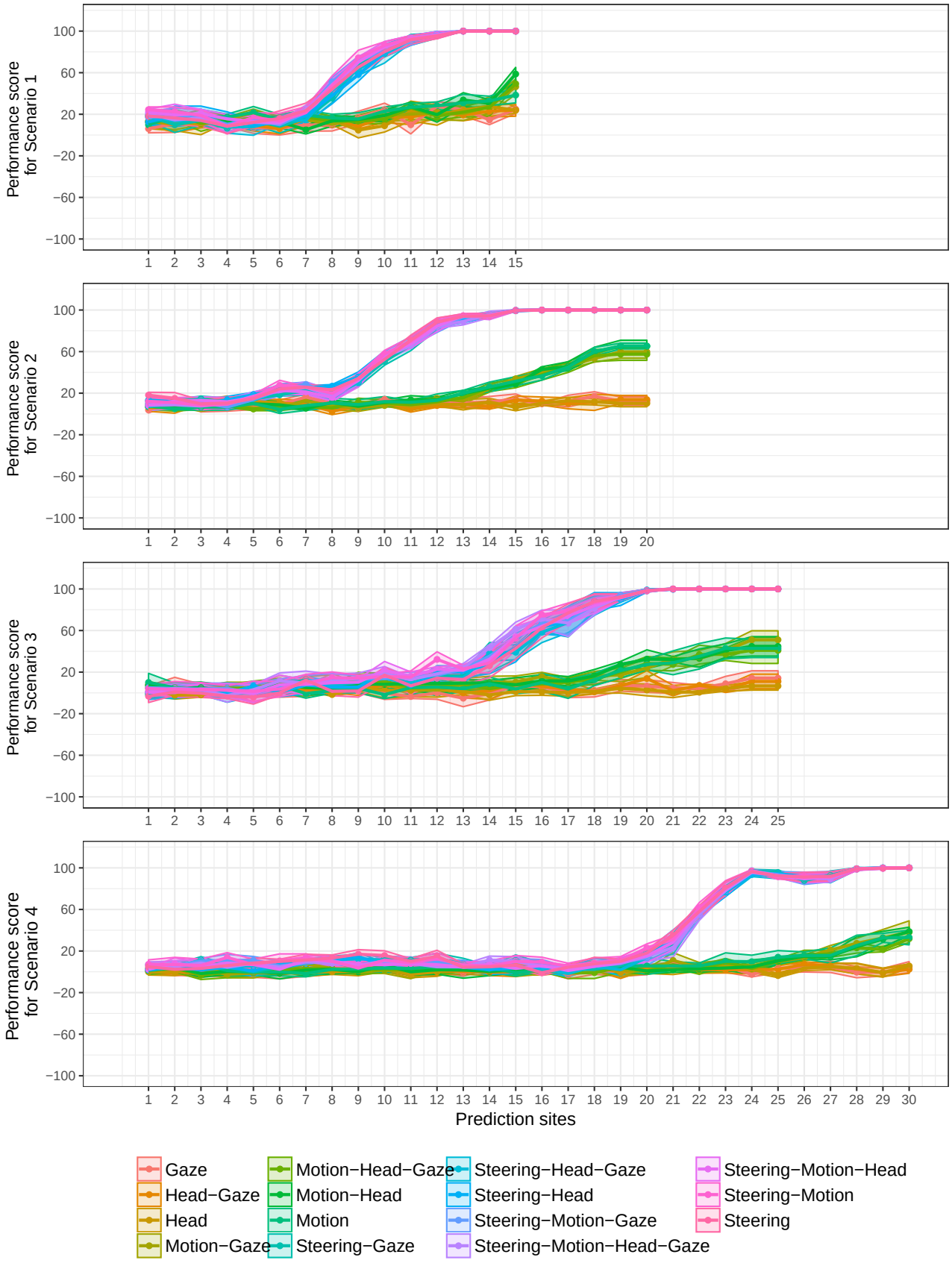

Figure A-11: Performance scores of AdaBoost with all features.

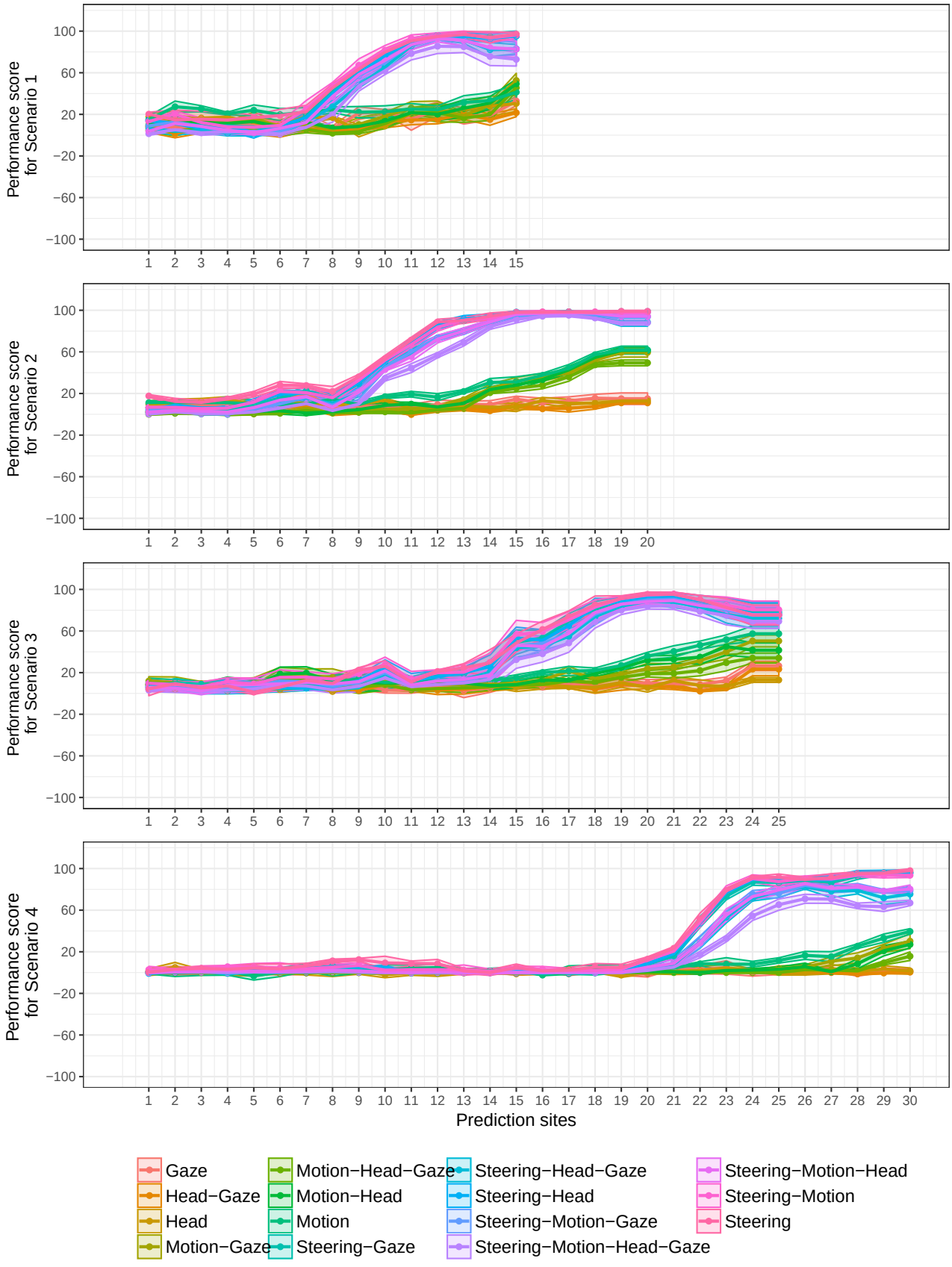

Figure A-12: Performance scores of random forest with all features.

B Effect Size Results in the Four Scenarios

Table B-1: Effect size results at Prediction Site 9 in Scenario 1.

Feature	Cohen's d	Rank
Steering-Motion-Head_with_logistic	9.633974	1
Steering-Motion-Head-Gaze_with_HMMLogistic	9.25089	2
Steering-Motion-Head-Gaze_with_logistic	9.25089	2
Steering-Motion-Head_with_HMMLogistic	9.031955	4
Steering-Motion-Gaze_with_HMMSVMlinear	8.635495	5
Steering-Motion-Gaze_with_SVMlinear	8.635495	5
Steering-Motion_with_SVMpoly	8.529764	7
Steering-Motion_with_logistic	8.39962	8
Steering-Motion-Gaze_with_HMMLogistic	8.282874	9
Steering-Motion-Gaze_with_logistic	8.282874	9
Steering-Motion_with_HMMLogistic	8.271929	11
Steering-Motion_with_HMMSVMpoly	8.239428	12
Steering-Motion_with_SVMrbf	8.238887	13
Steering-Motion-Gaze_with_HMMSVMpoly	8.090066	14
Steering-Gaze_with_Ada	8.068367	15
Steering-Gaze_with_HMMAda	8.068367	15
Steering-Motion-Gaze_with_SVMpoly	8.03073	17
Steering-Motion_with_HMMSVMrbf	8.005058	18
Steering-Motion_with_HMMSVMlinear	7.958817	19
Steering-Motion_with_SVMlinear	7.958817	19
Steering-Motion-Gaze_with_Ada	7.76075	21
Steering-Motion-Gaze_with_HMMAda	7.76075	21
Steering-Motion-Head_with_SVMrbf	7.569072	23
Steering-Motion-Head_with_Ada	7.426857	24
Steering-Motion-Head_with_HMMAda	7.426857	24
Steering-Motion-Head-Gaze_with_HMMSVMpoly	7.35205	26
Steering-Motion-Head-Gaze_with_SVMpoly	7.35205	26
Steering-Motion-Head-Gaze_with_SVMlinear	7.229652	28
Steering-Motion-Head_with_HMMSVMrbf	7.082734	29
Steering-Motion-Head-Gaze_with_Ada	7.003279	30
Steering-Motion-Head-Gaze_with_HMMAda	7.003279	30
Steering-Motion-Head_with_HMMSVMlinear	6.99497	32
Steering-Motion-Head_with_SVMlinear	6.924799	33
Steering_with_HMMRF	6.759392	34
Steering_with_RF	6.759392	34
Steering-Motion-Head-Gaze_with_HMMSVMlinear	6.666996	36

Continued on next page

Table B-1 – continued from previous page

Feature	Cohen's d	Rank
Steering-Gaze_with_HMMRF	6.493755	37
Steering-Gaze_with_RF	6.493755	37
Steering-Motion-Head_with_HMMSVMpoly	6.474157	39
Steering-Motion-Head_with_SVMpoly	6.474157	39
Steering-Motion-Gaze_with_HMMSVMrbf	6.344669	41
Steering-Motion-Gaze_with_SVMrbf	6.344669	41
Steering-Motion_with_Ada	6.30509	43
Steering-Motion_with_HMMAda	6.30509	43
Steering-Motion_with_RF	6.129666	45
Steering-Motion-Gaze_with_HMMRF	6.099755	46
Steering-Motion-Head_with_RF	6.038518	47
Steering-Motion_with_HMMRF	6.035772	48
Steering-Head_with_HMMRF	5.948457	49
Steering-Head_with_RF	5.948457	49
Steering-Motion-Head_with_HMMRF	5.851821	51
Steering-Head-Gaze_with_Ada	5.738356	52
Steering-Head-Gaze_with_HMMAda	5.738356	52
Steering-Motion-Gaze_with_RF	5.640505	54
Steering_with_Ada	5.438933	55
Steering_with_HMMAda	5.438933	55
Steering-Motion-Head-Gaze_with_HMMSVMrbf	5.406714	57
Steering-Motion-Head-Gaze_with_SVMrbf	5.406714	57
Steering-Head_with_HMMLogistic	5.291763	59
Steering-Head-Gaze_with_HMMRF	5.052442	60
Steering-Head-Gaze_with_HMMSVMrbf	5.035826	61
Steering-Gaze_with_HMMSVMlinear	4.95578	62
Steering-Head-Gaze_with_HMMLogistic	4.948414	63
Steering-Head-Gaze_with_logistic	4.948414	63
Steering-Head-Gaze_with_RF	4.947423	65
Steering-Head_with_Ada	4.912313	66
Steering-Head_with_HMMAda	4.912313	66
Steering-Gaze_with_HMMLogistic	4.833477	68
Steering-Gaze_with_logistic	4.833477	68
Steering-Head-Gaze_with_HMMSVMpoly	4.81795	70
Steering-Head-Gaze_with_HMMSVMlinear	4.77612	71
Steering-Gaze_with_HMMSVMpoly	4.752769	72
Steering-Head-Gaze_with_SVMrbf	4.7385	73
Steering-Gaze_with_HMMSVMrbf	4.731572	74
Steering-Head_with_logistic	4.7047	75
Steering-Gaze_with_SVMlinear	4.637754	76

Continued on next page

Table B-1 – continued from previous page

Feature	Cohen's d	Rank
Steering-Head-Gaze_with_SVMpoly	4.625471	77
Steering-Gaze_with_SVMpoly	4.61876	78
Steering-Head-Gaze_with_SVMlinear	4.536658	79
Steering_with_HMMLogistic	4.525856	80
Steering_with_logistic	4.525856	80
Steering-Gaze_with_SVMrbf	4.432906	82
Steering_with_HMMSVMlinear	4.276327	83
Steering_with_SVMlinear	4.276327	83
Steering-Head_with_HMMSVMrbf	4.149998	85
Steering-Motion-Head-Gaze_with_RF	4.037306	86
Steering-Motion-Head-Gaze_with_HMMRF	3.958967	87
Steering-Head_with_HMMSVMpoly	3.933453	88
Steering-Head_with_SVMpoly	3.790475	89
Steering_with_SVMpoly	3.770218	90
Steering_with_HMMSVMpoly	3.731531	91
Steering-Head_with_HMMSVMlinear	3.663084	92
Steering-Head_with_SVMrbf	3.56341	93
Steering-Head_with_SVMlinear	3.075411	94
Steering_with_HMMSVMrbf	1.001903	95
Steering_with_SVMrbf	0.819817	96
Motion_with_RF	0.65593	97
Motion_with_HMMRF	0.625587	98
Gaze_with_RF	0.518556	99
Gaze_with_HMMRF	0.490973	100
Gaze_with_Ada	0	101
Gaze_with_HMMAda	0	101
Motion-Gaze_with_Ada	-0.15069	103
Motion-Gaze_with_HMMAda	-0.15069	103
Motion_with_Ada	-0.18483	105
Motion_with_HMMAda	-0.18483	105
Motion-Head_with_Ada	-0.31327	107
Motion-Head_with_HMMAda	-0.31327	107
Motion-Head-Gaze_with_Ada	-0.60908	109
Motion-Head-Gaze_with_HMMAda	-0.60908	109
Motion-Gaze_with_HMMRF	-0.77935	111
Motion-Gaze_with_RF	-0.78732	112
Motion-Head_with_HMMRF	-1.27064	113
Head_with_Ada	-1.33864	114
Head_with_HMMAda	-1.33864	114
Head-Gaze_with_Ada	-1.38109	116

Continued on next page

Table B-1 – continued from previous page

Feature	Cohen's d	Rank
Head-Gaze_with_HMMAda	-1.38109	116
Motion-Head_with_RF	-1.4211	118
Head_with_HMMRF	-1.59595	119
Head_with_RF	-1.59595	119
Head-Gaze_with_SVMrbf	-1.68551	121
Head-Gaze_with_HMMSVMrbf	-1.85497	122
Motion-Head-Gaze_with_HMMSVMrbf	-1.93756	123
Head-Gaze_with_HMMRF	-1.96048	124
Head-Gaze_with_RF	-1.9649	125
Motion-Head-Gaze_with_SVMrbf	-1.96621	126
Motion-Head-Gaze_with_HMMRF	-2.16845	127
Motion-Head-Gaze_with_RF	-2.28634	128
Motion-Head-Gaze_with_HMMLogistic	-2.50573	129
Motion_with_HMMSVMlinear	-2.64859	130
Motion_with_HMMSVMpoly	-2.64859	130
Motion_with_SVMlinear	-2.64859	130
Motion_with_SVMpoly	-2.64859	130
Motion-Gaze_with_HMMLogistic	-2.67602	134
Motion-Gaze_with_logistic	-2.67602	134
Motion-Head-Gaze_with_logistic	-2.67602	134
Motion-Head_with_HMMLogistic	-2.67602	134
Motion-Head_with_logistic	-2.67602	134
Motion_with_HMMLogistic	-2.67602	134
Motion_with_logistic	-2.67602	134
Motion-Head-Gaze_with_HMMSVMlinear	-2.78269	141
Motion-Head-Gaze_with_SVMlinear	-2.78269	141
Motion-Head_with_HMMSVMlinear	-2.78269	141
Motion-Head_with_HMMSVMpoly	-2.78269	141
Motion-Head_with_SVMlinear	-2.78269	141
Motion-Gaze_with_HMMSVMlinear	-2.87513	146
Motion-Gaze_with_HMMSVMpoly	-2.87513	146
Motion-Gaze_with_SVMlinear	-2.87513	146
Motion-Gaze_with_SVMpoly	-2.87513	146
Motion-Head-Gaze_with_HMMSVMpoly	-2.87513	146
Motion-Head-Gaze_with_SVMpoly	-2.87513	146
Motion-Head_with_SVMpoly	-2.87513	146
Gaze_with_HMMLogistic	-2.98075	153
Gaze_with_HMMSVMlinear	-2.98075	153
Gaze_with_HMMSVMpoly	-2.98075	153
Gaze_with_HMMSVMrbf	-2.98075	153

Continued on next page

Table B-1 – continued from previous page

Feature	Cohen's d	Rank
Gaze_with_logistic	-2.98075	153
Gaze_with_SVMlinear	-2.98075	153
Gaze_with_SVMpoly	-2.98075	153
Gaze_with_SVMrbf	-2.98075	153
Head-Gaze_with_HMMLogistic	-2.98075	153
Head-Gaze_with_HMMSVMlinear	-2.98075	153
Head-Gaze_with_HMMSVMpoly	-2.98075	153
Head-Gaze_with_logistic	-2.98075	153
Head-Gaze_with_SVMlinear	-2.98075	153
Head-Gaze_with_SVMpoly	-2.98075	153
Head_with_HMMLogistic	-2.98075	153
Head_with_HMMSVMlinear	-2.98075	153
Head_with_HMMSVMpoly	-2.98075	153
Head_with_HMMSVMrbf	-2.98075	153
Head_with_logistic	-2.98075	153
Head_with_SVMlinear	-2.98075	153
Head_with_SVMpoly	-2.98075	153
Head_with_SVMrbf	-2.98075	153
Motion-Head_with_HMMSVMrbf	-2.98075	153
Motion-Head_with_SVMrbf	-2.98075	153
Motion_with_SVMrbf	-2.98075	153
Motion-Gaze_with_HMMSVMrbf	-3.03722	178
Motion-Gaze_with_SVMrbf	-3.03722	178
Motion_with_HMMSVMrbf	-3.03722	178

Table B-2: Top algorithm-feature combinations at Prediction Site 10 in Scenario 1.

Feature	Cohen's d	Rank
Steering-Motion-Head_with_HMMLogistic	10.02995	1
Steering-Motion-Head_with_logistic	10.02995	1
Steering-Motion_with_HMMLogistic	9.955481	3
Steering-Motion_with_SVMpoly	9.93187	4
Steering-Motion_with_HMMSVMlinear	9.913956	5

Table B-3: Top algorithm-feature combinations at Prediction Site 11 in Scenario 1.

Feature	Cohen's d	Rank
Steering-Motion_with_HMMLogistic	10.25055	1
Steering-Motion_with_logistic	10.25055	1
Steering-Gaze_with_logistic	9.973498	3
Steering-Motion-Gaze_with_HMMLogistic	9.896043	4
Steering-Motion_with_HMMAda	9.887678	5

Table B-4: Top algorithm-feature combinations at Prediction Site 12 in Scenario 1.

Feature	Cohen's d	Rank
Steering-Gaze_with_HMMLogistic	17.90049	1
Steering-Gaze_with_logistic	17.90049	1
Steering-Head-Gaze_with_HMMLogistic	17.90049	1
Steering-Head-Gaze_with_logistic	17.90049	1
Steering-Head_with_HMMLogistic	17.90049	1
Steering-Head_with_logistic	17.90049	1
Steering-Motion-Gaze_with_HMMLogistic	17.90049	1
Steering-Motion-Gaze_with_logistic	17.90049	1
Steering-Motion-Head-Gaze_with_logistic	17.90049	1
Steering-Motion-Head_with_HMMLogistic	17.90049	1
Steering-Motion-Head_with_logistic	17.90049	1
Steering-Motion_with_HMMLogistic	17.90049	1
Steering-Motion_with_logistic	17.90049	1
Steering_with_HMMLogistic	17.90049	1
Steering_with_logistic	17.90049	1

Table B-5: Top algorithm-feature combinations at Prediction Site 12 in Scenario 2.

Feature	Cohen's d	Rank
Steering-Gaze_with_HMMRF	27.52974	1
Steering-Gaze_with_RF	27.52974	1
Steering-Motion-Head-Gaze_with_Ada	24.97318	3
Steering-Motion-Head-Gaze_with_HMMAda	24.97318	3
Steering_with_RF	22.33317	5

Table B-6: Top algorithm-feature combinations at Prediction Site 13 in Scenario 2.

Feature	Cohen's d	Rank
Steering-Motion-Head-Gaze_with_HMMLogistic	19.97185	1
Steering-Motion-Head-Gaze_with_logistic	19.97185	1
Steering-Motion-Head_with_HMMLogistic	19.09531	3
Steering-Motion-Head_with_logistic	19.09531	3
Steering-Motion-Head_with_HMMAda	18.89744	5

Table B-7: Top algorithm-feature combinations at Prediction Site 14 in Scenario 2.

Feature	Cohen's d	Rank
Steering-Gaze_with_HMMLogistic	17.71208	1
Steering-Gaze_with_logistic	17.71208	1
Steering-Head-Gaze_with_HMMLogistic	17.71208	1
Steering-Head-Gaze_with_logistic	17.71208	1
Steering-Head_with_HMMLogistic	17.71208	1
Steering-Head_with_logistic	17.71208	1
Steering-Motion-Gaze_with_HMMLogistic	17.71208	1
Steering-Motion-Gaze_with_logistic	17.71208	1
Steering-Motion-Head-Gaze_with_HMMLogistic	17.71208	1
Steering-Motion-Head-Gaze_with_logistic	17.71208	1
Steering-Motion_with_HMMLogistic	17.71208	1
Steering-Motion_with_logistic	17.71208	1
Steering_with_HMMLogistic	17.71208	1
Steering_with_logistic	17.71208	1

Table B-8: Top algorithm-feature combinations at Prediction Site 15 in Scenario 2.

Feature	Cohen's d	Rank
Steering-Gaze_with_HMMSVMrbf	17.43946	1
Steering-Head-Gaze_with_HMMLogistic	17.43946	1
Steering-Head-Gaze_with_logistic	17.43946	1
Steering-Head_with_HMMLogistic	17.43946	1
Steering-Head_with_logistic	17.43946	1
Steering-Motion-Gaze_with_HMMLogistic	17.43946	1
Steering-Motion-Head-Gaze_with_HMMLogistic	17.43946	1
Steering-Motion-Head-Gaze_with_logistic	17.43946	1
Steering-Motion-Head_with_HMMLogistic	17.43946	1
Steering-Motion-Head_with_logistic	17.43946	1
Steering-Motion_with_HMMLogistic	17.43946	1
Steering-Motion_with_logistic	17.43946	1
Steering_with_HMMLogistic	17.43946	1
Steering_with_logistic	17.43946	1

Table B-9: Top algorithm-feature combinations at Prediction Site 17 in Scenario 3.

Feature	Cohen's d	Rank
Steering-Motion_with_HMMLogistic	18.18166	1
Steering-Motion_with_logistic	18.11886	2
Steering-Motion-Gaze_with_logistic	17.31795	3
Steering-Motion-Head_with_HMMSVMrbf	17.3067	4
Steering-Motion-Head-Gaze_with_logistic	17.17958	5

Table B-10: Top algorithm-feature combinations at Prediction Site 18 in Scenario 3.

Feature	Cohen's d	Rank
Steering-Motion-Head_with_logistic	15.32932	1
Steering-Head_with_logistic	15.15852	2
Steering-Motion-Head_with_HMMLogistic	14.97366	3
Steering-Motion-Head-Gaze_with_logistic	14.9204	4
Steering-Motion_with_HMMLogistic	14.9204	4

Table B-11: Top algorithm-feature combinations at Prediction Site 19 in Scenario 3.

Feature	Cohen's d	Rank
Steering-Motion-Head_with_logistic	17.5753	1
Steering-Motion-Gaze_with_logistic	17.43653	2
Steering-Motion-Head-Gaze_with_logistic	17.43653	2
Steering-Motion_with_logistic	17.43653	2
Steering-Motion-Head_with_HMMLogistic	17.14777	5

Table B-12: Top algorithm-feature combinations at Prediction Site 20 in Scenario 3.

Feature	Cohen's d	Rank
Steering-Motion-Gaze_with_HMMLogistic	16.06123	1
Steering-Motion-Gaze_with_HMMSVMlinear	16.06123	1
Steering-Motion-Gaze_with_HMMSVMpoly	16.06123	1
Steering-Motion-Head-Gaze_with_HMMLogistic	16.06123	1
Steering-Motion-Head_with_HMMLogistic	16.06123	1
Steering-Motion-Head_with_HMMSVMlinear	16.06123	1
Steering-Motion_with_HMMLogistic	16.06123	1

Table B-13: Top algorithm-feature combinations at Prediction Site 25 in Scenario 4.

Feature	Cohen's d	Rank
Steering-Motion_with_HMMLogistic	22.32261	1
Steering-Head_with_HMMLogistic	21.99521	2
Steering-Motion_with_logistic	21.78051	3
Steering-Head_with_HMMRF	21.21625	4
Steering-Gaze_with_HMMAda	21.15539	5

Table B-14: Top algorithm-feature combinations at Prediction Site 26 in Scenario 4.

Feature	Cohen's d	Rank
Steering_with_HMMAda	25.67759	1
Steering-Motion_with_HMMLogistic	25.66025	2
Steering-Head-Gaze_with_HMMSVMlinear	24.4891	3
Steering-Head-Gaze_with_HMMSVMpoly	24.4891	3
Steering-Head_with_HMMSVMlinear	24.4891	3

Table B-15: Top algorithm-feature combinations at Prediction Site 27 in Scenario 4.

Feature	Cohen's d	Rank
Steering-Motion_with_HMMRF	17.92307	1
Steering-Motion-Gaze_with_HMMSVMlinear	17.91624	2
Steering-Motion-Gaze_with_HMMSVMpoly	17.91624	2
Steering-Motion_with_HMMSVMlinear	17.91624	2
Steering-Motion_with_HMMSVMpoly	17.91624	2

Table B-16: Top algorithm-feature combinations at Prediction Site 28 in Scenario 4.

Feature	Cohen's d	Rank
Steering-Head_with_logistic	19.72534	1
Steering-Motion-Head-Gaze_with_HMMAda	19.72534	1
Steering-Motion_with_HMMRF	19.72534	1
Steering-Motion_with_logistic	19.72534	1
Steering-Gaze_with_HMMRF	19.49685	5

C Box Plots for the Evaluation of the Features and the Algorithms

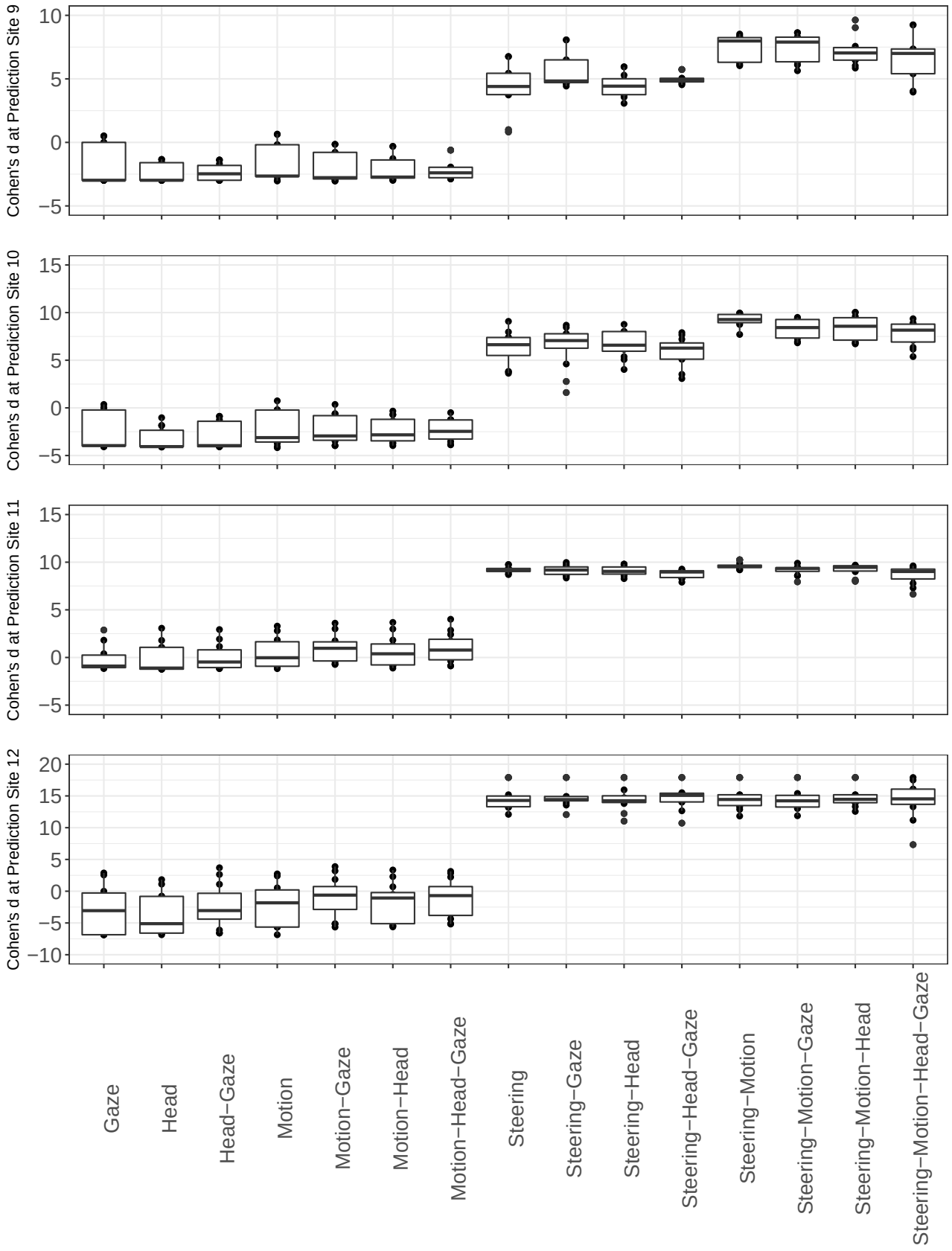

Figure C-1: Box plots of the features over different algorithms in Scenario 1.

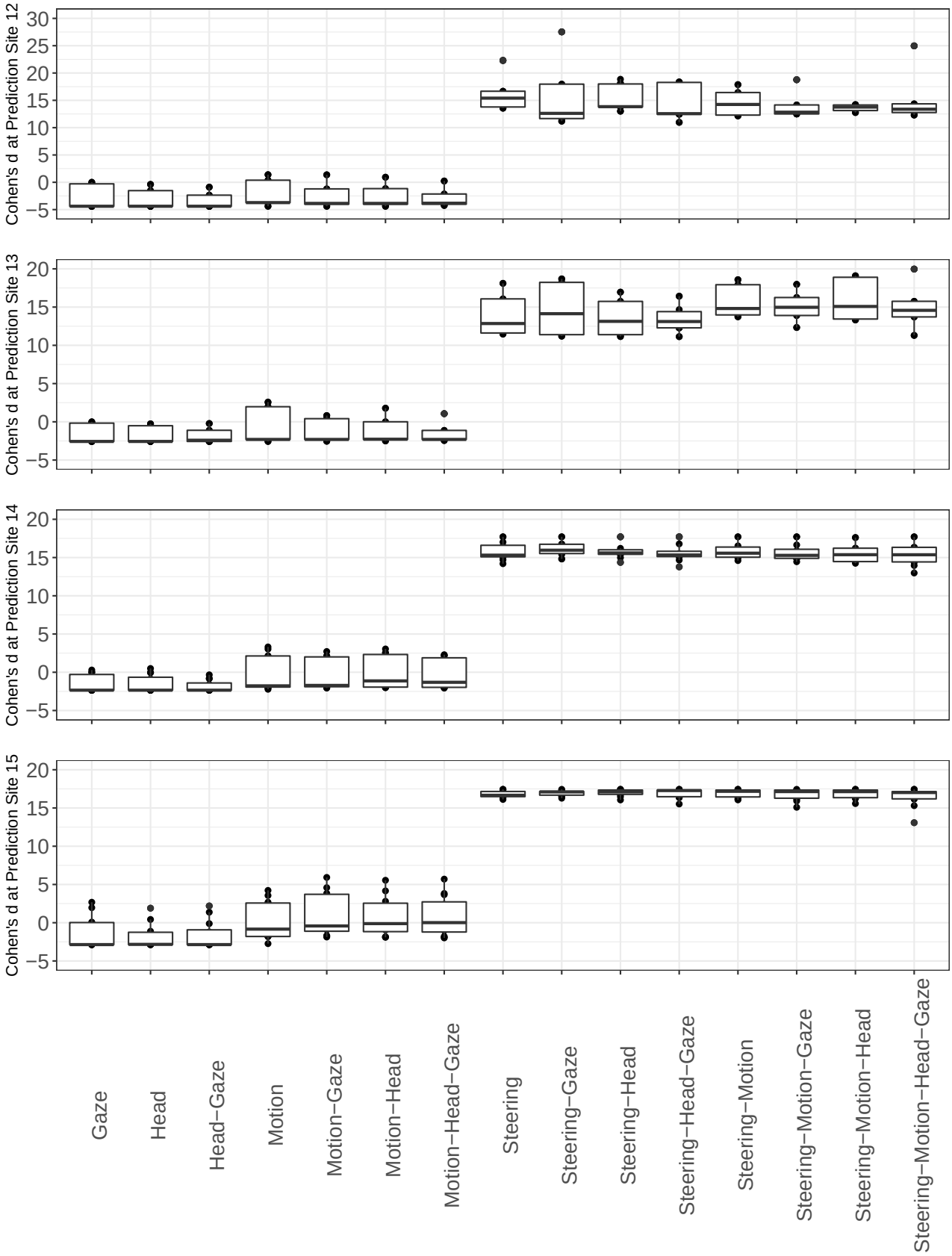

Figure C-2: Box plots of the features over different algorithms in Scenario 2.

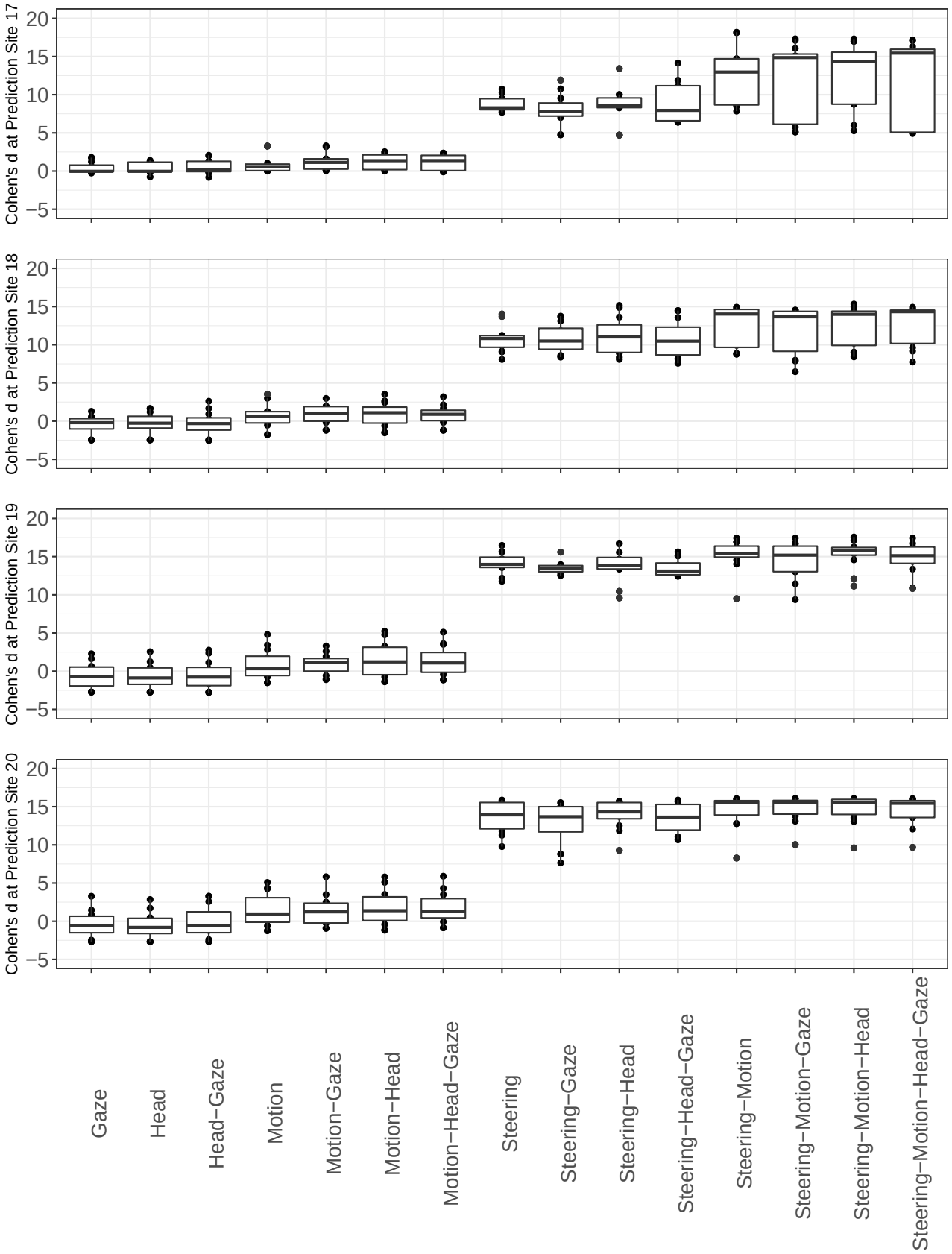

Figure C-3: Box plots of the features over different algorithms in Scenario 3.

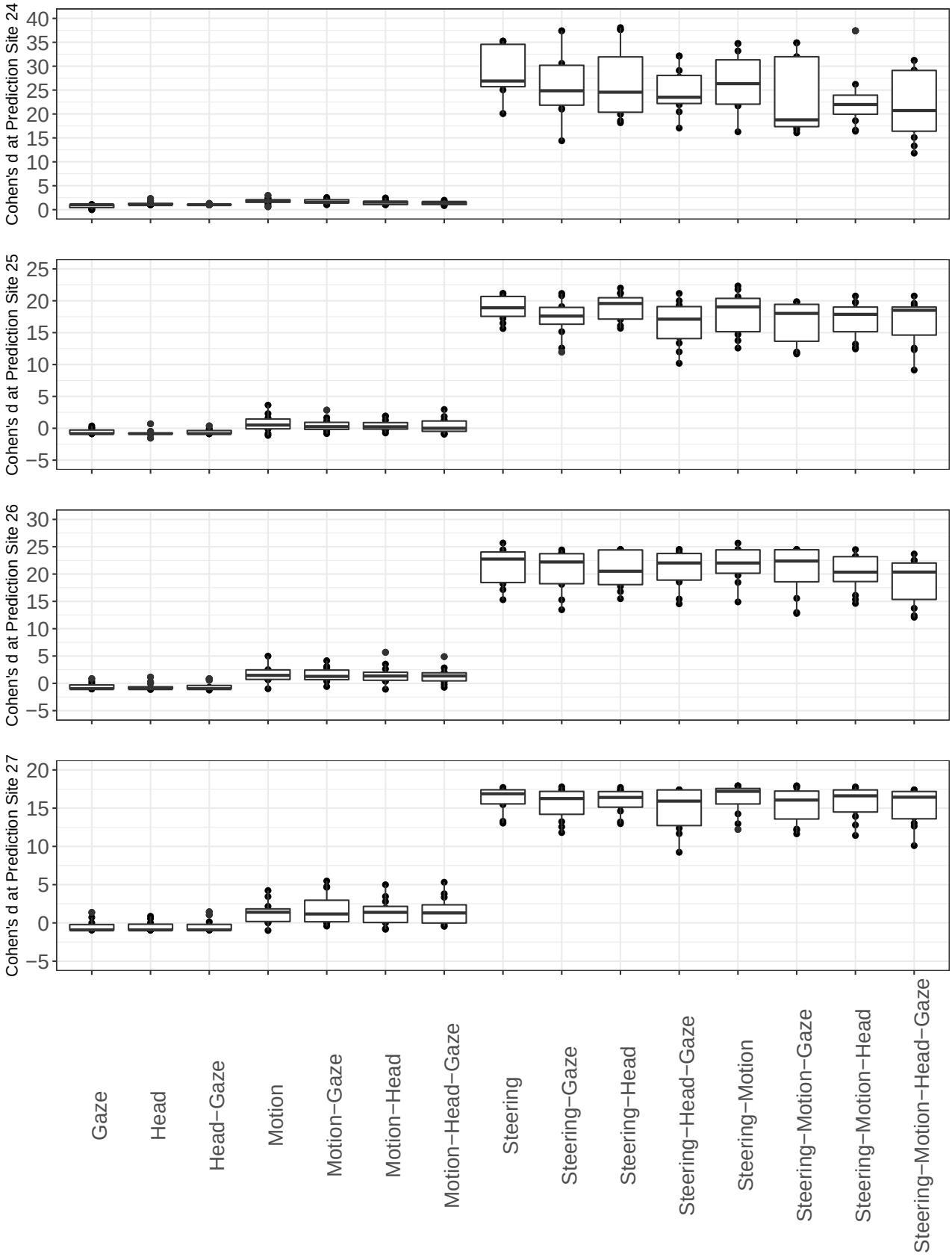

Figure C-4: Box plots of the features over different algorithms in Scenario 4.

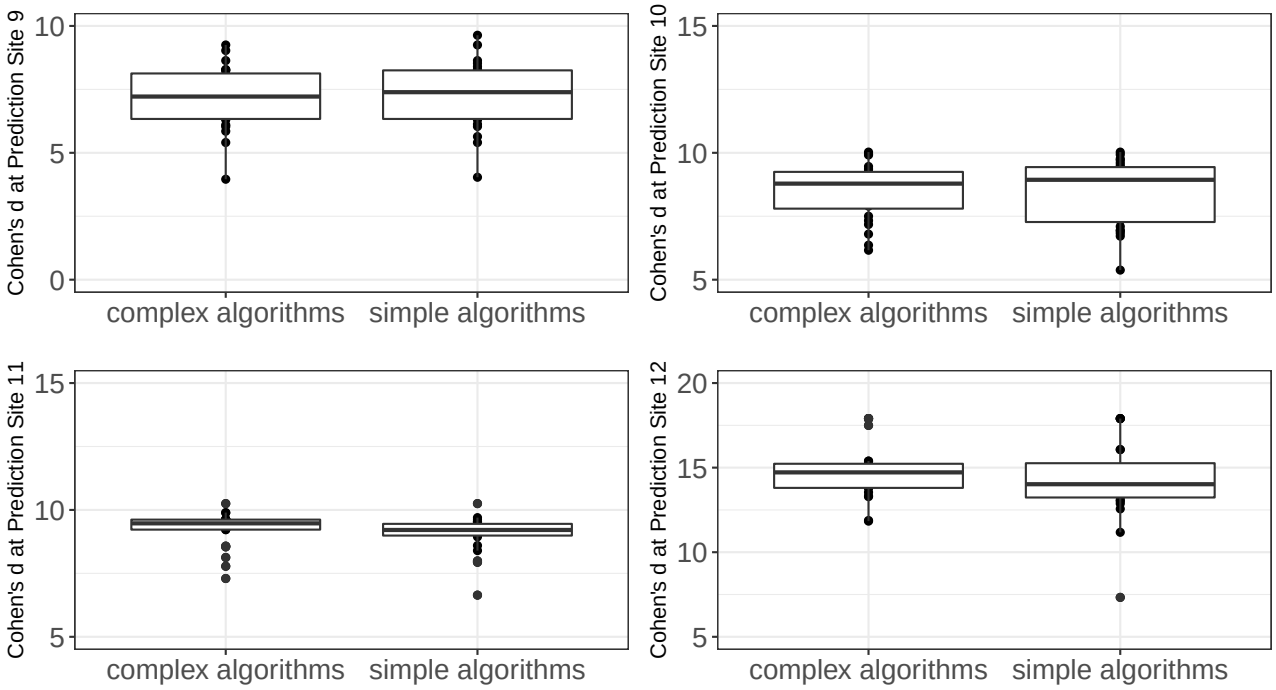

Figure C-5: Box plots of the complex algorithms and the simple algorithms in Scenario 1.

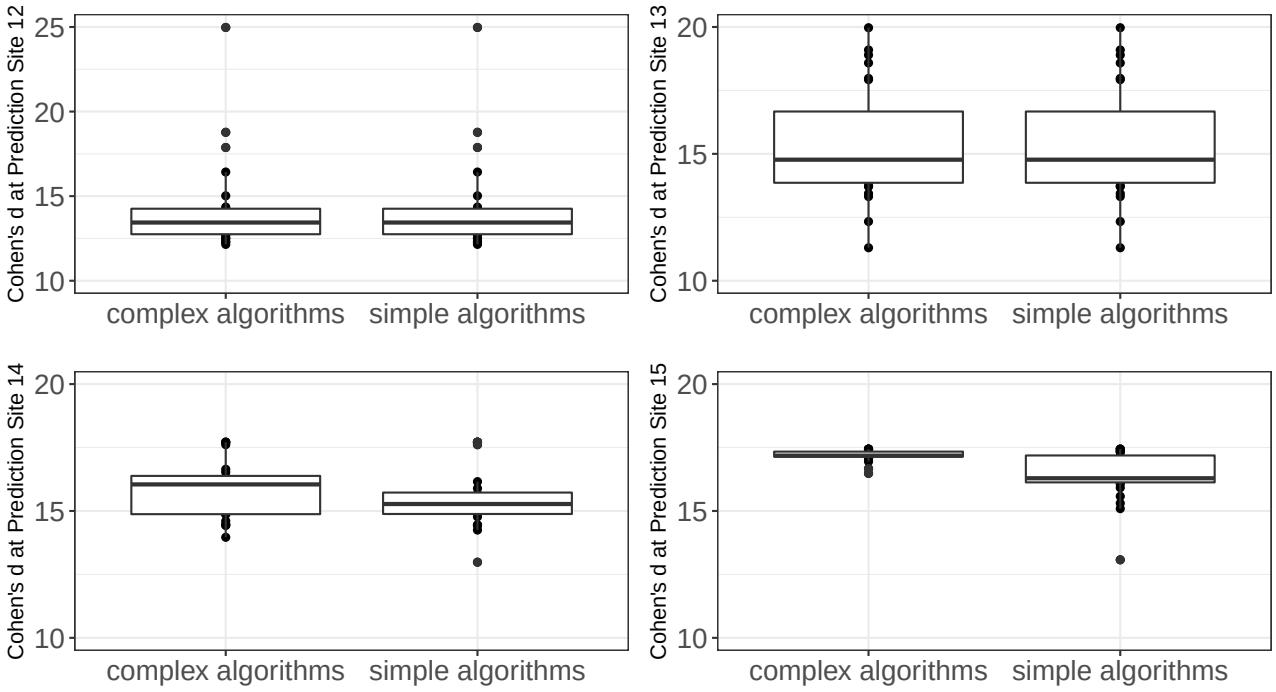

Figure C-6: Box plots of the complex algorithms and the simple algorithms in Scenario 2.

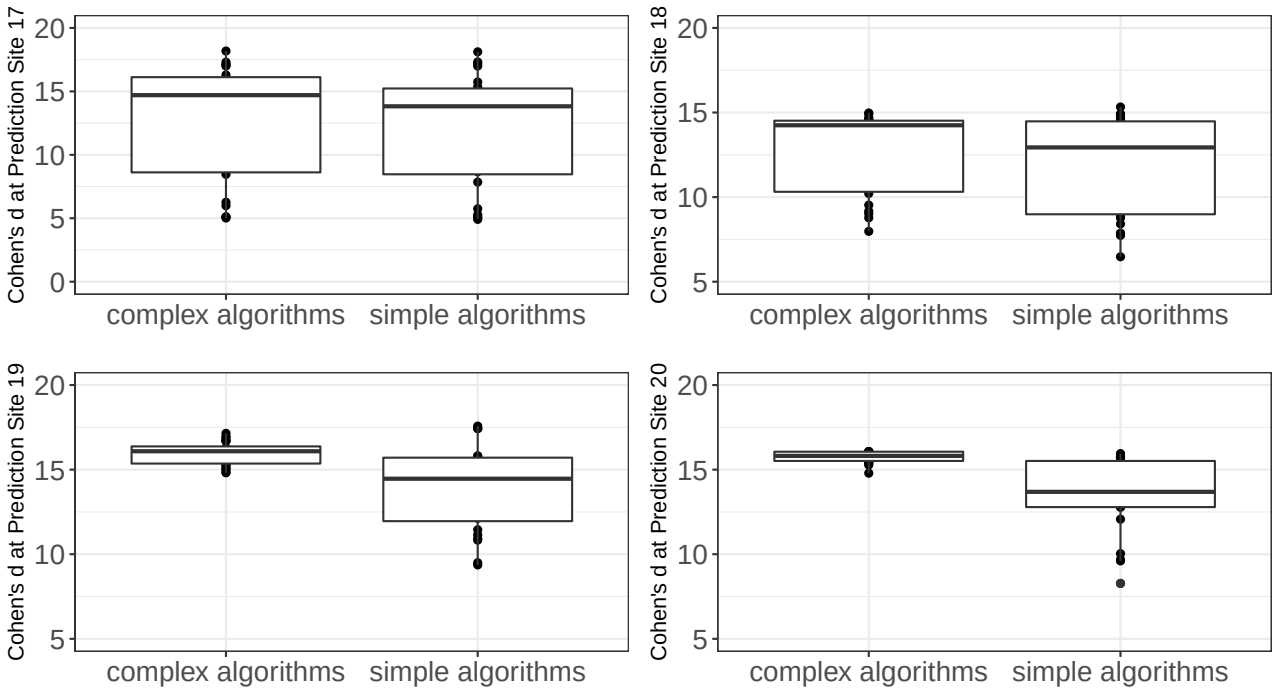

Figure C-7: Box plots of the complex algorithms and the simple algorithms in Scenario 3.

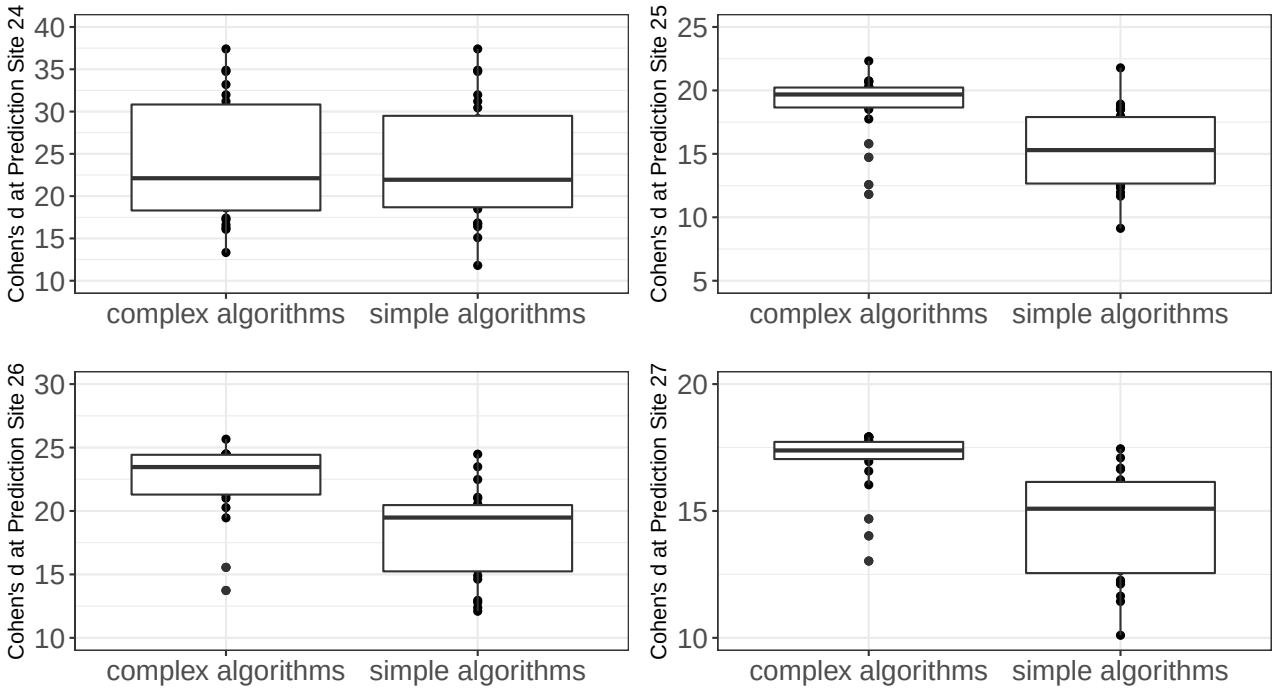

Figure C-8: Box plots of the complex algorithms and the simple algorithms in Scenario 4.

D Outputs of the Soft-Classification Algorithms

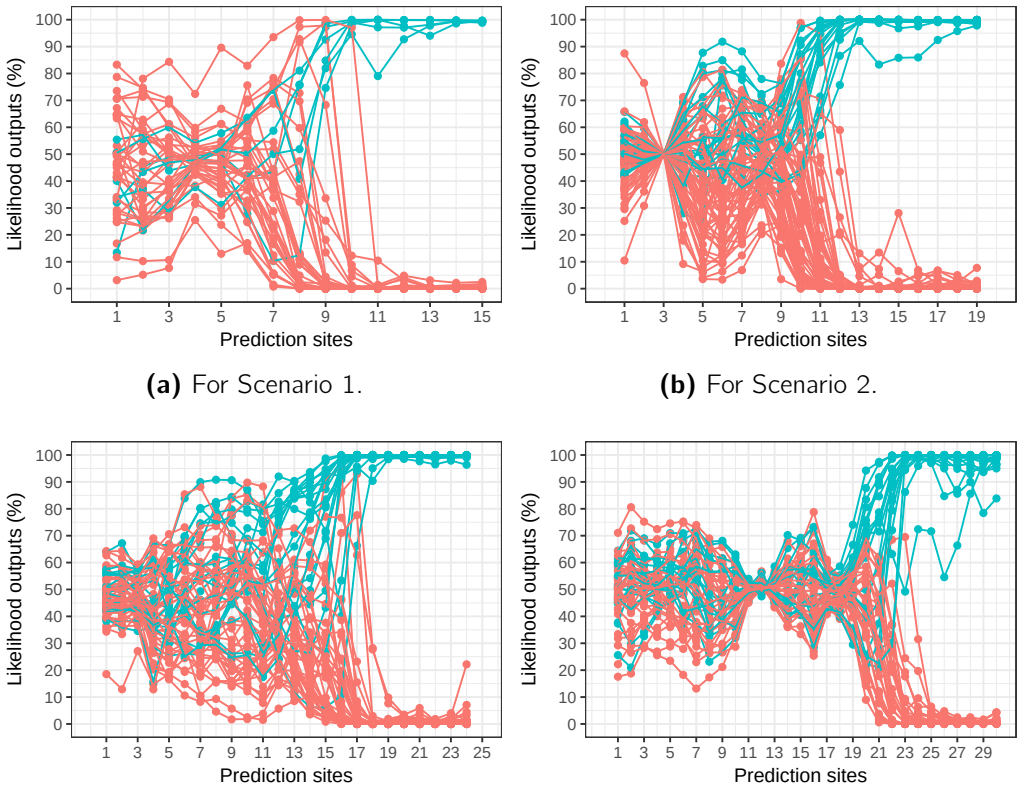

(a) For Scenario 1.

(b) For Scenario 2.

(c) For Scenario 3.

(d) For Scenario 4.

Figure D-1: Soft-decision outputs of linear SVM.

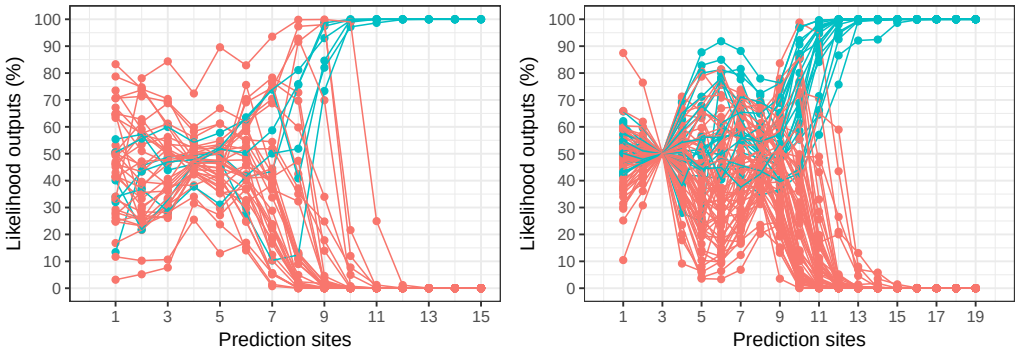

(a) For Scenario 1. **(b)** For Scenario 2.

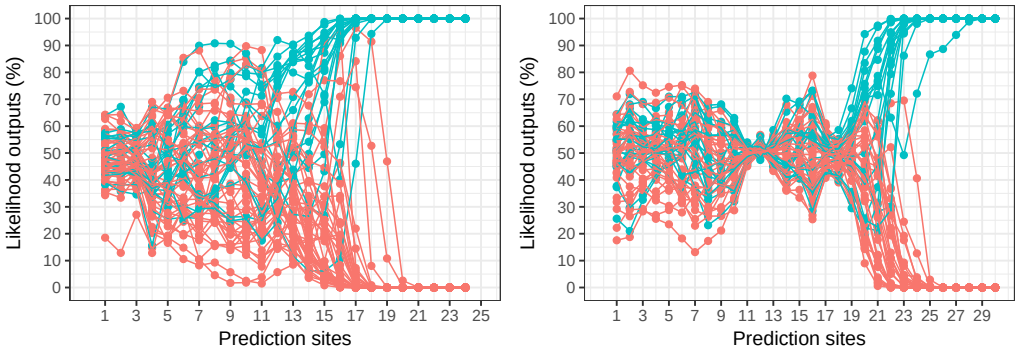

(c) For Scenario 3. **(d)** For Scenario 4.

Figure D-2: Soft-decision outputs of linear SVM-based quasi-HMM.

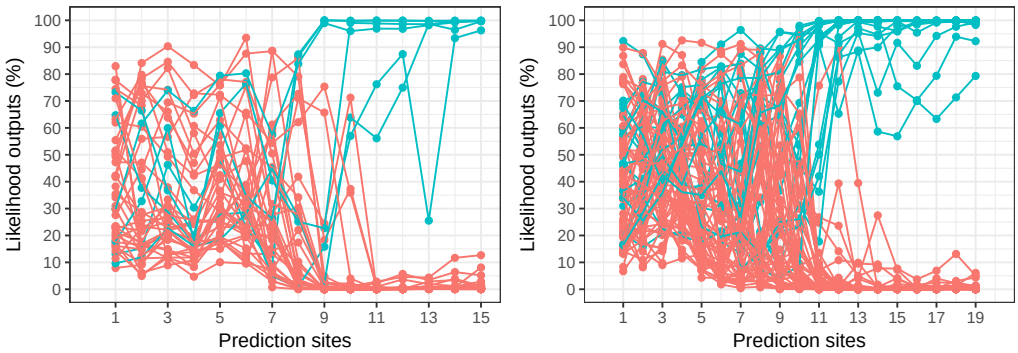

(a) For Scenario 1. **(b)** For Scenario 2.

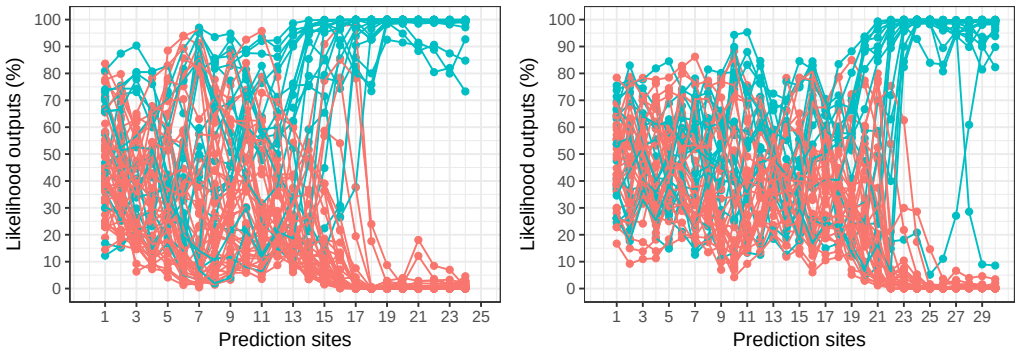

(c) For Scenario 3. **(d)** For Scenario 4.

Figure D-3: Soft-decision outputs of Gaussian SVM.

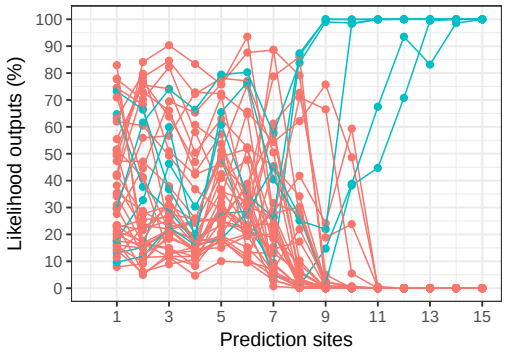

(a) For Scenario 1.

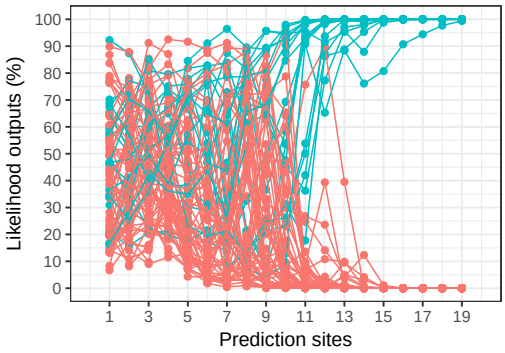

(b) For Scenario 2.

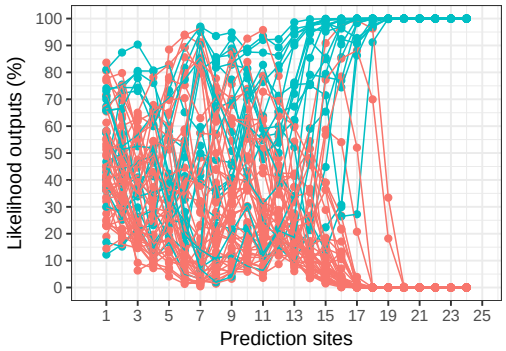

(c) For Scenario 3.

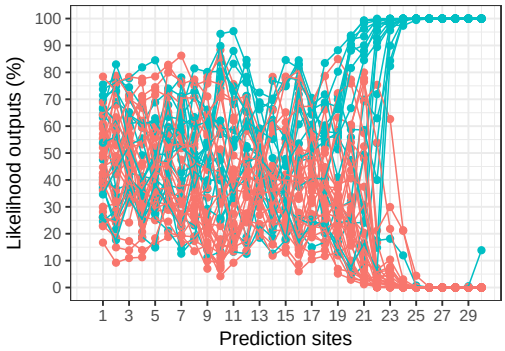

(d) For Scenario 4.

Figure D-4: Soft-decision outputs of Gaussian SVM-based quasi-HMM.

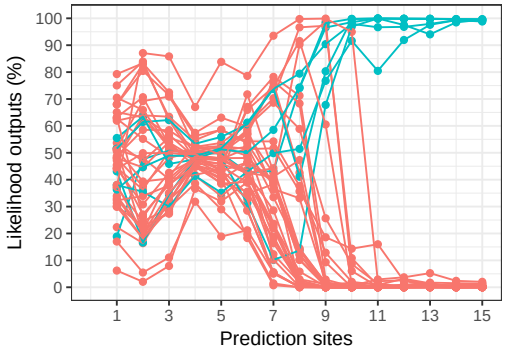

(a) For Scenario 1.

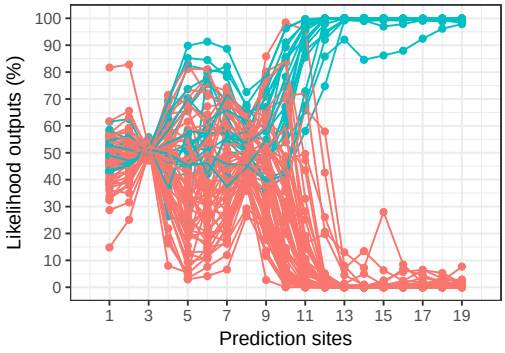

(b) For Scenario 2.

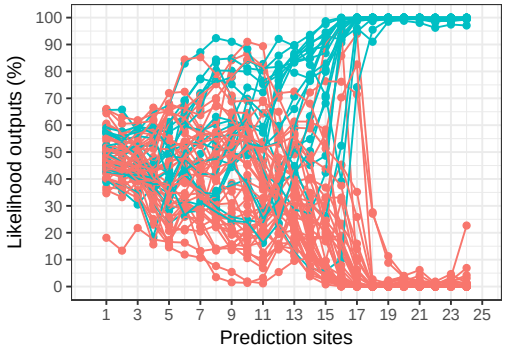

(c) For Scenario 3.

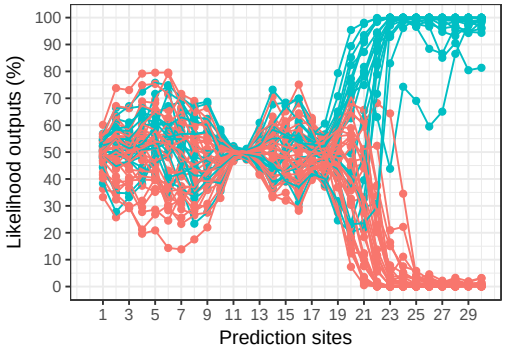

(d) For Scenario 4.

Figure D-5: Soft-decision outputs of polynomial SVM.

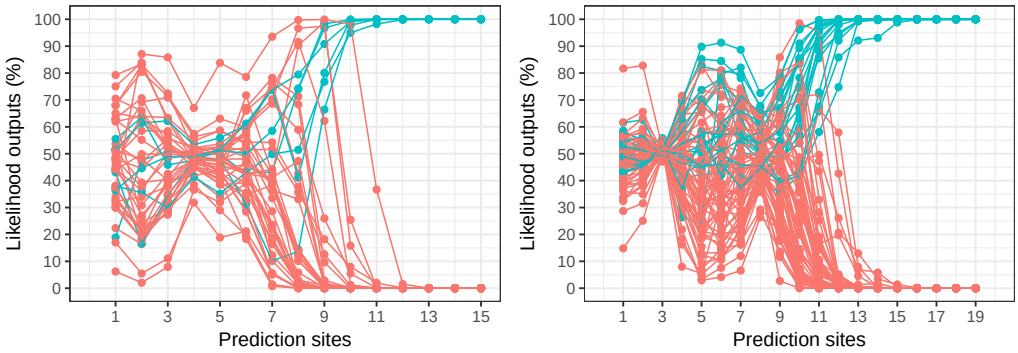

(a) For Scenario 1. **(b)** For Scenario 2.

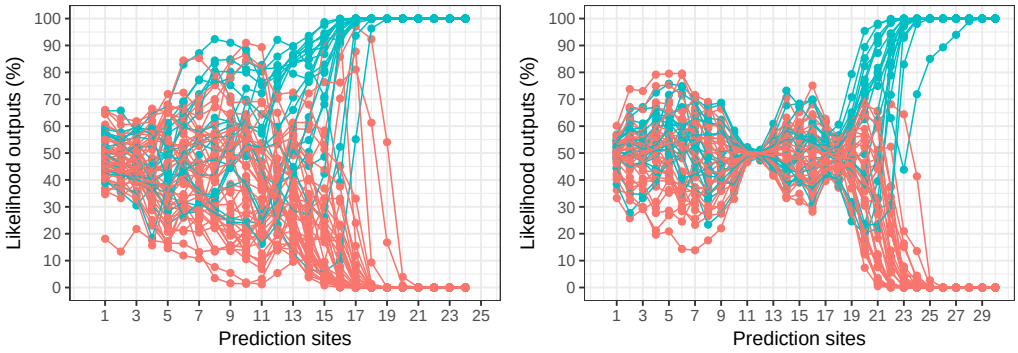

(c) For Scenario 3. **(d)** For Scenario 4.

Figure D-6: Soft-decision outputs of polynomial SVM-based quasi-HMM.

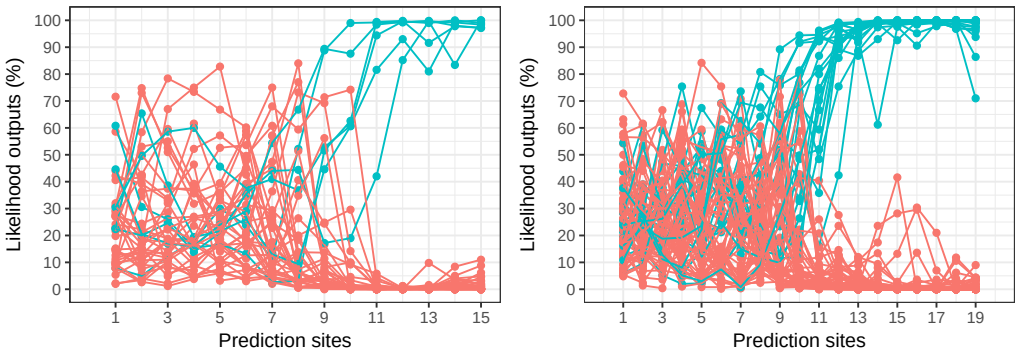

(a) For Scenario 1. **(b)** For Scenario 2.

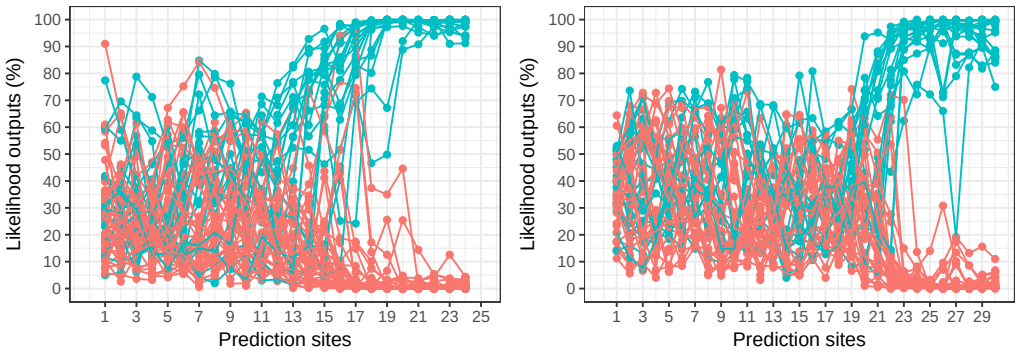

(c) For Scenario 3. **(d)** For Scenario 4.

Figure D-7: Soft-decision outputs of random forest (RF).

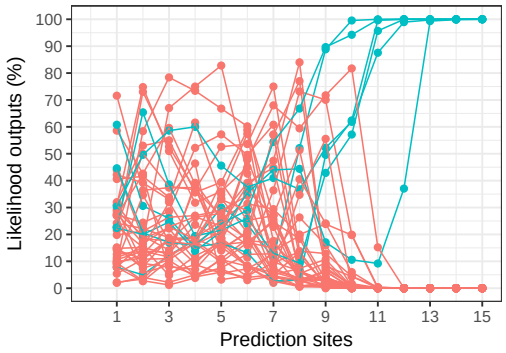

(a) For Scenario 1.

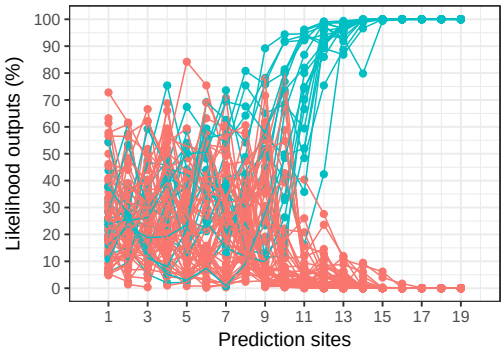

(b) For Scenario 2.

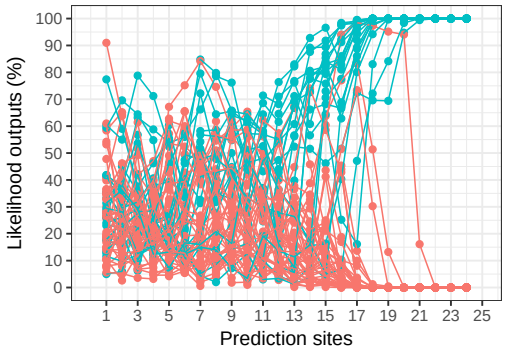

(c) For Scenario 3.

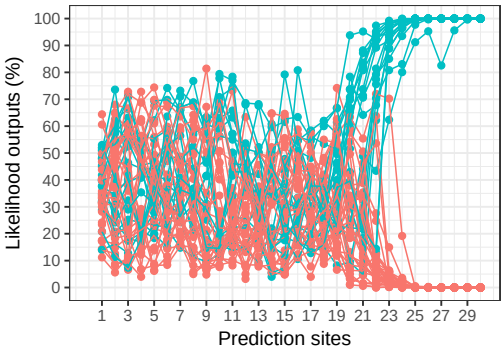

(d) For Scenario 4.

Figure D-8: Soft-decision outputs of RF-based quasi-HMM.

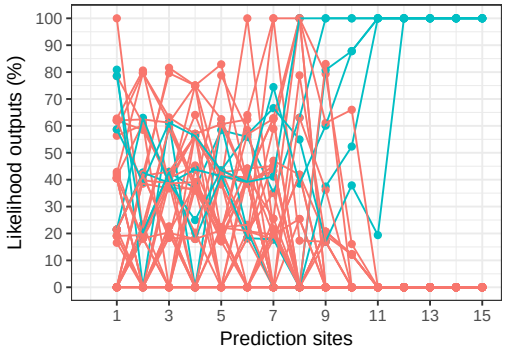

(a) For Scenario 1.

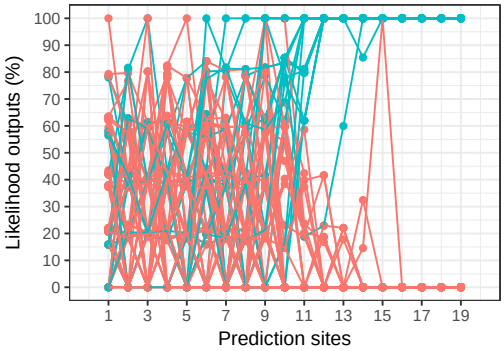

(b) For Scenario 2.

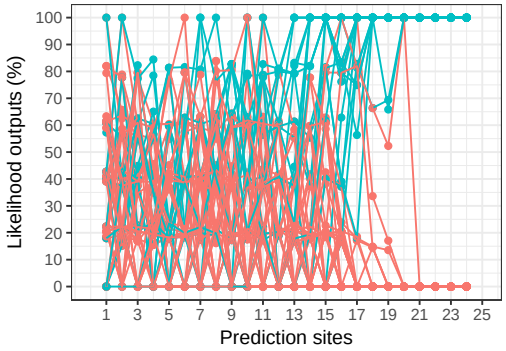

(c) For Scenario 3.

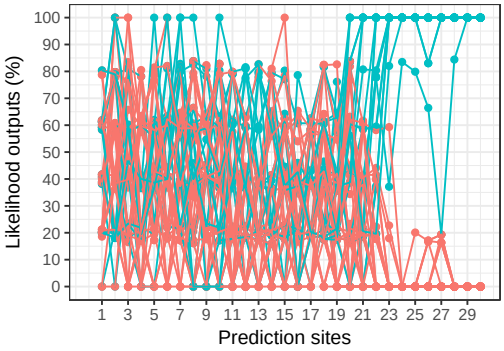

(d) For Scenario 4.

Figure D-9: Soft-decision outputs of AdaBoost.

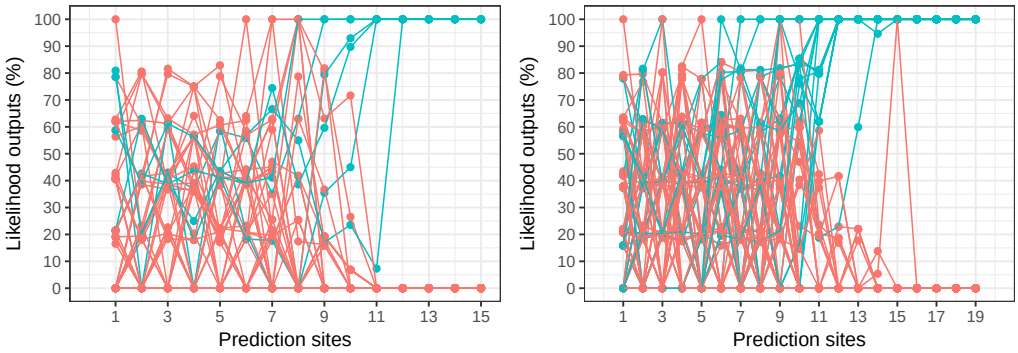

(a) For Scenario 1. **(b)** For Scenario 2.

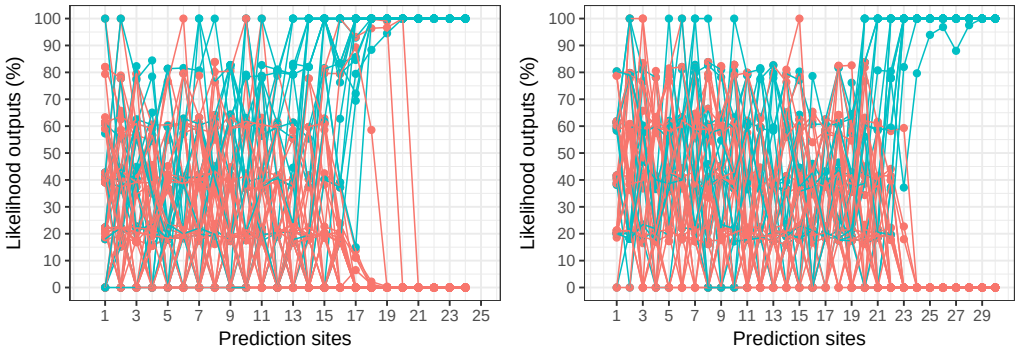

(c) For Scenario 3. **(d)** For Scenario 4.

Figure D-10: Soft-decision outputs of AdaBoost-based quasi-HMM.

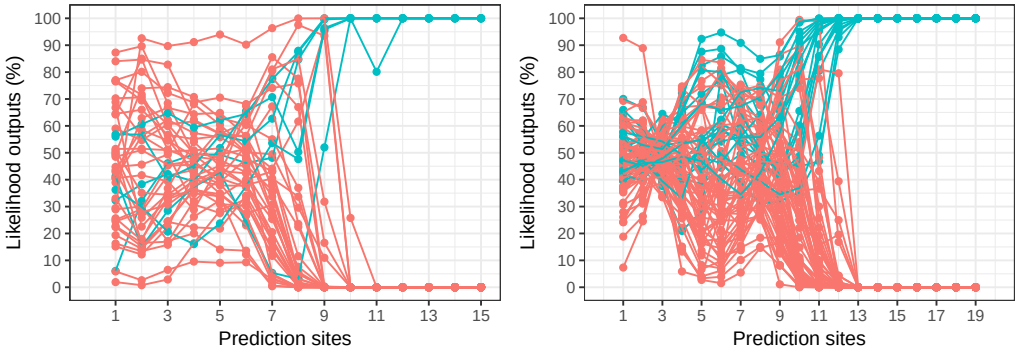

(a) For Scenario 1. **(b)** For Scenario 2.

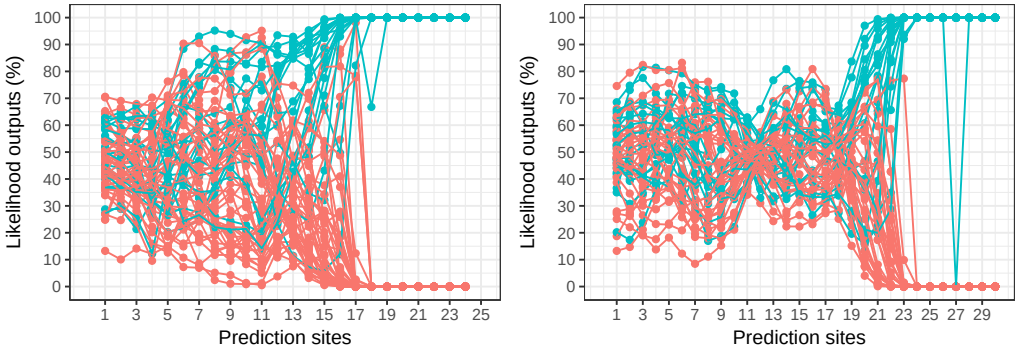

(c) For Scenario 3. **(d)** For Scenario 4.

Figure D-11: Soft-decision outputs of logistic regression.

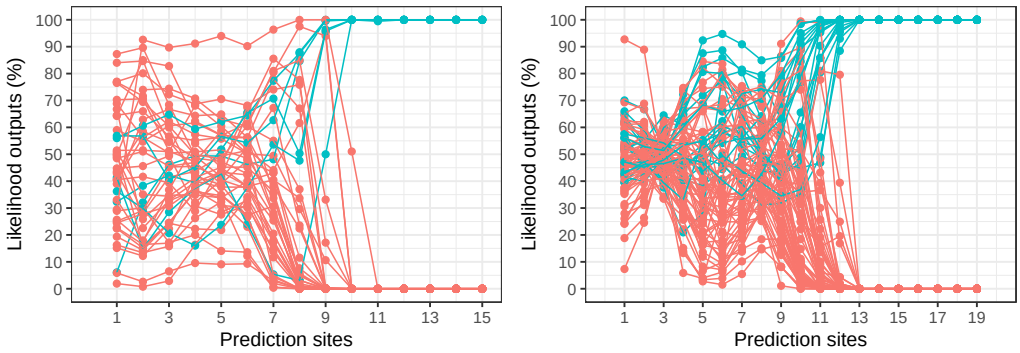

(a) For Scenario 1.

(b) For Scenario 2.

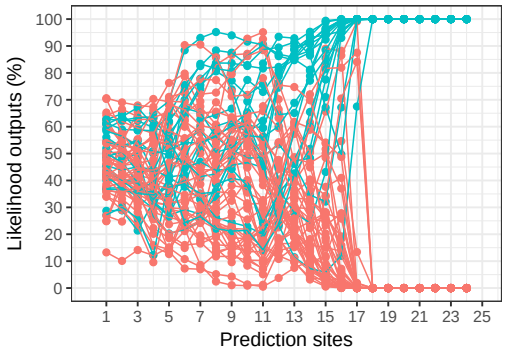

(c) For Scenario 3.

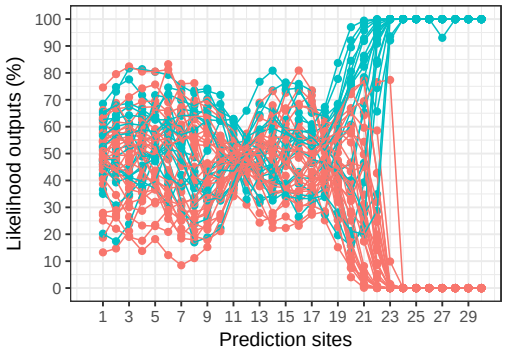

(d) For Scenario 4.

Figure D-12: Soft-decision outputs of logistic-based quasi-HMM.

E Symbols and Acronyms

EM	expectation maximization
SVM	support vector machines
ML	maximum likelihood
RF	random forest
HMM	hidden Markov models
VC	Vapnik and Chervonenkis
ROC	receiver operating characteristic curve

Bibliography

[Alb18] Chris Albon. Nested cross validation. `https://chrisalbon.com/machine_learning/model_evaluation/nested_cross_validation/`, 2018. Accessed: 06-30-2018.

[BD09] Holger Berndt and Klaus Dietmayer. Driver intention inference with vehicle onboard sensors. In *Vehicular Electronics and Safety (ICVES), 2009 IEEE International Conference on*, pages 102–107. IEEE, 2009.

[BED08] Holger Berndt, Jorg Emmert, and Klaus Dietmayer. Continuous driver intention recognition with hidden Markov models. In *Intelligent Transportation Systems, 2008. ITSC 2008. 11th International IEEE Conference on*, pages 1189–1194. IEEE, 2008.

[Ben12] Staffan Bengtsson. *Detection and prediction of lane-changes: A study to infer driver intent using support vector machine*. Master thesis, KTH Industrial Engineering and Management, 2012.

[BH89] Eric B Baum and David Haussler. What size net gives valid generalization? In *Advances in neural information processing systems*, pages 81–90, 1989.

[BLSIG17] Mathieu Barbier, Christian Laugier, Olivier Simonin, and Javier Ibanez-Guzman. Classification of drivers manoeuvre for road intersection crossing with synthethic and real data. In *Intelligent Vehicles Symposium (IV), 2017 IEEE*, pages 224–230. IEEE, 2017.

[Bre96] Leo Breiman. Bagging predictors. *Machine Learning*, 24(2):123–140, 1996.

[Bri11] Werner Brilon. Studies on roundabouts in germany: Lessons learned. In *Proceedings of International Roundabout Conference, Carmel, IN, USA*, 2011.

[BSB+96] Volker Blanz, Bernhard Schölkopf, HCBVV Bülthoff, Chris Burges, Vladimir Vapnik, and Thomas Vetter. Comparison of view-based object recognition algorithms using realistic 3d models. In *International Conference on Artificial Neural Networks*, pages 251–256. Springer, 1996.

[CGK12] Gary Charness, Uri Gneezy, and Michael A Kuhn. Experimental methods: Between-subject and within-subject design. *Journal of Economic Behavior & Organization*, 81(1):1–8, 2012.

[CV95] Corinna Cortes and Vladimir Vapnik. Support-vector networks. *Machine Learning*, 20(3):273–297, 1995.

[DMT11] Anup Doshi, Brendan Morris, and Mohan Trivedi. On-road prediction of driver's intent with multimodal sensory cues. *IEEE Pervasive Computing*, 10(3):22–34, 2011.

[DNW08] Stijn Daniels, Erik Nuyts, and Geert Wets. The effects of roundabouts on traffic safety for bicyclists: An observational study. *Accident Analysis & Prevention*, 40(2):518–526, 2008.

[DT11] Anup Doshi and Mohan M Trivedi. Tactical driver behavior prediction and intent inference: A review. In *Intelligent Transportation Systems (ITSC), 2011 14th International IEEE Conference on*, pages 1892–1897. IEEE, 2011.

[EHVS09] Rune Elvik, Alena Høye, Truls Vaa, and Michael Sørensen. *The Handbook of Road Safety Measures*. Emerald Group Publishing Limited, 2009.

[Eur08] Auto Club Europa. Reviere der Blinkmuffel. 2008.

[FHT+00] Jerome Friedman, Trevor Hastie, Robert Tibshirani, et al. Additive logistic regression: A statistical view of boosting (with discussion and a rejoinder by the authors). *The Annals of Statistics*, 28(2):337–407, 2000.

[FS95] Yoav Freund and Robert E Schapire. A desicion-theoretic generalization of on-line learning and an application to boosting. In *European Conference on Computational Learning Theory*, pages 23–37. Springer, 1995.

[GJW+16] Florian Gross, Justus Jordan, Felix Weninger, Felix Klanner, and Björn Schuller. Route and stopping intent prediction at intersections from car fleet data. *IEEE Transactions on Intelligent Vehicles*, 1(2):177–186, 2016.

[GKO14] Vijay Gadepally, Ashok Krishnamurthy, and Umit Ozguner. A framework for estimating driver decisions near intersections. *IEEE Transactions on Intelligent Transportation Systems*, 15(2):637–646, 2014.

[GSBD06] Joakim Gunnarsson, Lennart Svensson, E Bengtsson, and Lars Danielsson. Joint driver intention classification and tracking of vehicles. In *Nonlinear Statistical Signal Processing Workshop, 2006 IEEE*, pages 95–98. IEEE, 2006.

[Han98] James A Hanley. Receiver operating characteristic (ROC) curves. *Encyclopedia of Biostatistics*, 29:307–335, 1998.

[HKBL11] Thomas Hummel, Matthias Kühn, Jenö Bende, and Antje Lang. Advanced driver assistance systems. *German Insurance Association Insurers Accident Research.*, 6(01):2015, 2011.

[HL02] Chih-Wei Hsu and Chih-Jen Lin. A simple decomposition method for support vector machines. *Machine Learning*, 46(1-3):291–314, 2002.

[HMK06] Kurt Hornik, David Meyer, and Alexandros Karatzoglou. Support vector machines in R. *Journal of Statistical Software*, 15(9):1–28, 2006.

[HOB07] Tove Hels and Ivanka Orozova-Bekkevold. The effect of roundabout design features on cyclist accident rate. *Accident Analysis & Prevention*, 39(2):300–307, 2007.

[Hof14] Ulrike Hofmann. *Manual for Road Construction (German: Planungshandbuch Straße- und Wegebau)*. Forum Verlag Herkert GmbH, 2014.

[HV00] Christer Hydén and András Várhelyi. The effects on safety, time consumption and environment of large scale use of roundabouts in an urban area: A case study. *Accident Analysis & Prevention*, 32(1):11–23, 2000.

[HZW12] Lei He, Changfu Zong, and Chang Wang. Driving intention recognition and behaviour prediction based on a double-layer hidden Markov model. *Journal of Zhejiang University SCIENCE C*, 13(3):208–217, 2012.

[KLM96] Leslie Pack Kaelbling, Michael L Littman, and Andrew W Moore. Reinforcement learning: A survey. *Journal of Artificial Intelligence Research*, 4:237–285, 1996.

[Kru08] John Krumm. A Markov model for driver turn prediction. In *Society of Automotive Engineers 2008 World Congress*, volume 2008-01-0201, 2008.

[KYSL00] Nobuyuki Kuge, Tomohiro Yamamura, Osamu Shimoyama, and Andrew Liu. A driver behavior recognition method based on a driver model framework. *Society of Automotive Engineers*, 109(6):469–476, 2000.

[Lak13] Daniël Lakens. Calculating and reporting effect sizes to facilitate cumulative science: A practical primer for t-tests and anovas. *Frontiers in Psychology*, 4:863–900, 2013.

[LIGL11] Stéphanie Lefèvre, Javier Ibañez-Guzmán, and Christian Laugier. Context-based estimation of driver intent at road intersections. In *Computational Intelligence in Vehicles and Transportation Systems (CIVTS), 2011 IEEE Symposium on*, pages 67–72. IEEE, 2011.

[LKB+13] Martin Liebner, Felix Klanner, Michael Baumann, Christian Ruhhammer, and Christoph Stiller. Velocity-based driver intent inference at urban intersections in the presence of preceding vehicles. *IEEE Intelligent Transportation Systems Magazine*, 5(2):10–21, 2013.

[LLIG11] Stéphanie Lefèvre, Christian Laugier, and Javier Ibañez-Guzmán. Exploiting map information for driver intention estimation at road intersections. In *Intelligent Vehicles Symposium (IV), 2011 IEEE*, pages 583–588. IEEE, 2011.

[LRKS13] Martin Liebner, Christian Ruhhammer, Felix Klanner, and Christoph Stiller. Generic driver intent inference based on parametric models. In *Intelligent Transportation Systems-(ITSC), 2013 16th International IEEE Conference on*, pages 268–275. IEEE, 2013.

[LWWL13] Miao Liu, Mingjun Wang, Jun Wang, and Duo Li. Comparison of random forest, support vector machine and back propagation neural network for electronic tongue data classification: Application to the recognition of orange beverage and Chinese vinegar. *Sensors and Actuators B: Chemical*, 177:970–980, 2013.

[LZW11] Yufeng Liu, Hao Helen Zhang, and Yichao Wu. Hard or soft classification? Large-margin unified machines. *Journal of the American Statistical Association*, 106(493):166–177, 2011.

[Mac03] Charles C Macadam. Understanding and modeling the human driver. *Vehicle System Dynamics*, 40(1-3):101–134, 2003.

[MHCG14] Abhisek Mudgal, Shauna Hallmark, Alicia Carriquiry, and Konstantina Gkritza. Driving behavior at a roundabout: A hierarchical Bayesian regression analysis. *Transportation Research Part D: Transport and Environment*, 26:20–26, 2014.

[Mic85] John A Michon. A critical view of driver behavior models: What do we know, what should we do. *Human Behavior and Traffic Safety*, pages 485–520, 1985.

[MM15] Gys Albertus Marthinus Meiring and Hermanus Carel Myburgh. A review of intelligent driving style analysis systems and related artificial intelligence algorithms. *Sensors*, 15(12):30653–30682, 2015.

[Mon11] Alfonso Montella. Identifying crash contributory factors at urban roundabouts and using association rules to explore their relationships to different crash types. *Accident Analysis & Prevention*, 43(4):1451–1463, 2011.

[MS04] Hiren Mansukhlal Mandalia and D Salvucci. *Pattern recognition techniques to infer driver intentions*. PhD thesis, Drexel University, 2004.

[MS05] Hiren M Mandalia and Mandalia Dario D Salvucci. Using support vector machines for lane-change detection. In *Proceedings of the Human Factors and Ergonomics Society Annual Meeting*, volume 49, pages 1965–1969. SAGE Publications Sage CA: Los Angeles, CA, 2005.

[NMI+08] Takahiro Naito, Hiroshi Morimoto, Takafumi Ito, Toshimasa Yamamoto, and Harutsugu Fukumoto. Driver turning behavior prediction at intersections: Improving prediction performance with driver behavior adaptation. *Review of Automotive Engineering*, 29(2):157–163, 2008.

[OYT04] L Ohashi, Toru Yamaguchi, and Ikuo Tamai. Humane automotive system using driver intention recognition. In *SICE 2004 Annual Conference*, volume 2, pages 1164–1167. IEEE, 2004.

[PE07] Manfred Plöchl and Johannes Edelmann. Driver models in automobile dynamics application. *Vehicle System Dynamics*, 45(7-8):699–741, 2007.

[PLI02] Chao-Ying Joanne Peng, Kuk Lida Lee, and Gary M Ingersoll. An introduction to logistic regression analysis and reporting. *The Journal of Educational Research*, 96(1):3–14, 2002.

[Pow11] David Martin Powers. Evaluation: From precision, recall and f-measure to roc, informedness, markedness and correlation. *Journal of Machine Learning Technologies*, 2(1):37–63, 2011.

[PWK17] Derek J Phillips, Tim A Wheeler, and Mykel J Kochenderfer. Generalizable intention prediction of human drivers at intersections. In *Intelligent Vehicles Symposium (IV), 2017 IEEE*, pages 1665–1670. IEEE, 2017.

[Raa17] Raaijmakers. *Towards Environment Perception for Highly Automated Driving*. PhD thesis, Technische Universiteit Eindhoven, 2017.

[Ran94] Thomas A Ranney. Models of driving behavior: A review of their evolution. *Accident Analysis & Prevention*, 26(6):733–750, 1994.

[RJ86] Lawrence Rabiner and B Juang. An introduction to hidden Markov models. *IEEE ASSP Magazine*, 3(1):4–16, 1986.

[Rom05] Elpidio Romano. Modeling drivers' roundabout behavior. In *Proceedings of the SIIV Conference*, volume 39, 2005.

[RPGL01] Richard A Retting, Bhagwant N Persaud, Per E Garder, and Dominique Lord. Crash and injury reduction following installation of roundabouts in the united states. *American Journal of Public Health*, 91(4):628–631, 2001.

[SASMMI13] Paul St-Aubin, Nicolas Saunier, Luis Miranda-Moreno, and Karim Ismail. Use of computer vision data for detailed driver behavior analysis and trajectory interpretation at roundabouts. *Transportation Research Record: Journal of the Transportation Research Board*, (2389):65–77, 2013.

[SB98] Richard S Sutton and Andrew G Barto. *Reinforcement Learning: An Introduction*, volume 1. MIT press Cambridge, 1998.

[Sch13] Robert E Schapire. Explaining AdaBoost. In *Empirical Inference*, pages 37–52. Springer, 2013.

[SH14] Thomas Streubel and Karl Heinz Hoffmann. Prediction of driver intended path at intersections. In *Intelligent Vehicles Symposium Proceedings, 2014 IEEE*, pages 134–139. IEEE, 2014.

[SLSH10] Lisa Sakshaug, Aliaksei Laureshyn, Åse Svensson, and Christer Hydén. Cyclists in roundabouts - different design solutions. *Accident Analysis & Prevention*, 42(4):1338–1351, 2010.

[SSH12] Amardeep Sathyanarayana, Seyed Omid Sadjadi, and John HL Hansen. Leveraging sensor information from portable devices towards automatic driving maneuver recognition. In *Intelligent Transportation Systems (ITSC), 2012 15th International IEEE Conference on*, pages 660–665. IEEE, 2012.

[Sta04] Mark Stamp. A revealing introduction to hidden Markov models. *Department of Computer Science San Jose State University*, pages 26–56, 2004.

[SWRT14] Michaela Spitzer, Jan Wildenhain, Juri Rappsilber, and Mike Tyers. Boxplotr: A web tool for generation of box plots. *Nature Methods*, 11(2):121–122, 2014.

[TB13] Fabio Tango and Marco Botta. Real-time detection system of driver distraction using machine learning. *IEEE Transactions on Intelligent Transportation Systems*, 14(2):894–905, 2013.

[TIS+07] Shun Taguchi, Shinkichi Inagaki, Tatsuya Suzuki, Soichiro Hayakawa, and Nuio Tsuchida. Modeling and analysis of driver's decision making based on logistic regression model. In *SICE, 2007 Annual Conference*, pages 2390–2395. IEEE, 2007.

[TKG15] Bo Tang, Salman Khokhar, and Rakesh Gupta. Turn prediction at generalized intersections. In *Intelligent Vehicles Symposium (IV), 2015 IEEE*, pages 1399–1404. IEEE, 2015.

[TMF16] Ashish Tawari, Teruhisa Misu, and Kikuo Fujimura. Predicting unexpected maneuver while approaching intersection. In *Intelligent Transportation Systems (ITSC), 2016 IEEE 19th International Conference on*, pages 2225–2229. IEEE, 2016.

[ZKJ+17] Min Zhao, David Käthner, Meike Jipp, Dirk Söffker, and Karsten Lemmer. Modeling driver behavior at roundabouts: Results from a field study. In *Intelligent Vehicles Symposium (IV), 2017 IEEE*, pages 908–913. IEEE, 2017.

[ZKS+17] Min Zhao, David Käthner, Dirk Söffker, Meike Jipp, and Karsten Lemmer. Impact of surrounding cyclists on car driver behavior recognition at roundabouts. In *2017 IEEE International Conference on Intelligent Transportation Systems*. Accepted. IEEE, 2017.